

Concepts and mechanisms of trained immunity in pulmonary macrophages

Doctoral thesis at the Medical University of Vienna
for obtaining the academic degree

Doctor of Philosophy

Submitted by

Sophie Zahalka, M.Sc.

Supervisor:

Univ. Prof. Sylvia Knapp, MD, PhD

Department of Medicine I, Research Division of Infection Biology,
Medical University of Vienna

Research Center for Molecular Medicine (CeMM) of the
Austrian Academy of Sciences, Vienna

Vienna, 05/2022

Declaration

I, Sophie Zahalka, hereby declare that I have authored this doctoral thesis, entitled “Concepts and mechanisms of trained immunity in pulmonary macrophages”, and was substantially involved in the design and execution of the presented work. I have conducted my doctoral studies under the supervision of Prof. Sylvia Knapp, MD, PhD at the Medical University of Vienna (MUW), Austria and at the Research Center for Molecular Medicine (CeMM) of the Austrian Academy of Sciences, Vienna, Austria. As part of the MUW doctoral program, I have spent six months at the Max Planck Institute of Immunobiology and Epigenetics in Freiburg, Germany under the supervision of Prof. Edward J. Pearce, PhD. This stay abroad was granted by the FWF-funded PhD program “Cell Communication in Health and Disease (CCHD)” with additional funding provided by the European Molecular Biology Organization (EMBO short term fellowship).

The experimental work of my PhD studies is presented in the publication “Trained immunity of alveolar macrophages requires metabolic rewiring and type 1 interferon signaling”, which is embedded and substantially discussed in this thesis. Individual contributions are listed below. The majority of experiments was conducted in Vienna (MUW & CeMM). I hereby further declare that all additional parts of the thesis were solely written by me, with input and feedback from Prof. Sylvia Knapp, MD, PhD.

First author publication (accepted for publication in *Mucosal Immunology*):

Trained immunity of alveolar macrophages requires metabolic rewiring and type 1 interferon signaling

Sophie Zahalka, Philipp Starkl, Martin L. Watzenboeck, Asma Farhat, Mariem Radhouani, Florian Deckert, Anastasiya Hladik, Karin Lakovits, Felicitas Oberndorfer, Caroline Lassnig, Birgit Strobl, Kristaps Klavins, Mai Matsushita, David E. Sanin, Katarzyna M. Grzes, Edward J. Pearce, Anna-Dorothea Gorki, Sylvia Knapp.

Individual author contributions:

SZ, SK and ADG conceptualized the study. SK and EJP provided funding. SK, ADG and EJP supervised the project. SZ, PS, AF, MR, AH, KL, ADG, KK, KMG and MM conducted the experiments. MLW, FD and DES performed bioinformatic analyses. MLW provided statistical consulting. CL and BS coordinated mouse breeding and supply. FO evaluated histological samples. SZ and SK wrote the manuscript with input from co-authors.

Table of contents

Declaration	ii
Table of contents.....	iii
List of Figures and Tables	v
Abstract	vii
Zusammenfassung.....	viii
Publications arising from this thesis	x
Abbreviations	xi
Acknowledgements	xvi
1. General introduction.....	1
1.1 Innate immunity of the lungs.....	2
1.2 Alveolar macrophages – key players in lung homeostasis and host defense	9
1.2.1 Ontogeny and development	9
1.2.2 AMs in homeostasis	14
1.2.3 AM polarization.....	17
1.2.4 AM metabolism.....	19
1.2.5 The role of AMs in antimicrobial defense	20
1.3 Pneumococcal pneumonia	22
1.3.1 Epidemiology of lower respiratory tract infections	22
1.3.2 <i>Streptococcus pneumoniae</i> virulence factors.....	23
1.3.3 Host immune response to <i>Streptococcus pneumoniae</i>	23
1.3.4 Current treatment and vaccination strategies.....	25
1.4 Trained immunity.....	27
1.4.1 Evolutionary perspective and basic concepts.....	27
1.4.2 Inducers of trained immunity	30
1.4.3 Mechanistic regulation of trained immunity	32
1.4.4 Cellular mediators of trained immunity	35
1.4.5 Therapeutic targeting of trained immunity	37
1.5 Aims of the thesis	39

2. Results	40
2.1 Abstract	41
2.2 Introduction.....	41
2.3 Results.....	43
2.3.1 LPS exposure induces trained immunity in alveolar macrophages	43
2.3.2 AM training depends on type 1 interferon signaling	45
2.3.3 Trained AMs exhibit an altered transcriptional profile upon secondary bacterial challenge	47
2.3.4 Secondary metabolic AM responses are modulated by prior LPS exposure	49
2.3.5 LPS training induces changes in AM metabolite and lipid composition.....	51
2.3.6 LPS-induced rewiring of AM metabolism is critical for memory induction	53
2.3.7 LPS training modulates pneumonia outcome.....	53
2.4 Discussion	55
2.5 Materials and Methods	59
2.6 Supplementary Methods.....	62
2.7 Supplementary Figures	68
2.8 Supplementary Tables.....	76
Extended discussion	87
References.....	97
<i>Curriculum vitae</i>	113

List of Figures and Tables

Thesis figures

Thesis figure 1 - Innate defense strategies of the respiratory system.....	3
Thesis figure 2 - Ontogeny of tissue-resident macrophages.....	10
Thesis figure 3 - Alveolar macrophage development.....	11
Thesis figure 4 - Alveolar macrophage turnover in steady state and inflammation.....	13
Thesis figure 5 - Negative regulators of alveolar macrophage activity.....	16
Thesis figure 6 - Global leading causes of death	22
Thesis figure 7 - Immunological events during <i>S. pneumoniae</i> infection	25
Thesis figure 8 - Basic concepts of trained immunity.....	28
Thesis figure 9 - Schematic representation of innate adaptation programs.....	29
Thesis figure 10 - TLR4 signaling pathways	31
Thesis figure 11 - Metabolic regulation of trained immunity	33
Thesis figure 12 - Epigenetic regulation of trained immunity	34
Thesis figure 13 - Graphical abstract	94

Publication figures

Figure 1 - LPS exposure induces trained immunity in alveolar macrophages.	44
Figure 2 - LPS-induced AM training is driven by type 1 interferon signaling.....	46
Figure 3 - LPS-trained AMs display an altered gene expression profile upon <i>ex vivo</i> challenge.	48
Figure 4 - LPS exposure persistently alters the metabolic state and responsiveness of AMs.	50
Figure 5 - LPS-induced metabolic activation contributes to the establishment of AM memory.	52
Figure 6 - LPS exposure modulates pneumonia outcome in a context-dependent manner. 54	

Published supplementary figures

Figure S1 - FACS analysis of post-lavage lung tissue following LPS exposure.	68
Figure S2 - Analysis of AM cytokines, efferocytosis and turnover following <i>in vivo</i> LPS exposure.	69
Figure S3 - Cytokine analysis of HISP-challenged <i>Ifngr1^{-/-}</i> , <i>Rag2^{-/-}</i> and <i>Ifnar1^{-/-}</i> AMs six days after <i>in vivo</i> training.	70
Figure S4 - AM ATAC-seq analysis and inhibition of epigenetic enzymes during mexAM training.	71
Figure S5 - Maximum and spare respiratory capacity of AMs on day six after <i>in vivo</i> training.	72
Figure S6 - AM amino acids six days after <i>in vivo</i> training.	73
Figure S7 - Assessment of AM engraftment and post-infection FACS analysis after <i>in vivo</i> training.	74

Published supplementary tables

Table S1 - Differentially expressed genes identified in AMs six days after <i>in vivo</i> training. ...	76
Table S2 - Differentially expressed genes identified in HISP-challenged AMs six days after <i>in vivo</i> training.	77
Table S3 - Differentially accessible chromatin regions identified in AMs on day six after <i>in vivo</i> training.	82
Table S4a - Reagents, disposables and antibodies.	83
Table S4b - Flow cytometry antibodies.	86
Table S4c - Instruments.	86

Abstract

The development and functionality of our immune system is substantially influenced by microbial exposures. Such interactions may induce long-term changes in the functional program of innate immune cells, enhancing their responsiveness to secondary triggers. This phenomenon, referred to as trained immunity or innate memory, has revolutionised our understanding of the immunological memory, a process traditionally ascribed to adaptive immune cells. Trained immunity can be induced by a variety of microbial and non-microbial compounds, and has been described for multiple innate cell populations, including monocytes, macrophages and natural killer cells. Research of the past decade provided insights into the mechanistic regulation of trained immunity, demonstrating an important role of cellular metabolism and epigenetic remodelling processes. However, our knowledge about the tissue-specific characteristics and consequences of innate memory remains limited.

Alveolar macrophages (AMs), tissue-resident macrophages of the lungs, are continuously and directly exposed to inhaled environmental agents, which may reprogram AM function by establishing trained immunity. In this study, we investigated whether a ubiquitous microbial compound, lipopolysaccharide (LPS), has the potential to induce AM training in mice. We discovered that intranasal exposure to ambient concentrations of LPS established a robust AM memory response, which was characterized by increased cytokine production and phagocytosis upon subsequent challenge with *Streptococcus pneumoniae*, the major causative agent of bacterial pneumonia. Exploring the mechanistic basis of AM memory, we identified a critical role of type 1 interferon signaling and found that LPS-exposed (trained) AMs displayed an altered metabolite and lipid composition. Based on these observations, we assessed a potential role of metabolic reprogramming and demonstrated that inhibition of fatty acid oxidation and glutaminolysis significantly attenuated the training effect.

Finally, we assessed whether AM training can modulate the outcome of a subsequent pneumococcal infection and found that adoptive transfer of trained AMs, isolated from their tissue-specific context, led to increased lung inflammation and impaired bacterial clearance. In contrast, intranasal administration of LPS resulted in enhanced anti-pneumococcal resistance six days later, indicating that the local microenvironment plays an important role in determining the ultimate, physiological consequence of prior LPS exposure.

Collectively, our findings highlight the immunomodulatory impact of microbial encounters and reveal novel, tissue-specific aspects of AM memory.

Zusammenfassung

Unsere Lungen ermöglichen den lebensnotwendigen Austausch von Sauerstoff und Kohlendioxid – die Atmung. Im Zuge dieses Prozesses inhalieren wir eine Vielfalt an Umweltpartikeln und Mikroben, welche einen starken Einfluss auf die Entwicklung und Funktion unseres respiratorischen Immunsystems haben. Dies kann wiederum die Immunantwort auf zukünftig folgende Atemwegsinfektionen modulieren indem wir ein immunologisches Gedächtnis entwickeln. Während dieses Konzept klassischerweise den Zelltypen des adaptiven Immunsystems (T und B Zellen) zugeschrieben wurde, ist mittlerweile bekannt, dass auch Zellen des angeborenen Immunsystems (z.B. Monozyten und Makrophagen) ein Immungedächtnis entwickeln können. Dieser Prozess (im Englischen bekannt als „trained immunity“) wird durch eine primäre Stimulation mit mikrobiellen oder auch nicht-mikrobiellen Stoffen ausgelöst und führt zu einer erhöhten Immunantwort selbiger Zellen bei einer darauffolgenden (unspezifischen) Restimulation. Studien des letzten Jahrzehnts ermöglichten einen Einblick in die zugrunde liegenden Mechanismen von „trained immunity“ und konnten zeigen, dass diese komplexe epigenetische sowie metabolische Prozesse umfassen. Dennoch ist unser momentaner Wissensstand über die tatsächlich im Organismus (i.e. *in vivo*) stattfindenden mechanistischen Grundlagen und Konsequenzen des trainierten angeborenen Gedächtnisses limitiert.

Alveolarmakrophagen (AM), welche in den terminalen Lungenbläschen, den Alveolen, angesiedelt sind, sind aufgrund dieser einzigartigen Lage in ständigem Kontakt mit Stimuli und Partikeln aus der Umwelt. Dadurch besteht die Möglichkeit, dass ihre Immunantwort durch eine Etablierung von „trained immunity“ beeinflusst wird. Im Zuge dieser Studie wurde untersucht, ob ein allgegenwärtiger mikrobieller Bestandteil, Lipopolysaccharid (LPS), zur Entwicklung eines angeborenen Immungedächtnisses in AM führen kann. Wir konnten zeigen, dass AM von Mäusen, welche eine intranasale Behandlung mit LPS erhalten hatten, sechs Tage später eine erhöhte Reaktivität bei *ex vivo* Restimulation mit dem klinisch hochrelevanten Erreger *Streptococcus pneumoniae* aufwiesen. Dies zeichnete sich durch vermehrte Produktion wichtiger immunologischer Mediatoren, wie z.B. Interleukin (IL)-6 und IL-1 β , sowie erhöhte Phagozytose aus. Durch mechanistische Analysen konnten wir weiters ermitteln, dass Typ 1 Interferone, welche im Zuge der primären *in vivo* Stimulation mit LPS produziert werden, eine kritische Rolle in diesem Prozess spielen. Des Weiteren beobachteten wir Veränderungen in der zellulären Metabolit- und Lipid-Zusammensetzung trainierter AM und fanden heraus, dass zwei zentrale Stoffwechselwege, Glutaminolyse und Fettsäureoxidation, für die Etablierung der trainierten Immunantwort essentiell sind.

Mittels intratrachealer Transfer-Experimente konnten wir schließlich zeigen, dass isolierte, und demnach dem Gewebe-Kontext entnommene, LPS-trainierte AM den Verlauf einer folgenden Pneumokokken-Infektion negativ beeinflussen können. Im Gegensatz dazu führte intranasale Gabe von LPS zu einer verbesserten Bekämpfung der Folgeinfektion, was darauf hindeutet, dass der Gewebe-spezifische Kontext die tatsächliche, physiologische Auswirkung einer vorangehenden LPS-Exposition maßgeblich beeinflusst.

Im Gesamten konnten wir zeigen, dass mikrobielle Bestandteile, welchen wir im Zuge des täglichen Atmungsprozesses ausgesetzt sind, ein immunologisches Gedächtnis in Lungenmakrophagen auslösen können. Des Weiteren unterstreicht unsere Studie die mechanistischen Besonderheiten des AM Gedächtnisses, sowie die Notwendigkeit, die Folgen von „trained immunity“ unter Berücksichtigung Gewebe- und Krankheits-spezifischer Parameter zu untersuchen.

Publications arising from this thesis

Trained immunity of alveolar macrophages requires metabolic rewiring and type 1 interferon signaling (accepted for publication in *Mucosal Immunology*)

Sophie Zahalka, Philipp Starkl, Martin L. Watzenboeck, Asma Farhat, Mariem Radhouani, Florian Deckert, Anastasiya Hladik, Karin Lakovits, Felicitas Oberndorfer, Caroline Lassnig, Birgit Strobl, Kristaps Klavins, Mai Matsushita, David E. Sanin, Katarzyna M. Grzes, Edward J. Pearce, Anna-Dorothea Gorki* and Sylvia Knapp*.

* These authors contributed equally.

Abbreviations

AA-MP	alternatively activated macrophage
AEC	airway epithelial cell
AGM	aorta-gonad-mesonephros
AM	alveolar macrophage
AMP	antimicrobial peptide
AP-1	activator protein 1
ATAC	assay for transposase-accessible chromatin
ATP	adenosine triphosphate
BAL	bronchoalveolar lavage
BCG	Bacille Calmette-Guérin
BETi	bromodomain and extraterminal domain inhibitor
BPTES	bis-2-(5-phenylacetamido-1,3,4-thiadiazol-2-yl)ethyl sulfide
CAP	community-acquired pneumonia
CBP	choline-binding protein
CD200R	CD200 receptor
cDC	conventional dendritic cell
Cer	ceramide
CFU	colony forming unit
COPD	chronic obstructive pulmonary disease
CRP	C-reactive protein
CXCL	CXC motif ligand
DALY	disability-adjusted life-year
DAMP	danger-associated molecular pattern
DC	dendritic cell
DEG	differentially expressed gene
2-DG	2-deoxyglucose

ECAR	extracellular acidification rate
EMP	erythromyeloid progenitor
ERK	extracellular signal-regulated kinase
ETC	electron transport chain
EU	endotoxin unit
FAD	flavin adenine dinucleotide
FAO	fatty acid oxidation
FCCP	carbonyl cyanide p-trifluoromethoxyphenylhydrazone
FL-MO	fetal liver monocyte
Foxp3	forkhead box P3
GLUT1	glucose transporter 1
GM-CSF	granulocyte-macrophage colony-stimulating factor
GRO	growth-regulated oncogene
H3K27ac	histone 3 lysine 27 acetylation
H3K4me1	histone 3 lysine 4 monomethylation
H3K4me3	histone 3 lysine 4 trimethylation
HAP	hospital-acquired pneumonia
HAT	histone acetyl transferase
HDL	high density cholesterol
HIDS	hyper-IgD syndrome
HIF1 α	hypoxia-inducible factor 1 α
HISP	heat-inactivated <i>Streptococcus pneumoniae</i>
HSC	hematopoietic stem cell
IFN	interferon
Ifnar1	type 1 interferon receptor
Ifngr1	interferon γ receptor
IKK	I κ B kinase
IL	interleukin

ILC	innate lymphoid cell
IM	interstitial macrophage
iNOS	inducible nitric oxide synthase
IRAK	interleukin-1 receptor associated kinase
IRF	interferon regulatory factor
ISG	interferon-stimulated gene
ISGF3	interferon-stimulated gene factor 3
JAK	Janus kinase
JNK	JUN N-terminal kinase
KEGG	Kyoto Encyclopedia of Genes and Genomes
α -KG	α -ketoglutarate
LPS	lipopolysaccharide
LRTI	lower respiratory tract infection
<i>M. tuberculosis</i>	<i>Mycobacterium tuberculosis</i>
MAPK	mitogen-activated protein kinase
MARCO	macrophage receptor with collagenous structure
MCMV	murine cytomegalovirus
mexAM	murine <i>ex vivo</i> cultured alveolar macrophage
MHC	major histocompatibility complex
moAM	monocyte-derived AM
moDC	monocyte-derived DC
MOI	multiplicity of infection
MR-1	mannose receptor-1
MTA	5'-deoxy-5'-methylthioadenosine
mTOR	mammalian target of rapamycin
MyD88	myeloid differentiation primary response 88
NAD	nicotinamide adenine dinucleotide
NET	neutrophil extracellular trap

NF κ B	nuclear factor κ -light-chain-enhancer of activated B cells
NK cell	natural killer cell
NLR	NOD-like receptor
NLRP3	NLR family pyrin domain containing 3
NO	nitric oxide
NOD	nucleotide-binding oligomerization domain
OCR	oxygen consumption rate
oxLDL	oxidized low-density lipoprotein
OXPHOS	oxidative phosphorylation
PAMP	pathogen-associated molecular pattern
PAP	pulmonary alveolar proteinosis
PC	phosphatidylcholine
PCA	principal component analysis
PCV	pneumococcal conjugate vaccine
PE	phosphatidylethanolamine
PGE2	prostaglandin E2
PitA	pneumococcal iron transporter A
PPAR- γ	peroxisome proliferator-activated receptor γ
PPSV	pneumococcal polysaccharide vaccine
PRR	pattern recognition receptor
PspA	pneumococcal surface protein A
R/A	rotenone/antimycin A
RIG I	retinoic acid-inducible gene I
RNAi	RNA interference
ROS	reactive oxygen species
<i>S. pneumoniae</i>	<i>Streptococcus pneumoniae</i>
SAM	S-adenosyl-methionine
SAP	serum amyloid P

sCD14	soluble CD14
SCID	severe combined immunodeficiency
sIgA	secretory IgA
Siglec F	sialic acid-binding immunoglobulin-like lectin F
SIRP α	signal-regulatory protein α
SM	sphingomyelin
SOCS3	cytokine signaling 3
SP	surfactant protein
SRC	spare respiratory capacity
STAT	signal transducer and activator of transcription
TAG	triacylglyceride
TBK1	TANK binding kinase 1
TCA cycle	tricarboxylic acid cycle
TGF- β	transforming growth factor β
TIM	T cell immunoglobulin mucin receptor
TLR	Toll-like receptor
TNF	tumor necrosis factor
TR-AM	tissue-resident alveolar macrophage
TRAF	TNF receptor associated factor
TRAM	TRIF-related adapter molecule
T _{reg}	regulatory T cell
TREM	triggering receptor expressed on myeloid cells
TRIF	TIR domain-containing adaptor-inducing interferon- β
TRM	tissue-resident macrophage
TSLP	thymic stromal lymphopoietin
TYK2	tyrosine kinase 2
YS	yolk sac

Acknowledgements

The completion of my PhD studies would not have been possible without the kind and continuous support of many people, whom I would like to acknowledge on the following pages.

First and foremost, I want to express my sincere gratitude to my supervisor Sylvia Knapp for her excellent mentorship and guidance, her scientific input and personal advice, her sense of humor and her outstanding kindness. Thank you, Sylvia, for constantly believing in me, especially in times when I did not believe in myself. You are – and will always be – very important to me.

Being part of both, the CCHD and the CeMM PhD program, I considered myself very fortunate as it allowed me to interact with and learn from many talented and inspiring researchers. I am very thankful for the great times I shared with the fellow students of my year, who were wonderful colleagues and friends. I feel privileged to have worked in a truly unique research environment and would like to thank every single CeMM member for making my PhD an unforgettable experience. Thank you for the great administrative support, for the valuable input I received during my Friday Seminar presentations, and for your motivating and collaborative spirit! I am further thankful to the members of my thesis committee: Christoph Bock, Christoph Binder and Florentina Porsch. Thank you for your helpful feedback and advice!

I would like to thank all members of the Knapp group for making me feel at home in the lab. Thank you for your intellectual contributions during lab meetings and office chats, for your incredible experimental support, and for not only being my colleagues but also my cherished friends. Thea, Martin, Fede, Mariem, Asma, Lisa, Dorothea, Dörte, Henri, Mina, Alina, Lenka Florian M., Florian D., Riem, Stefanie and Philipp – you were the best lab mates one could imagine. You were the ones, who made me laugh, cheered for me and cheered me up. My office desk wall is decorated with handwritten motivation messages and little drawings that I received from many of you over the past couple of years. I will keep all of them and couldn't be more thankful to have worked with and amongst all of you. Special thanks go to Karin, Anastasiya and Nina, otherwise known as our lab angels. Thank you for your continuous help with experiments and administration, but also for being just the way you are – smart, funny, warmhearted and irreplaceable.

I am further particularly grateful to Thea, who co-supervised my project and supported me throughout my PhD studies, even when she no longer worked at our institute. You provided me with exactly the right amount of guidance that allowed me to think independently, learn from my mistakes and speak my own mind. On top of this, you were always able to calm my

anger and dry my tears, which is usually very difficult to achieve. Thank you for always being there for me!

Being part of the CCHD program I was granted with the opportunity to spend six months in the lab of Edward Pearce at the Max Planck Institute in Freiburg, where I met incredibly talented scientists and formed many new friendships. I would like to thank Ed and every member of his lab for this great experience!

During my PhD studies, I learned the enormous value of scientific collaborations and I am truly convinced that the completion of my PhD would not have been feasible without the substantial support and contributions of my co-authors. A sincere and heart-felt thank you to each and every one of you!

I further would like to thank my amazing family and friends, who never stopped believing in me. I know that it can be difficult to relate to and accept the “special” life style of a PhD student and I am very thankful for your concerns, your patience and your understanding.

Last but definitely not least, I would like to express my deepest gratitude to Philipp, the best scientist and boyfriend I know. I feel very blessed to have you in my life and I am beyond grateful for the numerous times you listened to my worries, encouraged me, built me up and made me not give up. Thank you for coping with me throughout these challenging times – and thank you for your unconditional love and support.

1

General introduction

The following introduction provides a detailed overview of the major topics related to our study “Trained immunity of alveolar macrophages requires metabolic rewiring and type 1 interferon signaling”, which is presented in the *Results* section (chapter 2) of this thesis. Introductory chapters are subdivided into four main parts and aim to summarize:

- I) the key mediators and mechanisms of pulmonary innate host defense.
- II) developmental aspects, cellular features and effector functions of alveolar macrophages in steady state and inflammation.
- III) epidemiological and immunological aspects of pneumococcal pneumonia.
- IV) general concepts and mechanisms of trained immunity.

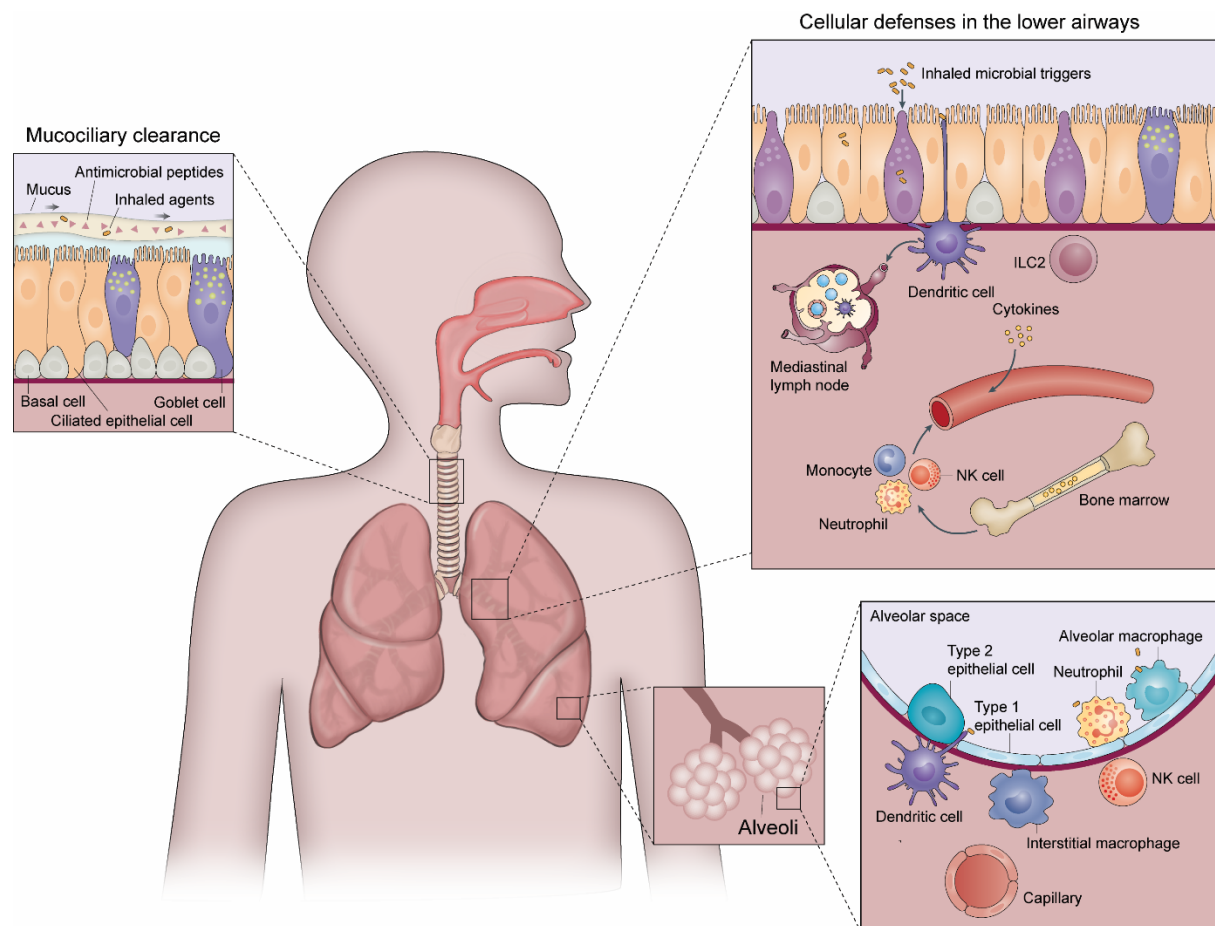
1.1 Innate immunity of the lungs

The respiratory system has evolved to facilitate gas exchange of oxygen and carbon dioxide between the external environment and our circulation. Fuelling this process, which occurs in the alveoli of the distal airways, our lungs are faced with 10.000 litres of inhaled air every day (Hartl *et al*, 2018). As such, they are continuously exposed to airborne environmental compounds and microbial triggers. While some of these agents may be innocuous, others can be toxic or harmful, posing an injurious threat to the host. To protect the airways from respiratory pathogens and other deleterious substances, the respiratory system has developed a complex and highly sophisticated immune system.

The first line of pulmonary immune defense comprises mechanical barriers, as well as cellular and humoral components, which predominantly belong to the innate part of the immune system (Nicod, 2005) (s. Thesis figure 1). These defense mechanisms act in concert to promote an effective immune response that follows a structured, step-wise program (Iwasaki *et al*, 2017). The upper and lower airways are protected by physical and anatomical factors that limit the deposition of inhaled particles (s. subsection “Physical and anatomical barriers”). Upon intrusion of infectious agents or foreign material, secreted innate immune proteins (s. subsection “Antimicrobial peptides”) recognize conserved microbial patterns via pattern recognition receptors (PRRs), providing immediate, non-specific defense (Weinberger *et al*, 2019). At the same time, airway epithelial cells (AECs), dendritic cells (DCs), and AMs act as the frontline of cellular innate defense (s. respective subsections) and initiate downstream immune responses to attract inflammatory cells to the bronchoalveolar and lung parenchymal compartments (Hartl *et al*, 2018). Additional cellular players of innate immunity include natural killer (NK) cells and innate lymphoid cells (ILCs) (Zhang *et al*, 2021b).

The recruitment of leukocytes into the pulmonary microenvironment is orchestrated by a variety of chemoattractants, including complement factors, lipid mediators and chemokines. The CXC family chemokines CXC motif ligand (CXCL) 1-8 and CXCL12, as well as the CC family chemokines CC chemokine ligand (CCL) 2, CCL17, CCL18 and CCL20 are particularly important for the recruitment of bone marrow-derived leukocytes. Additional cytokines, including interleukin (IL)-1 α , IL-1 β , IL-10, IL-17, IL-23, IL-25 and IL-33, assist in the orchestration of cellular trafficking and, together with the afore-mentioned factors, serve to induce a microenvironmentally tailored immune milieu (Hartl *et al*, 2018). During an acute inflammatory reaction, neutrophils are typically the first inflammatory cells to be recruited to the bronchoalveolar space. There, they promote pathogen clearance by a diversity of mechanisms, including phagocytosis and production of reactive oxygen radicals (Nicod, 2005). In the course of the inflammatory response, DCs process ingested antigens and migrate to the draining lymph nodes of the lungs in order to interact with naïve T-cells and

kick-start adaptive immunity (Weinberger *et al*, 2019). The complex interplay of cellular and non-cellular mechanisms shapes the immune response of our respiratory tract, and ultimately determines the outcome of infections, allergies and other forms of lung insult. In the following subchapters, important mediators of innate pulmonary defense will be discussed in more detail.



Thesis figure 1 - Innate defense strategies of the respiratory system

Inhaled antigens are trapped by physical and anatomical barriers of the respiratory tract. In the lower airways, invading pathogens are eliminated by cell-mediated immune processes that promote the influx of inflammatory cells, initiate adaptive immunity, and restore tissue homeostasis. *Adapted and modified from (Alon et al, 2021).*

Physical and anatomical barriers

During the process of respiration, the laminar air flow becomes more turbulent as it traverses the progressively branching airways of the respiratory system, enabling the deposition of inhaled particles at these locations. This allows for effective sequestration of particles with a diameter greater than 5 μm (Nicod, 2005). Smaller particles, however, can further intrude into the distal parenchyma of the lungs, where they are removed by two important processes:

cough and mucociliary transport. The latter refers to a process, during which coordinated ciliary beats of pulmonary epithelial cells move a “blanket” of mucus (as well as inhaled materials, trapped within) from distal to proximal airways (Nicod, 2005). The mucous film comprises an aqueous *sol layer*, located adjacent to surface epithelium, and a superficial, viscous *gel layer* (Weinberger *et al*, 2019). While mucus predominantly consists of water (Ohar *et al*, 2019), its physical properties are largely determined by heavily glycosylated proteins termed mucins, as well as by proteoglycans and phospholipids (Nicod, 2005). These components are produced by goblet cells and mucous glands and collectively provide optimal viscosity and elasticity (Puchelle *et al*, 1995) for trapping inhaled particles and microbes within the mucous layers.

Antimicrobial peptides

Antimicrobial peptides (AMPs) are central innate effector molecules, that display a wide range of antimicrobial and immunomodulatory activities. Recognising conserved pathogen-associated structures, they have the capacity to interfere with vital microbial processes, e.g. by inducing membrane lysis or impairing cell wall synthesis (Hiemstra *et al*, 2016). The main AMPs detected in lung tissue and secretions are listed below.

Lysozyme, a lytic enzyme that is present throughout the respiratory tract, causes bacterial cell death by cleaving the peptidoglycan moieties of their cell walls (Hiemstra *et al*, 2016). It is mainly produced by AECs, serous glandular cells and macrophages (Weinberger *et al*, 2019).

Lactoferrin is an iron binding glycoprotein found in airway fluid. It is synthesized by serous cells and neutrophils, and has the capacity to impair bacterial viability via the sequestration of iron. Furthermore, it promotes the agglutination of bacteria and enhances neutrophil effector functions (Weinberger *et al*, 2019).

Defensins are a family of small proteins that possess intrinsic microbicidal activity, which is exerted via permeabilization of microbial cell walls. The two important types of defensins found in the respiratory tract are α -defensins, produced by neutrophils, and β -defensins, produced by AECs. In addition to their lytic activity, defensins possess chemotactic properties, and thus are capable of promoting both innate and adaptive immune responses (Teclé *et al*, 2010).

Collectins are small cationic proteins that aggregate and opsonize microbes, facilitating recognition and clearance by phagocytic cells (Grubor *et al*, 2006). Lung collectins were originally identified as components of pulmonary surfactant (Haczku, 2008), a mixture of phospholipids and surfactant proteins (SPs) that facilitates respiration and gas exchange by reducing surface tension (Mirastschijski *et al*, 2020). SP-A and SP-D can directly interact with

macrophages to modulate their ability of phagocytosis and reactive oxygen species (ROS) production (Sano & Kuroki, 2005).

Airway epithelial cells

The airway epithelium is strategically located at the interface to the external environment, and thus represents the first line of cellular innate defense. Despite their classification as (non-immune) structural cell types, AECs actively contribute to the innate pulmonary immune response (Bals & Hiemstra, 2004). They are capable of sensing a variety of conserved microbe-derived compounds via different PRRs, including Toll-like receptors (TLRs), retinoic acid-inducible gene I (RIG-I)-like receptors, nucleotide-binding oligomerization domain (NOD)-like receptors (NLRs) and C-type lectin receptors (Hartl *et al*, 2018). Upon ligand binding, downstream signaling cascades induce changes in gene expression that increase AEC defenses by promoting the production of AMPs, cytokines and chemoattractants (Bals & Hiemstra, 2004). Apart from their central function in pulmonary host defense, AECs provide a physical mucosal barrier, which serves to protect the lungs from invasion of pathogens. Using mouse models of pneumococcal pneumonia and sterile acute lung injury, our group identified type 1 interferons (IFNs) as critical regulators of lung epithelial barrier integrity, as they selectively antagonized inflammation-induced cell obstruction of type II AECs, thereby limiting bacterial dissemination and tissue damage (Maier *et al*, 2016).

Monocytes and tissue-resident macrophages

Monocytes and macrophages are mononuclear phagocytes that play a central role in homeostasis and host defense. Human monocytes can be subdivided into classical (CD14⁺ CD16⁻) monocytes, non-classical patrolling (CD14^{low} CD16⁺) monocytes and (CD14⁺ CD16⁺) intermediate monocytes (Chiu & Bharat, 2016). Upon infection or injury, classical monocytes proliferate in the bone marrow and spleen, and are mobilized to the site of interest, where they perform key effector functions, including phagocytosis, release of chemokines and presentation of antigens in combination with major histocompatibility complex (MHC) II molecules. Furthermore, these cells are capable of differentiating into tissue-resident DCs and macrophages. (Chiu & Bharat, 2016).

Non-classical monocytes are known for their ability to crawl along the luminal side of the endothelium. They phagocytose injured endothelium and recruit neutrophils to the site of damage, which makes them important mediators of intraluminal surveillance (Carlin *et al*, 2013). In the lung, they can differentiate into CD11b⁺ CD103⁻ DCs (Jakubzick *et al*, 2008). Intermediate monocytes were reported to be involved in antigen processing/presentation and trans-endothelial migration, but are generally less well characterized (Kapellos *et al*, 2019).

Tissue-resident macrophages (TRMs) are distributed in different microanatomical niches of our body and are considered as immunological gate keepers of tissue integrity and homeostasis. Different TRM populations display heterogeneous, organ-specific phenotypes, which are strongly influenced by their developmental origin and local environment (Zhang *et al*, 2021a). The lungs harbour two main types of macrophages: AMs, which are located in the alveolar space, and interstitial macrophages (IMs), which reside in the parenchyma between the microvascular and alveolar epithelium (Hu & Christman, 2019). AMs constitute the first line of innate cellular host defense, and are critically involved in a variety of essential mucosal processes, including phagocytic clearance of inhaled pathogens and cellular debris, initiation and resolution of inflammation, and maintenance of tissue homeostasis (Hu & Christman, 2019). The unique developmental and biological aspects of AMs will be discussed in detail in chapter 1.2.

While IMs are less well characterized than AMs, they are well known for their capacity to spontaneously produce high amounts of the anti-inflammatory cytokine IL-10 (Sabatell *et al*, 2017), whereby they promote tissue homeostasis, and display moderate phagocytic activity (Schyns *et al*, 2018). Moreover, recent evidence suggests an important role of IMs in the prevention of allergic asthma via modulation of DC activity (Schyns *et al*, 2018). IMs were reported to have a dual origin. A subset of yolk sac-derived pre-macrophages was shown to seed the developing lungs around embryonic day E10.5 and persist as “primitive” IMs. During the first week of life, an additional wave of bone marrow-derived, “definitive” IMs populates the lung interstitium and continues to be maintained by circulating progenitors (Tan & Krasnow, 2016). In mice, two major IM populations have been described in a recent publication by Chakarov *et al*: Lyve-1^{low} MHC II^{high} IMs, which are located adjacent to neurons and specialized in antigen presentation, and Lyve-1^{high} MHC II^{low} IMs, which can be found in proximity to blood vessels and support tissue remodelling (Chakarov *et al*, 2019).

Neutrophils

Neutrophils represent the most abundant leukocyte population in human blood and play a pivotal role in innate host defense (Hartl *et al*, 2018). Patrolling in the circulation, they continuously search for potential injurious or inflammatory stimuli (e.g. pathogen- or danger-associated compounds, cytokines or chemoattractants), which induce their recruitment to peripheral sites. In addition to freely circulating neutrophils, a large fraction of these cells transits through distinct organs, forming so-called marginated (intravascular) pools within the bone marrow, spleen, liver and lungs (Summers *et al*, 2010). While the size of the pulmonary marginated granulocyte pool is currently under debate (Summers *et al*, 2010), it serves to rapidly recruit neutrophils to the site of injury or inflammation (Hartl *et al*, 2018).

In steady state, only a small proportion of neutrophils resides in the small airways and alveoli. Depending on the pathogen load, local innate defenses may either be sufficient to combat infectious invaders, or require additional recruitment of inflammatory neutrophils. This process is initiated via host-derived factors, including chemokines (e.g. IL-8, growth-regulated oncogene (GRO)- α , GRO- β), cytokines, complement factors and leukotriens, and/or pathogen-derived compounds, which enter the circulation and cause neutrophil stimulation and activation. The following extravasation into the tissue is a multi-step process that depends on the adhesive interactions between neutrophils and vascular endothelial cells and involves four major stages, i.e. (1) capture and rolling, (2) firm adhesion, (3) crawling and (4) transmigration (Lawrence *et al*, 2017). Upon their arrival in the inflamed airways, activated neutrophils employ a plethora of mechanisms in order to eliminate microbial agents. Major neutrophil effector functions include phagocytosis, the release of granule components (e.g. proteases, antimicrobial peptides, ROS) and the formation of neutrophil extracellular traps (NETs) (Kruger *et al*, 2015).

Dendritic cells

Lung DCs are located throughout the entire respiratory tract and can be subdivided into CD103⁺ conventional DCs (cDCs), CD11b^{high} cDCs and plasmacytoid DCs (pDCs) at steady state (Kim & Lee, 2014). Under inflammatory conditions, circulating CCR2^{high} monocytes can be additionally recruited to the lungs, where they upregulate MHCII and CD11c and differentiate into monocyte-derived DCs (moDCs) that can induce both T_{h1} and T_{h2} polarization (Chow *et al*, 2017). Being located in proximity to the respiratory epithelium, DCs continuously sample antigens from the local microenvironment by extending their dendrites through epithelial tight junctions (Condon *et al*, 2011). In addition to receptor-mediated antigen uptake, which is mostly mediated via C-type lectin- and Fc-receptors, full DC maturation requires the recognition of pathogen-associated molecular patterns (PAMPs) or endogenous danger-associated molecular patterns (DAMPs) and results in the upregulation of costimulatory molecules (Condon *et al*, 2011).

While pDCs control local immune responses and serve as an important source of type 1 IFNs (IFN- α and IFN- β) (Desch *et al*, 2013), cDCs can migrate to the draining lymph nodes, where they initiate T cell-mediated immune responses. CD103⁺ cDCs are specialized in antigen cross-presentation (i.e. presentation of exogenous, extracellular antigens via MHC I) and induction of cytotoxic CD8⁺ T cell immunity (Desch *et al*, 2011), whereas CD11b^{high} cDCs primarily prime CD4⁺ T_h cells via presentation of peptide-MHCII complexes (Beaty *et al*, 2007).

Innate lymphoid cells

The ILC family comprises five phenotypically distinct subsets (NK cells, ILC1, ILC2, ILC3 and lymphoid tissue-inducer cells), which originate from a common lymphoid progenitor and show transcriptional and functional parallels to the conventional T_h cell subsets (T_{h1}, T_{h2}, T_{h17}). In contrast to T cells, however, they lack clonally distributed, antigen-specific receptors and instead mediate unspecific, innate immune responses upon recognition of mucosal stress or danger signals (Borger *et al*, 2019).

The different subclasses are capable of antagonizing each other's functions and display remarkable cellular plasticity, allowing for an efficient adaptation to the requirements of the local microenvironment. The three prototypical ILC subsets (ILC1, ILC2, ILC3) play a role akin to their T_h cell counterparts, which is reflected by their expression of T-bet (ILC1), GATA-3 (ILC2) and retinoic acid-related orphan receptor (ROR) γ t (ILC3), while lymphoid tissue-inducer cells are involved in the development of secondary lymphoid organs (Borger *et al*, 2019). The ILC2 subset represents the dominant ILC population in steady-state mouse lungs (Yu *et al*, 2016). ILC2s maintain airway epithelial barrier integrity and lung tissue homeostasis through the release of IL-4, IL-5, IL-9, IL-13 and amphiregulin (Borger *et al*, 2019). Their activity is regulated by coordinated interactions with myeloid and epithelial cells, which reportedly promote ILC2 responses after influenza infection, allergen challenge and helminth exposure by producing IL-25, thymic stromal lymphopoietin (TSLP) and IL-33 (Borger *et al*, 2019). Investigating the homeostatic role of IL-33 in newborn mice, our group discovered that IL-33 production by type II AECs is increased shortly after birth, leading to the expansion and activation of lung ILC2s (Saluzzo *et al*, 2017). We could further show that ILC2-derived IL-13 induced an anti-inflammatory phenotype in AMs, which contributed to the quiescent state of homeostatic lungs, but caused a delay in the antibacterial defense against the respiratory pathogen *Streptococcus pneumoniae* (*S. pneumoniae*) (Saluzzo *et al*, 2017).

NK cells are cytotoxic lymphocytes that are specialized in eliminating virus-infected and malignantly transformed cells (Abel *et al*, 2018). Historically defined as cytolytic ILC1s, they have recently been categorized as a separate ILC population (Vivier *et al*, 2018). NK cells express a variety of activating receptors, which, upon recognition of "altered self" (e.g. cells displaying altered MHC expression), deliver activating signals to kill the infected/malignantly transformed cell, while inhibitory receptors prevent the elimination of uninfected/non-dysfunctional host cells. Stimulation of activating receptors is promoted by type 1 IFNs and selected macrophage- or DC-derived cytokines (e.g. IL-12, IL-18, tumor necrosis factor (TNF)), and causes the release of IFN- γ as well as direct killing of their targets via the expulsion of cytotoxic granules (Murphy & Weaver, 2016).

1.2 Alveolar macrophages – key players in lung homeostasis and host defense

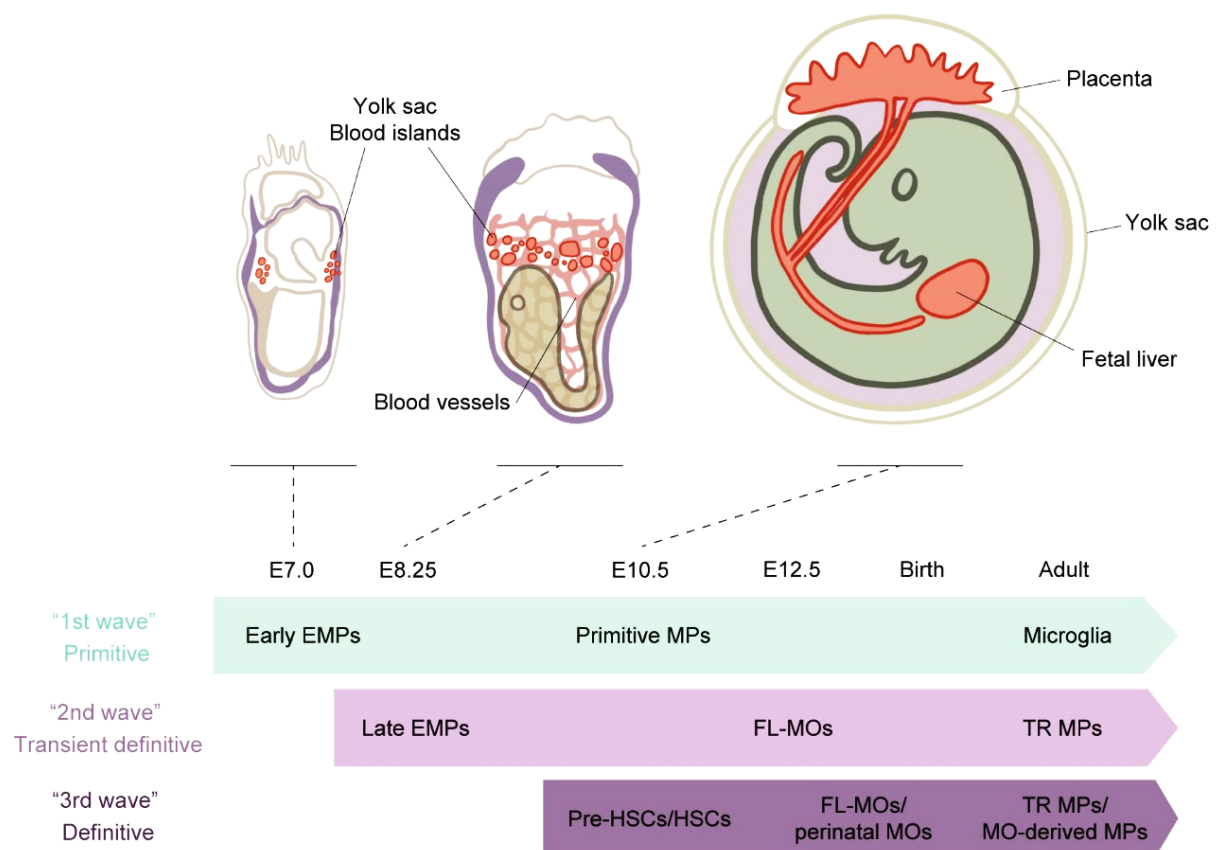
TRMs are central components of the innate immune system, which can be found in different anatomical locations of the human body. They exhibit a remarkable functional and phenotypic diversity, which is determined by their distinct origins and niche-specific microenvironments (Davies *et al*, 2013), and act as local immune sentinels that recognize and eliminate invading pathogens. In addition, they have been associated with a plethora of important biological processes, including tissue homeostasis, angiogenesis, iron processing, and resolution of inflammation (Wu & Hirschi, 2020).

AMs are TRMs of the lungs, which are located in the airspace of the alveoli, where they constitute the major cellular component (90-95%) at steady state (Kopf *et al*, 2015). Their phenotype, function and turnover is modulated by the unique microenvironment of the lungs, which includes intimate contact with respiratory epithelial cells, exposure to surfactant-rich fluids, high oxygen tension and low glucose availability (Baker & Baines, 2018; Hu & Christman, 2019). The following subchapters will provide detailed information on the developmental origin, cellular properties and key effector functions of AMs in steady state and inflammation.

1.2.1 Ontogeny and development

For several decades, it was believed that all TRM populations are derived from and continuously repopulated by circulating, bone marrow-derived monocytes. In the early 2000s, however, this dogma was challenged by a study demonstrating that Langerhans cells (macrophage-like cells of the epidermis) were only minimally depleted upon lethal irradiation, and repopulated independently of donor cells upon congenic bone marrow transplantation (Merad *et al*, 2002). Additional evidence for a monocyte-independent origin of distinct TRM populations came from experiments with parabiotic mice, which are surgically connected and thus share the same blood circulation, enabling continuous exchange of circulating precursor cells. These experiments revealed that certain TRM populations like Langerhans cells, microglia (i.e. the TRMs of the brain) and lung macrophages are not replenished by circulating precursors, whereas macrophages of the gut, dermis and heart were partially replaced by bone marrow-derived cells (Ginhoux & Guillemins, 2016). In 2013, a fate-mapping study by Yona *et al*. confirmed that major murine TRM populations, including lung, splenic, liver and peritoneal macrophages, arise prior to birth and are maintained independently of circulating monocytes throughout adulthood (Yona *et al*, 2013). While these models improved our understanding of macrophage ontogeny and constituted a conceptual breakthrough, mammalian embryonic hematopoiesis remains very complex and challenging to investigate.

Murine macrophages arise during three consecutive waves of hematopoiesis (Ginhoux & Guillems, 2016) (s. Thesis figure 2). The first wave (“primitive hematopoiesis”) occurs around E7 in the blood islands of the extra-embryonic yolk sac (YS) and generates early erythromyeloid progenitors (“early EMPs”). Characteristically, this process occurs independently of the transcription factor c-Myb (Ginhoux & Guillems, 2016) and gives rise to erythroblasts and megakaryocytes as well as primitive YS macrophages that develop without a monocyte intermediate stage. These primitive YS macrophages are trapped within the blood islands until the embryonic blood circulation is established (E8.5) and eventually seed every tissue of the body (E10.5). Around the same time, the second wave (“transient definitive hematopoiesis”) occurs in the hemogenic endothelium of the YS. This developmental pathway requires c-Myb expression and gives rise to “late EMPs” (Hoeffel & Ginhoux, 2018), which seed the fetal liver and establish a population of fetal liver monocytes (FL-MOs). FL-MOs subsequently infiltrate every tissue of the embryo (except the brain), and differentiate into most adult TRM populations, thereby replacing the initial pool of primitive YS macrophages (except microglia). The third wave (“definitive hematopoiesis”) starts around

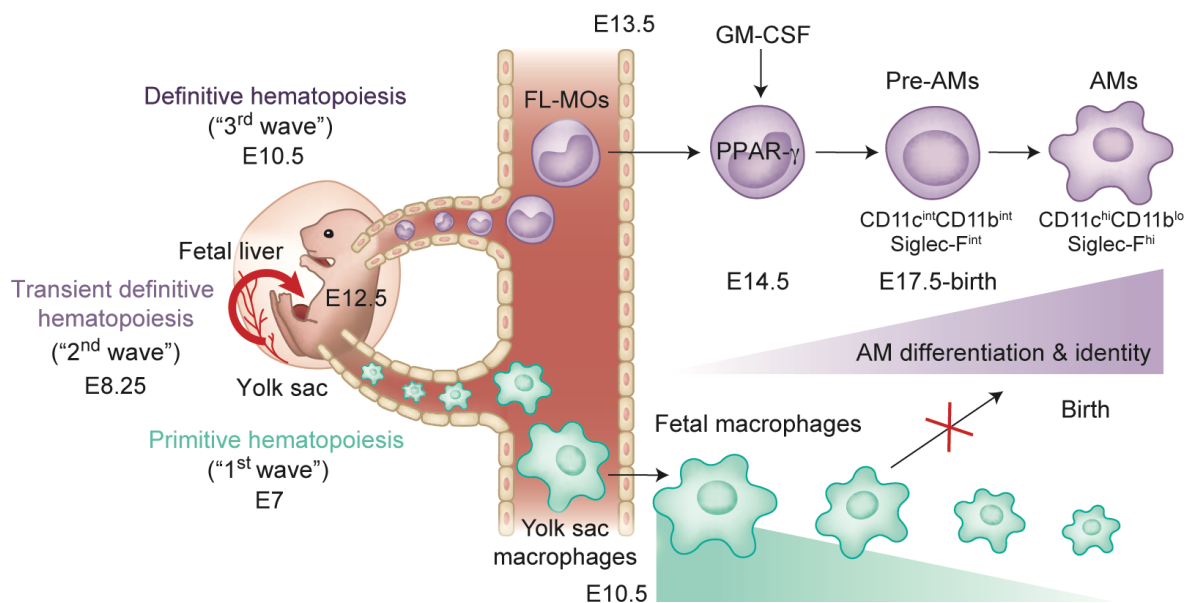


Thesis figure 2 - Ontogeny of tissue-resident macrophages

Macrophage development occurs in three consecutive ways. Created based on (Hoeffel & Ginhoux, 2018).

E10.5, as premature hematopoietic stem cells (HSCs) arise in the embryonic aorta-gonad-mesonephros (AGM) regions. These cells colonize the fetal liver, which becomes the main site of fetal hematopoiesis until gestation, and seed the bone marrow to generate a long-lived pool of HSCs (Wu & Hirschi, 2020). Importantly, fetal liver-derived HSCs can also differentiate into fetal monocytes that can give rise to a minor fraction of TRM populations in the perinatal period (Hoeffel & Ginhoux, 2018).

AMs predominantly originate from FL-MOs of the transient definitive wave, which colonize the lung rudiment around E13.5-14.5 (s. Thesis figure 3) (Ginhoux, 2014; van de Laar *et al*, 2016). Upon arrival in the premature lungs, these cells expand and start to differentiate into pre-AMs (detectable at E17.5), thereby superseding the pre-existing population of YS-derived primitive macrophages. This process is mediated by granulocyte-macrophage colony-stimulating factor (GM-CSF), mainly produced by type II AECs, which induces janus kinase (JAK) 2/signal transducer and activator of transcription (STAT) 5-mediated expression of the master transcription regulator peroxisome proliferator-activated receptor γ (PPAR- γ) (Ginhoux, 2014). In mice, local GM-CSF levels sharply increase with birth (Woo *et al*, 2021), promoting the development of mature AMs that are detectable around post-natal day 3 and characteristically express high levels of the surface markers CD11c and sialic acid-binding immunoglobulin-like lectin F (Siglec F) (Ginhoux, 2014).



Thesis figure 3 - Alveolar macrophage development

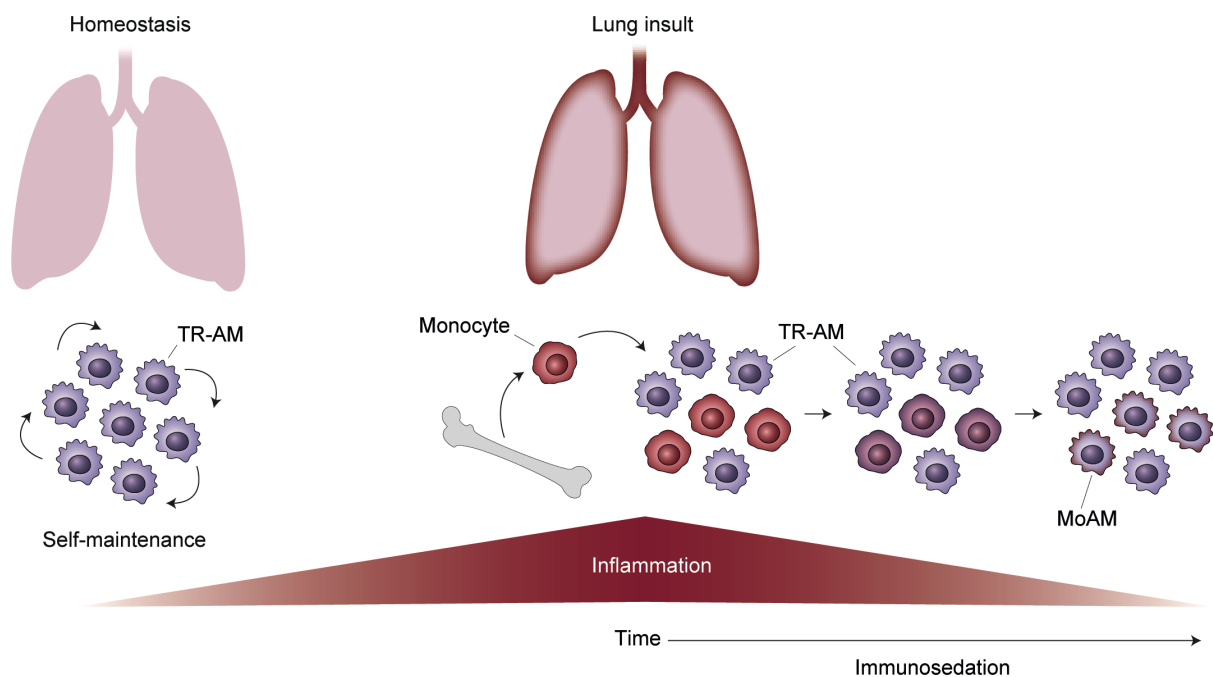
YS macrophages of the first wave seed the lungs around E10.5. FL-MOs, generated from late EMPs during the second wave of embryonic hematopoiesis, eventually replace the majority of these primitive macrophages around E13.5 and subsequently develop into pre-AMs and mature AMs under the influence of the lung environment. *Adapted and modified from (Ginhoux, 2014).*

CD11c, a cell adhesion receptor belonging to the leukointegrin family, binds a variety of ligands, including cellular adhesion molecules (e.g. ICAM1, ICAM2), complement fragments (e.g. iC3b) and matrix proteins, and has been associated with multiple immunological processes such as phagocytosis, cellular migration and cytokine production (Sadhu *et al*, 2007). Siglec F belongs to the family of sialic acid-recognizing lectins, whose biological role is largely unknown. While a critical role of Siglec F was reported for the resolution of lung eosinophilia in a mouse model of allergic asthma (Zhang *et al*, 2007), the function of Siglec F in AMs remains to be identified.

As previously mentioned, GM-CSF-induced PPAR- γ expression is critical to establish and maintain AM identity. In recent years, an additional mediator, transforming growth factor (TGF)- β , was identified to play an equally important role in AM development and self-maintenance (Yu *et al*, 2017). TGF- β activates PPAR- γ in a GM-CSF-independent, autocrine or paracrine manner (Woo *et al*, 2021). However, the exact molecular mechanisms of these processes remain to be investigated. Our group recently developed a novel AM culture model, which allows to expand and maintain murine *ex vivo* cultured AMs ("mexAMs") by providing a combination of GM-CSF, TGF- β and rosiglitazone, an antidiabetic drug which amplifies PPAR- γ signaling (Gorki *et al*, 2022). Continuous supply of these factors allowed for stable expression of primary AM surface markers as well as proper responsiveness to microbial ligands throughout culture. In addition, we could show that mexAMs are capable of engrafting the lungs of AM-depleted mice (Gorki *et al*, 2022).

Under homeostatic conditions, the local pool of AMs is repopulated via self-replenishment, with negligible input from inflammatory monocytes. Upon lung injury, however, the AM pool can get (partially) depleted, leading to the recruitment of bone marrow-derived monocytes, which accelerate the immune response and ultimately acquire a tissue-resident AM (TR-AM) profile. The dynamics of AM turnover and post-insult replenishment may be explained by the so-called niche model (Kulikauskaite & Wack, 2020): At steady state, the local AM niche is occupied by embryonically derived, resident AMs, thus denying access to circulating monocytes. In contrast, injurious insults such as influenza infection or irradiation may cause TR-AM depletion, rendering the niche temporarily available. Depending on the severity of depletion and the form of insult (e.g. type of infection/degree of damage), the empty niche may be replenished by *in situ* proliferation of TR-AMs (Hashimoto *et al*, 2013) and/or via recruitment of highly immunoreactive monocytes. The reactivity of monocyte-derived AMs (moAMs) is determined by the pulmonary environment, which ultimately confers an anti-inflammatory, „immunosedated“ phenotype to the recruited cells. The kinetics of this process depend on the inflammatory milieu as well as on the amount of time spent therein (s. Thesis figure 4).

In non-inflamed lungs, activating stimuli are largely absent, enabling a fast immunosedation of incoming cells, which is promoted by local exposure to colony stimulating factors, TGF- β , and tissue-specific concentrations of glucose or fatty acids (Kulikauskaite & Wack, 2020). In contrast, both pro- and anti-inflammatory stimuli are present following an inflammatory insult, resulting in a slower rate of sedation. Of note, recently recruited moAMs can modulate the outcome of asthma (Machiels *et al*, 2017), bacterial infections (Aegerter *et al*, 2020) or fibrosis (Misharin *et al*, 2017) as they display increased reactivity compared to TR-AMs.



Thesis figure 4 - Alveolar macrophage turnover in steady state and inflammation

Under homeostatic conditions, TR-AMs self-maintain locally with minimal contribution from incoming monocytes. Upon lung injury, the local TR-AM pool may be (partially) replenished by inflammatory monocytes. As they develop into moAMs, the local microenvironment imposes an immunosedated phenotype onto these cells.

In contrast to laboratory mice, which are typically housed under specific pathogen-free conditions, humans are continuously exposed to environmental particles and microbial triggers that potentially impact the functionality and replenishment of the AM pool. However, due to a lack of bona-fide markers and limitations in sampling/study methods, the origin and self-renewal capacity of human AMs remains largely unclear (Hou *et al*, 2021). Lung transplantation studies indicate that human AMs predominantly arise from recipient-derived hematopoietic precursors, implying an impaired self-renewal capacity under these conditions (Byrne *et al*, 2020; Nayak *et al*, 2016). This further suggests that human TR-AMs and moAMs

may co-exist throughout life. In a recent publication, Evren *et al.* offered important insights into the development and diversity of human macrophages (Evren *et al.*, 2021). Using a humanized mouse model that enables the reconstitution of a human blood monocyte and lung macrophage compartment upon transplantation of human CD34⁺ hematopoietic stem and progenitor cells, the authors could demonstrate that human CD14⁺ monocytes give rise to CD206⁺CD169⁺ TR-AMs and IMs. In addition, they identified a population of pulmonary intravascular macrophages, which originated from non-classical CD16⁺ monocytes (Evren *et al.*, 2021). Future research will be required to fully understand human AM turnover in homeostasis and disease.

1.2.2 AMs in homeostasis

The specialized microenvironment of the airspace prevents excessive inflammation in healthy individuals, which, in turn, impacts the function and phenotype of AMs (Hussell & Bell, 2014). Serving as gatekeepers of tissue integrity, AMs are responsible for efficient removal of apoptotic cells and cellular debris via a multi-step process termed efferocytosis (derived from the Latin term *effere*, “to take to the grave”) (Gheibi Hayat *et al.*, 2019). Apoptotic cells attract phagocytes via the release of soluble “find me”-signals, including modified membrane lipids (e.g. sphingosine 1-phosphate) or DAMPs (e.g. mitochondrial DNA, nucleotides or nuclear proteins). Subsequently, recognition of “eat-me”-signals enables recruited phagocytes to distinguish dead cells from their viable neighbors that bear “don’t eat-me”-signals (e.g. CD47, which binds to signal-regulatory protein α (SIRP α)) (Boada-Romero *et al.*, 2020). A primary signal exposed on apoptotic cells is the externalized expression of phosphatidylserines, which can interact with different phagocyte receptors, including T cell immunoglobulin mucin receptor (TIM)1, TIM4 and CD36. Additionally, signaling can occur via adaptor molecules (e.g. GAS6 or protein S), which enable indirect recognition of phosphatidylserines by phagocyte receptors (e.g. MerTK, Axl and Tyro3), or via interaction of calreticulin – CD91 interaction (Boada-Romero *et al.*, 2020). Following engulfment of apoptotic cells, GTPase-dependent actin remodelling processes result in the formation, maturation and trafficking of phagosomes, which ultimately fuse with lysosomes to degrade the apoptotic particles. This process promotes the secretion of anti-inflammatory mediators, including TGF- β and prostaglandin E2 (PGE2), which can suppress T cell activation (Roth & Golub, 1993) and thus contribute to the establishment of an overall immunosuppressive environment (Woo *et al.*, 2021).

Another important homeostatic task of AMs is the clearance and recycling of pulmonary surfactant, a functionality which is severely impaired in a rare disorder termed pulmonary alveolar proteinosis (PAP) (Hartl *et al.*, 2018). This condition is associated with defects in GM-CSF signaling, which, in the majority of cases, result from the development of anti-GM-CSF

autoantibodies (Carrington & Hershberger, 2022). In this context, we recently demonstrated that adoptive transfer of mexAMs restored impaired alveolar surfactant clearance in AM-deficient GM-CSFR^{-/-} mice, thus preventing the development of PAP (Gorki *et al*, 2022).

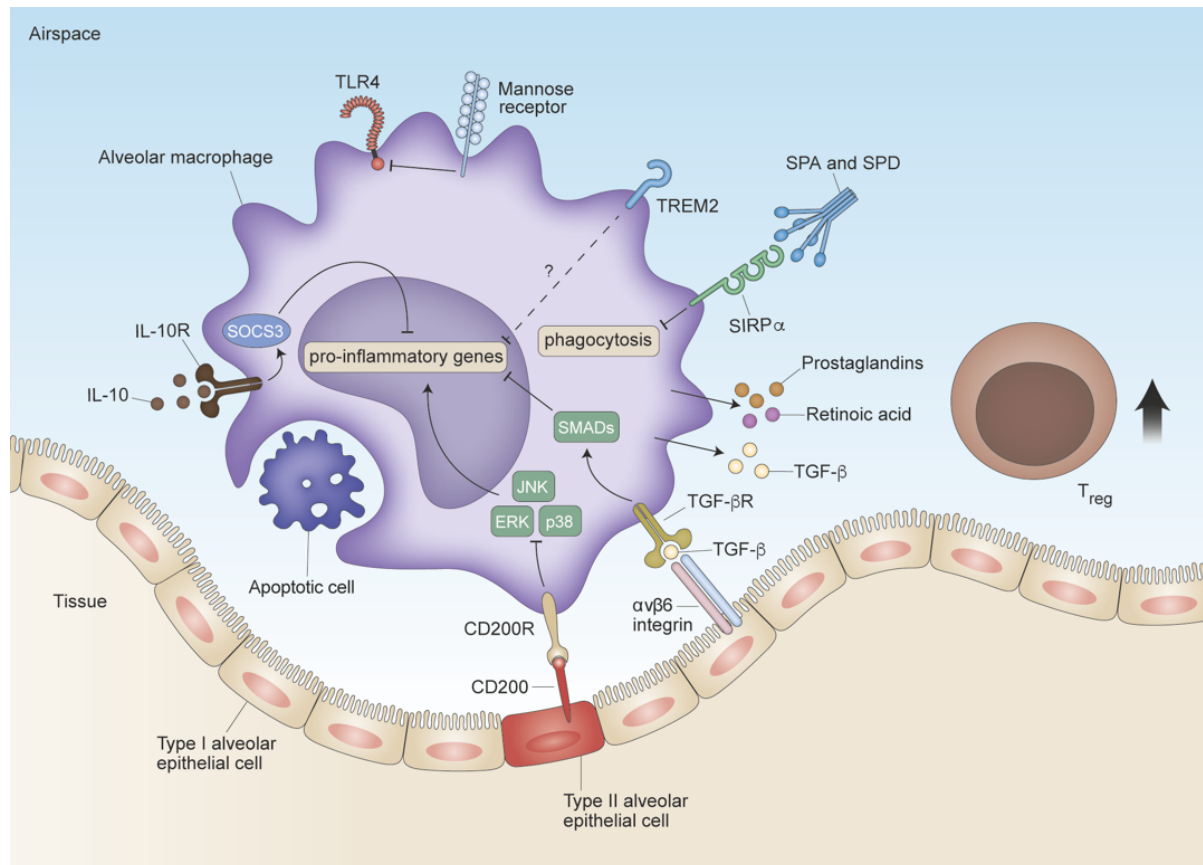
The immunosuppressive properties of AMs are further exemplified by their decreased phagocytic activity (compared to IMs), as well as their limited respiratory burst (Hussell & Bell, 2014). Despite their ability to transport antigens to the draining lymph nodes, AMs were reported to be poor at initiating antigen-specific T cell responses (Hussell & Bell, 2014). Their mediocre antigen presentation capacity, in combination with a lack of co-stimulatory molecule expression, was reported to promote T cell tolerance/unresponsiveness to innocuous antigens in humans (Blumenthal *et al*, 2001). Furthermore, AM-derived TGF- β and retinoic acid may promote the development of forkhead box P3 (Foxp3)⁺ regulatory T cells (T_{regs}).

AM activity is tightly controlled by cell-cell interactions and soluble mediators that create a regulatory microenvironment to limit undesired inflammation (s. Thesis figure 5). Exploring the cellular composition and interactions during murine development, we discovered that lung-resident basophils, educated by IL-33 and GM-CSF, critically regulated the maturation of AMs by imposing an anti-inflammatory, AM-specific identity on naïve developing macrophages (Cohen *et al*, 2018). In addition, we could show that selective depletion of basophils impaired the functionality of mature AMs, which was illustrated by a decreased phagocytic capacity (Cohen *et al*, 2018).

Compared to IMs and other TRMs, AMs express high levels of inhibitory molecules, including the CD200 receptor (CD200R). Binding of its ligand CD200, a transmembrane protein expressed by bronchial epithelial cells and type II AECs, inhibits activation of the pro-inflammatory extracellular signal-regulated kinase (ERK), JUN N-terminal kinase (JNK) and p38 mitogen-activated protein kinase (MAPK) pathways, thus limiting inflammatory AM responses (Hussell & Bell, 2014). In addition, type II AECs express various mannose receptor ligands, which are recognized by AM mannose receptors and block the recognition of TLR4 ligands (Woo *et al*, 2021). AM activity is further dampened by epithelial cell-derived IL-10, which, upon binding to the IL10 receptor, induces expression of cytokine signaling 3 (SOCS3), a negative regulator of pro-inflammatory cytokine production (Hussell & Bell, 2014). Apart from IL-10, TGF- β is abundantly expressed in mouse and human lungs (Coker *et al*, 1996) and its effects on AM biology can be exerted in an autocrine or paracrine manner. Tethered to the lung epithelium via α v β 6 integrin, it can interact with the TGF- β receptor (a heterodimer of TGF β R1 and TGF β R2 subunits) and regulate AM responses by SMAD-dependent and -independent processes (Hussell & Bell, 2014). Of note, the downstream consequences of TGF- β signalling are partly dictated by the expression level of the TGF β R2 subunit (Rojas

et al, 2009). Additional regulatory molecules expressed by AMs include SIRP α , which suppresses AM-mediated phagocytosis upon binding of surfactant-associated proteins, and triggering receptor expressed on myeloid cells (TREM)-2 (Hussell & Bell, 2014).

TREM proteins serve as important regulators of innate and adaptive immunity, with opposing functions reported for TREM-1, which is considered to amplify cellular immune responses, and TREM-2, a negative regulator of immune cell activation and inflammation (Sharif & Knapp, 2008). Dissecting the role of TREM-2 *in vivo*, our group could show that lack of endogenous TREM-2 led to augmented early inflammation and impaired phagocytosis during Gram-negative infection and LPS-induced sepsis (Gawish *et al*, 2015). In addition, we discovered that TREM-2, expressed on AMs, selectively suppressed the production of the complement component C1q, resulting in impaired phagocytosis and bacterial clearance during pneumococcal pneumonia (Sharif *et al*, 2014). In line with these findings, we could demonstrate a beneficial impact of TREM-1 in this infection model, as its engagement by an agonistic TREM-1 antibody accelerated bacterial elimination and significantly improved survival (Lagler *et al*, 2009).



Thesis figure 5 - Negative regulators of alveolar macrophage activity

AMs are restricted via cell-cell interactions and soluble mediators to prevent excessive lung inflammation at steady state. Adapted and modified from (Hussell & Bell, 2014).

1.2.3 AM polarization

The previous chapters highlighted that the identity of AMs is dictated by their developmental origin and immunosuppressive microenvironment. However, they need to exert a considerable amount of plasticity in order to fulfill the requirements of both homeostatic and diseased lungs. As such, they carry out disparate functions that preserve tissue integrity while enabling efficient anti-microbial immunity.

The ability of TRMs to exhibit different functional activation states has led to their classification as M1 (classically activated) versus M2 (alternatively activated) macrophages (Hussell & Bell, 2014). The origin of these terms dates back to the 1960s, when Mackaness first proposed the term “macrophage activation” to describe the enhanced antimicrobial activity of macrophages following primary bacterial stimulation (Mackaness, 1962), a phenomenon which was later linked to IFN- γ and T_{h1} immune responses (Nathan *et al*, 1983). In 1992, Stein, Doyle and colleagues discovered that the T_{h2} cytokines IL-4 and IL-13 induced a so-called alternative macrophage activation phenotype, which was distinct from IFN- γ induced (classical) activation (Doyle *et al*, 1994; Stein *et al*, 1992). A few years later, the traditional M1/M2 nomenclature was coined by Mills and colleagues, who revealed important metabolic differences between macrophages activated in mouse strains with T_{h1} versus T_{h2} background (Mills *et al*, 2000). These studies have collectively established the basic principles of macrophage polarization, which are summarized below.

Exposure to IFN- γ (a cytokine associated with T_{h1} immunity) and bacterial LPS promotes killing of intracellular pathogens, tumor resistance and secretion of pro-inflammatory mediators (e.g. IL-6, TNF, IL-1 β and IL-12) (Murray *et al*, 2014). In addition, M1 macrophages are known for their potent ability to produce nitric oxide (NO) due to increased expression of inducible nitric oxide synthase (iNOS) (Martinez & Gordon, 2014). M2 polarization, on the other hand, is driven by the T_{h2} cytokines IL-4 and IL-13 (Murray *et al*, 2014). M2 macrophages, also commonly referred to as “alternatively activated macrophages” (AA-MPs), produce increased amounts of anti-inflammatory mediators (e.g. IL-10), show an upregulation of mannose and scavenger receptors (Wang *et al*, 2014), and promote tissue repair as well as parasite containment (Martinez & Gordon, 2014). They characteristically express PPAR- γ and arginase-1 (encoded by the gene Arg1), which mediates the conversion of L-arginine into L-ornithine within the urea cycle (Briken & Mosser, 2011) and thus enhances cellular levels of ornithine and polyamines.

In recent years, the concept and nomenclature of macrophage polarization has been expanded in order to account for the diversity of activation scenarios, which are likely caused by differences in experimental conditions and stimuli. Mantovani and colleagues proposed an

extension to the classical M1/M2 concept, in which M1 polarization is induced by IFN- γ in combination with bacterial LPS or TNF, while M2 polarization is induced by IL-4/IL-13 (M2a polarization) but may also be elicited by immune complexes and TLR ligands (M2b polarization) or by IL10 and glucocorticoids (M2c polarization) (Mantovani *et al*, 2004). In order to counter-balance this increasing complexity, the macrophage field has come to the (partial) consensus that macrophage activation should be considered as a broad “spectrum” rather than specific activation states, with M1 and M2 representing the extreme edges of this dynamic spectrum (Murray, 2017).

Studies investigating the polarization states of mouse and human AMs are sparse and were mostly performed in inflammatory settings or upon *ex vivo* stimulation with recombinant cytokines. In mice, AMs constitutively express high levels of the classical M2 marker mannose receptor-1 (MR-1; also known as CD206), which can recognize unopsonized pathogens, resulting in the suppression of pro-inflammatory AM responses. Additionally, they display reduced phagocytic and respiratory burst activity compared to other TRM populations, further indicating a tendency for M2 polarization of murine AMs in homeostatic conditions. In humans, there are conflicting reports about the activation status of AMs. While some studies identified a minor proportion of M2-like AMs in the absence of disease (Kim *et al*, 2008; Shaykhiev *et al*, 2009), others have observed up to 50% of CD206⁺ AMs in human bronchoalveolar lavage (BAL) fluid (Melgert *et al*, 2011; Pechkovsky *et al*, 2010). A more recent publication investigating the polarization phenotypes of AMs in healthy lungs and upon development of smoking-induced chronic obstructive pulmonary disease (COPD) found the majority of AMs to display an M0 (iNOS⁻ CD206⁻) phenotype at steady-state, whereas M1 (iNOS⁺ CD206⁻) and M2 (iNOS⁻ CD206⁺) marker expression progressively increased with COPD severity (Bazzan *et al*, 2017). These opposing observations altogether indicate that there is no general consensus about the polarization state of human AMs in homeostasis.

However, increased M2 characteristics of both mouse and human AMs have been described in pathological settings, including asthma and fibrosis (Hussell & Bell, 2014). While asthma development and severity reportedly correlate with increased AA-MP numbers in mice (Melgert *et al*, 2010) and humans (Melgert *et al*, 2011), their functional contribution to the pathogenesis of asthma remains controversial (Abdelaziz *et al*, 2020). In 2010, Melgert *et al*. demonstrated that adoptive transfer of AA-MPs resulted in increased DC migration, elevated effector T cell numbers, and aggravated allergic airway inflammation in mice, indicating a direct impact on asthma development (Melgert *et al*, 2010). In contrast, a study by Nieuwenhuizen *et al*. showed that genetic ablation of macrophage IL-4R α expression did not affect the pathology of asthma, suggesting that increased AA-MPs may be a mere association to increased T_{H2} immunity (Nieuwenhuizen *et al*, 2012).

TRMs and inflammatory monocytes have been identified as key regulators of tissue regeneration and fibrosis, a disease characterized by excessive, aberrant wound healing following lung insult (Wynn & Vannella, 2016). During the (pre-fibrotic) lung injury phase, recruited moAMs display an M1 phenotype and promote myofibroblast proliferation and fibrocyte recruitment via the release of pro-inflammatory mediators. While this represents the starting point of the pro-fibrotic process, M1 macrophages have also been associated with an anti-fibrotic effect due to their release of metalloproteinases that degrade the extracellular matrix (Wynn & Vannella, 2016). Following the acute phase, macrophage M2 polarization is promoted by increased production of T_{H2} cytokines and phagocytosis of apoptotic cells. These M2 macrophages are intended to promote tissue repair and create an anti-inflammatory environment. However, if lesions persist, they take on a pro-fibrotic role and secrete large amounts of pro-fibrotic factors such as TGF- β and Galectin-3, ultimately promoting disease progression (Zhang *et al*, 2018). Therefore, modulation of lung macrophage polarization represents a central axis in the exacerbation and control of pulmonary fibrosis.

1.2.4 AM metabolism

Cellular metabolism comprises anabolic processes, which consume energy to synthesize cellular structures, and catabolic processes, which degrade nutrients to promote energy production. In brief, tissue fuels (e.g. glucose, lipids or amino acids) are converted into metabolites (e.g. pyruvate, tricarboxylic acid (TCA) cycle intermediates or free fatty acids), which are either used for the production of cellular building blocks, get fully oxidized, or are released to prevent toxicity (e.g. lactate, excess cholesterol) (Wculek *et al*, 2022).

The metabolic state of TRMs facilitates their tissue-specific functions and is strongly influenced by the availability of nutrients and metabolites. Being located in a lipid-rich environment, AMs are specialized in lipid catabolism and trafficking, which enables efficient clearance of pulmonary surfactant (mainly consisting of phospholipids and cholesterol (Fessler & Summer, 2016)) (Wculek *et al*, 2022). These metabolic features are critical for AM identity, which is illustrated by the fact that loss of PPAR- γ , a potent regulator of lipid metabolism, alters AM-specific transcriptional and phenotypic features (Schneider *et al*, 2014b). While AMs utilize glucose, glutamine, pyruvate or fatty acids to maintain a high basal respiration, they display an impaired glycolytic metabolism and thus do not rely on glycolysis to meet their metabolic demands (Wculek *et al*, 2022). Accordingly, transcriptional analysis of *Mycobacterium tuberculosis* (*M. tuberculosis*)-infected murine AMs revealed increased expression of genes related to oxidative phosphorylation (OXPHOS), fatty acid metabolism, and cholesterol homeostasis, while IMs additionally expressed glycolysis-related genes (Huang *et al*, 2018).

However, it needs to be indicated that the metabolic profile of lung macrophages may be modulated in different disease settings.

1.2.5 The role of AMs in antimicrobial defense

As a result of their strategic location, AMs act as important sentinels of the lower airways that play a fundamental role in innate host defense against respiratory pathogens (Schneider *et al*, 2014a). Their ability to switch from an immuno-sedated house-keeping function to a pro-inflammatory, antimicrobial program requires a tightly balanced act of activation that overrides the local inhibitory mechanisms governing AM biology. This process is believed to be facilitated by loss of regulatory ligands due to damage of airway epithelial cells as well as by sensing of necrotic target cells, which liberates a pro-inflammatory program in AMs (Hussell & Bell, 2014). Another crucial factor determining the threshold of AM activation is the ability to sense microbe-derived products via multi-receptor signaling. In addition to C-type lectin receptors, nucleotide-binding oligomerization domain (NOD)-like receptors and scavenger receptors, AMs express a diversity of TLRs, including TLR2, TLR4, TLR5 and TLR9, which sense bacterial lipoteichoic acid, LPS, flagellin or unmethylated CpG DNA respectively. The binding of such ligands is followed by specific intracellular signaling cascades that result in the production of pro-inflammatory cytokines and type 1 IFNs (El-Zayat *et al*, 2019). TLR signaling classically includes two distinct pathways: the myeloid differentiation primary response 88 (MyD88)-dependent pathway, which is common to all TLRs except TLR3 and leads to production of pro-inflammatory cytokines, and the TIR domain-containing adaptor-inducing interferon- β (TRIF)-dependent pathway, which is characteristic for TLR3 and TLR4 and associated with induction of type 1 IFNs. Additionally, stimulation of TLR2, TLR4 or TLR9 reportedly inhibits IL-10R signaling and thereby counteracts the suppressive effects of epithelial cell-derived IL-10 (Fernandez *et al*, 2004). Similarly, T cell-mediated inhibition of AM responses are overcome by locally produced inflammatory cytokines, such as GM-CSF and TNF (Hussell & Bell, 2014). Furthermore, recent evidence suggests that NETs can modulate the inflammatory potential of AMs by promoting M1-like polarization in a model of LPS-induced acute lung injury, thus aggravating tissue damage (Song *et al*, 2019).

Once activated, AMs shape local immunity by phagocytosis, production of ROS or NO, and via release of pro-inflammatory cytokines (e.g. TNF- α , IL-6, IL-12, IL-1 β) and chemokines (e.g. IL-8, MCP-1) that attract circulating neutrophils and monocytes (Aberdein *et al*, 2013). AM-mediated initiation and augmentation of the early inflammatory response was shown to be critical for efficient clearance of bacterial pathogens (e.g. *Streptococcus pneumoniae*). Moreover, during pulmonary viral infections, AMs are the main cellular source of type 1 IFNs,

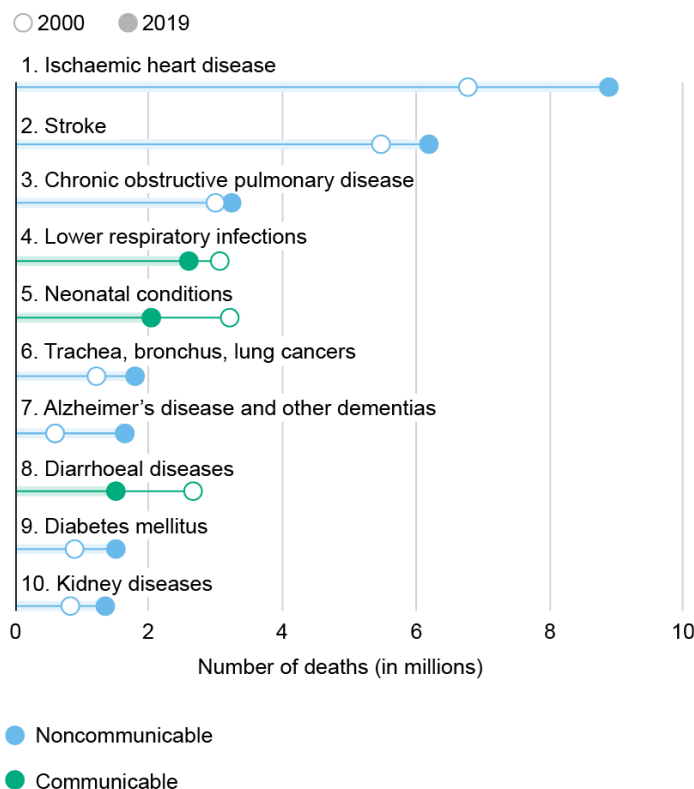
which can act in an autocrine or paracrine fashion. As such, they promote the induction of IFN-stimulated antiviral genes, restricting viral dissemination (Divangahi *et al*, 2015).

Apart from their important role in early host defense, AMs serve to limit tissue damage and resolve inflammation during the resolution phase of infections. AM-mediated efferocytosis (described in chapter 1.2.2) prevents the release of pro-inflammatory or toxic contents into the mucosal microenvironment, and triggers the production of pro-resolving factors, including TGF- β - a potent suppressor of T_{H1} cell differentiation (Travis & Sheppard, 2014) - and PGE₂, which was shown to suppress NK cell activity and decrease DC-mediated antigen presentation (Allard *et al*, 2018). While tissue damage control is critical for the restoration of homeostasis, it needs to be noted that dampened host immunity can create a permissive niche for many intracellular bacteria. Notably, *M. tuberculosis* was reported to actively promote M2 polarization of infected macrophages while dampening the production of ROS, thereby facilitating bacterial survival (Rajaram *et al*, 2010).

1.3 Pneumococcal pneumonia

1.3.1 Epidemiology of lower respiratory tract infections

While global health, measured by age-standardized disability-adjusted life-year (DALY) rates, has steadily improved over the past thirty years (Diseases & Injuries, 2020), infectious respiratory diseases continue to present a major global health concern. The twenty-first century has faced a wave of severe disease outbreaks, including the severe acute respiratory coronavirus outbreak (2003), the Ebola virus disease epidemic in West Africa (2013-2016), the Zika virus disease epidemic (2015) and the recent COVID-19 pandemic, leading to a substantial increase in morbidity and mortality around the globe (Baker *et al*, 2022). According to the Global Burden of Disease Study 2019, lower respiratory tract infections (LRTIs) affected 489 million people globally (Diseases & Injuries, 2020), thus remaining a leading cause of death worldwide (s. Thesis figure 6). LRTIs include pneumonia, bronchitis and bronchiolitis (among other infections of the airways or alveoli) and can be caused by a variety of bacteria, viruses, fungi and parasites (Noviello & Huang, 2019).



Thesis figure 6 - Global leading causes of death

In 2019, 7 out of 10 leading global causes of death were non-communicable diseases, accounting for 44% of all deaths or 80% of the top ten depicted death causes. The major cause of death, ischaemic heart disease, was responsible for 16% of the world's total deaths in 2019. Stroke and chronic obstructive pulmonary diseases accounted for approximately 11% and 6% of total deaths, respectively. LRTIs ranked as the 4th leading cause of death, remaining the world's most deadly communicable disease (WHO, 2020, December 9).

Communicable diseases are caused by a pathogenic agent, whereas non-communicable diseases (also known as chronic diseases) arise from a combination of genetic, physiological, behavioral and environmental factors. Source: (WHO, 2020, December 9).

Pneumonia, a common acute respiratory infection of the alveoli and distal bronchial trees, is a predominant infectious cause of death in immunocompromised people, such as children

under 5 years of age and the elderly (Torres *et al*, 2021). The disease is broadly classified into community-acquired pneumonia (CAP, most common) and hospital-acquired pneumonia (HAP, including ventilation-associated pneumonia). In Europe, the annual incidence of CAP was estimated to range from 1.07–1.2 incidents per 1000 people, with up to 14 cases per 1000 individuals reported for adults over 65 years of age (Torres *et al*, 2013). *S. pneumoniae* is a major causative agent of bacterial CAP and a leading cause of various other infectious diseases (Weiser *et al*, 2018). The following chapters provide a concise overview of *S. pneumoniae*-related pathology and host immunity, as well as current treatment options for pneumococcal pneumonia.

1.3.2 *Streptococcus pneumoniae* virulence factors

S. pneumoniae is a Gram-positive, opportunistic commensal, which colonizes the mucosal surface of the human nasopharynx (upper respiratory tract). Upon local spread and migration to sterile tissues, however, it may cause invasive diseases, such as pneumonia, otitis media, sepsis and meningitis (Weiser *et al*, 2018). Pneumococcal dissemination is promoted by the production of various virulence factors, which hinder the host's defense mechanisms and prevent bacterial clearance. *S. pneumoniae*'s extracellular polysaccharide capsule effectively promotes adherence while preventing recognition by complement factors, host receptors, NETs and phagocytes (Brooks & Mias, 2018). These effects are amplified by pneumococcal surface proteins, including choline-binding proteins (CBPs; e.g. pneumococcal surface protein A (PspA)) and lipoproteins (e.g. pneumococcal iron transporter A (PitA)), which prevent *S. pneumoniae* opsonization, and transport substrates across membranes, respectively (Weiser *et al*, 2018). Moreover, pneumococci produce pore-forming toxins, such as pneumolysin (which induces host cell lysis and DNA damage) and autolysins (which lead to bacterial autolysis, thereby promoting release of cell wall- and cytoplasmic components; e.g. LytA). Other important virulence factors include pili, biofilms and IgA1 protease, an enzyme capable of cleaving the human immunoglobulin isotype IgA1, thus hindering antibody-mediated bacterial clearance (Brooks & Mias, 2018).

1.3.3 Host immune response to *Streptococcus pneumoniae*

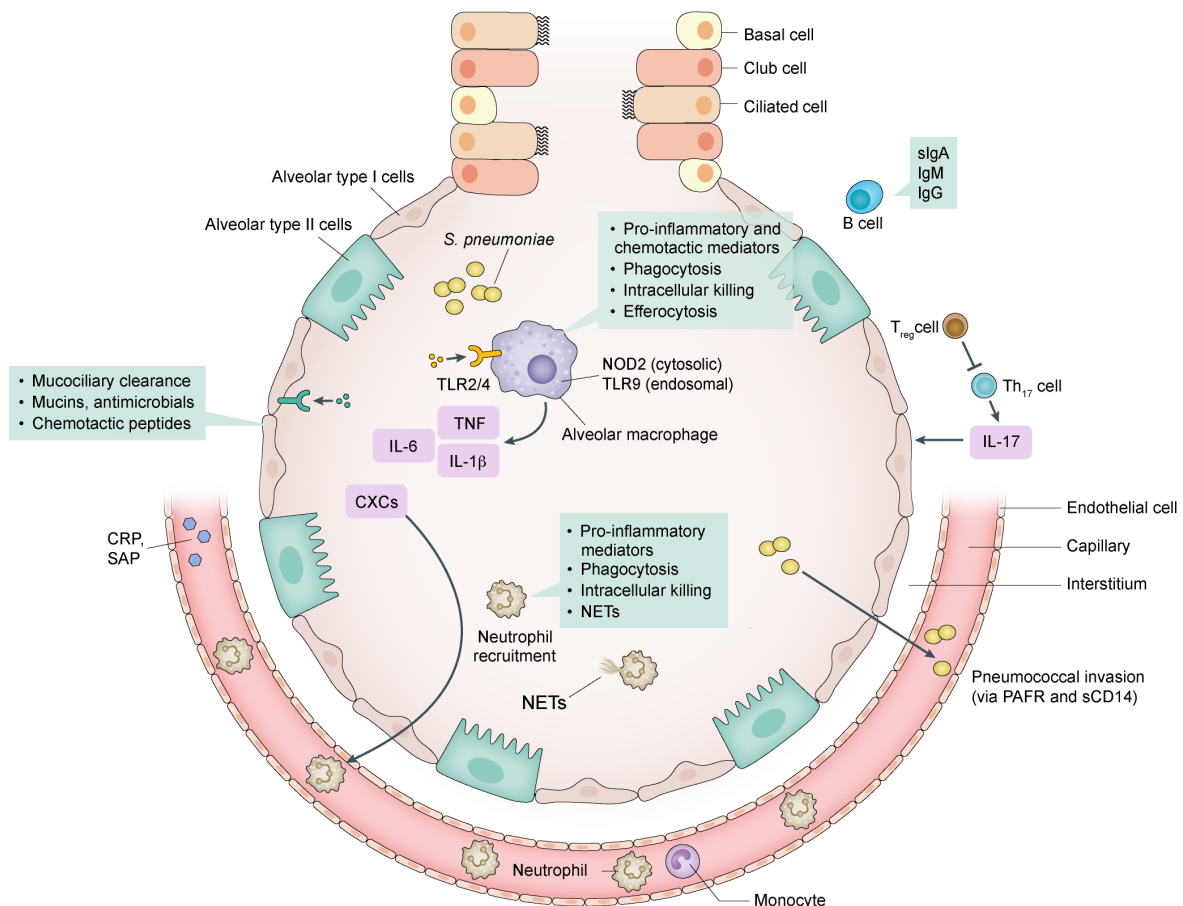
Anti-pneumococcal immunity involves a variety of innate and adaptive defense strategies (s. Thesis figure 7). Respiratory epithelial cells play a prominent role during the early phase of infection as they continuously perform mucocilliary clearance and can directly eliminate invading pneumococci via production of AMPs (discussed in chapter 1.1). Within the alveoli, AMs act as the first line of innate host defense and can eliminate small infectious doses through phagocytosis-mediated killing. While opsonized microbial particles can be engulfed

via complement- and Fc γ -receptor-mediated endocytosis, AMs can sense non-opsonized particles (e.g. polyanions, low density lipoproteins) with the aid of surface receptors, e.g. the macrophage receptor with collagenous structure (MARCO) (Brooks & Mias, 2018). Recognition of *S. pneumoniae* is mediated via PRRs, which bind pneumococcal ligands and kickstart anti-bacterial immune responses. In 2004, we could show that TLR2, an important sensor of major Gram-positive cell wall components (e.g. peptidoglycan and lipoproteins), is critically required for AM-mediated sensing of *S. pneumoniae* (Knapp *et al*, 2004). However, while TLR2 contributed to the early inflammatory response established upon pneumococcal infection, it did not influence the overall outcome of pneumonia (Knapp *et al*, 2004), suggesting a requirement for additional microbial sensors. Malley *et al*. found that interaction of TLR4 and pneumolysin plays an important role in the innate immune defense against nasopharyngeal *S. pneumoniae* infections that remain confined to the upper respiratory tract (Malley *et al*, 2003). In contrast, our group identified a moderate influence of TLR4 signaling during *S. pneumoniae* infection of the lower respiratory tract (Branger *et al*, 2004), indicating distinct roles for TLR4 with regards to the degree of pneumococcal invasiveness.

Within the cytoplasm, NOD-2 can recognize pneumococcal peptidoglycan components, while CpG motifs, specific to bacterial DNA, are sensed via TLR9 within endosomal compartments (van der Poll & Opal, 2009). TLR ligation leads to the activation of intracellular signaling cascades, which were described in chapter 1.2.5, enabling the induction of potent antibacterial immune responses. Upon activation, AMs secrete a wide range of pro-inflammatory cytokines (e.g. IL-6, IL-1 β , IL-18 and TNF) and chemokines (e.g. CXCL1, CXCL5 and CXCL8) to recruit neutrophils (Brooks & Mias, 2018), which subsequently engage in bacterial killing via various mechanisms (described in chapter 1.1). Aside from their crucial role in the initiation of inflammation, AMs also exert indispensable anti-inflammatory functions, which are equally important for the outcome of pneumococcal pneumonia. Dissecting the role of AMs in anti-pneumococcal host defense, we discovered that AM-depletion led to increased mortality (but not bacterial clearance) during murine *S. pneumoniae* infection, which was accompanied by exacerbated local inflammation and accumulation of apoptotic neutrophils (Knapp *et al*, 2003).

If alveolar defense mechanisms fail to locally pertain the bacterial load, *S. pneumoniae* invades into the bloodstream via abusive interaction with host platelet-activating factor receptor (PAFR), which recognizes the pneumococcal cell wall component phosphorylcholine, and soluble CD14 (sCD14) (van der Poll & Opal, 2009). In the blood, the bacteria are faced with a variety of host mediators, including natural IgM antibodies and acute phase proteins (most importantly C-reactive protein (CRP) and serum amyloid P (SAP)), which bind *S. pneumoniae* cell wall components, thus promoting the deposition of complement proteins (Brooks & Mias, 2018).

Adaptive immunity transpires several days post-infection. While B cells are critically involved in pathogen opsonization (e.g. via production of pneumococcal-specific secretory IgA (sIgA)), CD4⁺ T cells polarize into different subsets, which provide antibacterial protection. Th₁₇ cells are of particular importance as they release IL-17 to recruit inflammatory cell types to the site of infection, a process which is tightly regulated by T_{reg}s to prevent excessive inflammation (Brooks & Mias, 2018).



Thesis figure 7 - Immunological events during *S. pneumoniae* infection

Early antibacterial defense is predominantly mediated by respiratory epithelial cells, AMs, monocytes and neutrophils. If the infection cannot be locally pertained, the bacteria proceed to invade the bloodstream, where they encounter soluble immunoglobulins and acute phase proteins. Adaptive immune cells further promote pathogen opsonization and bacterial elimination. *Adapted and modified from (Torres et al, 2021).*

1.3.4 Current treatment and vaccination strategies

Pneumococcal pneumonia is typically treated via administration of antibiotics (e.g. penicillin), which are essential to reduce bacterial loads. However, with increased antibiotics use, *S. pneumoniae* acquires multi-resistance genes, thus impeding successful treatment. In addition, over 90 serologically different serotypes have been described to date (Brooks & Mias,

2018). Currently, there are two major types of vaccines administered to protect against pneumococcal pneumonia: pneumococcal polysaccharide vaccines (PPSVs), which contain purified capsular polysaccharides, and pneumococcal conjugate vaccines (PCVs), which consist of purified polysaccharides that are covalently linked to a carrier protein (Pletz *et al*, 2008). Polysaccharide antigens are recognized by surface-bound antibody molecules specific for the respective carbohydrate moiety, leading to B cell activation and IgM secretion (T cell-independent). In contrast, polysaccharide-protein conjugates induce T- and B cell-dependent mucosal immunity as they can additionally be processed by DCs, which present peptides (derived from the protein portion of the conjugate) to T_{h2} cells (T cell-dependent). Activated T_{h2} cells then enable IgG class switching of B cells with polysaccharide specificity (Pletz *et al*, 2008).

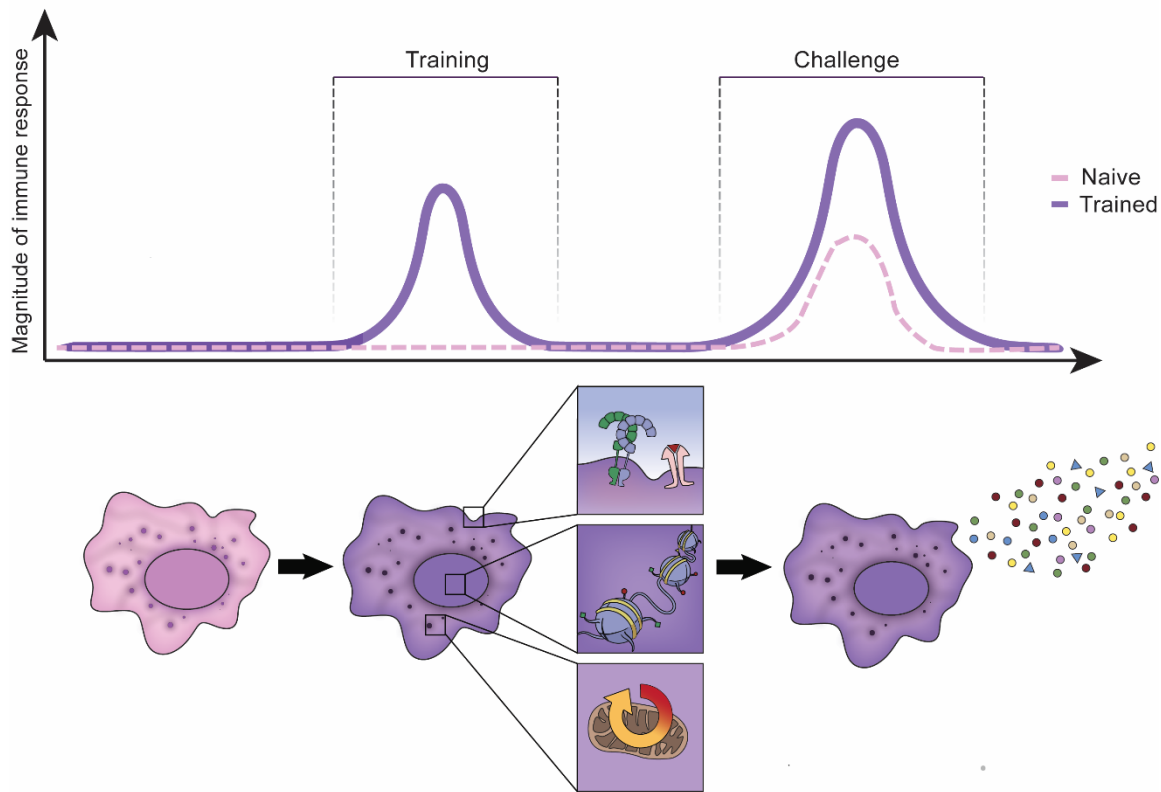
PPSV23, the current approved PPSV, is routinely administered to adults > 65 years of age and protects against 23 *S. pneumoniae* serotypes, but displays low efficacy and immunogenicity among infants. PCV13, the current approved PCV, protects against 13 different *S. pneumoniae* serotypes and provides long-lasting immunity in young children (Torres *et al*, 2021). Patients who are at high risk of developing pneumococcal disease (e.g. due to pre-existing conditions) are typically vaccinated via prime-boost strategy, i.e. PCV13 vaccination, followed by PPSV23 vaccination (Brooks & Mias, 2018). While the development of vaccines has significantly reduced the incidence of invasive pneumococcal infections, it needs to be considered that a large number of (especially non-invasive) serotypes cannot be targeted by the current vaccination regimen (Brooks & Mias, 2018). Furthermore, future research will be required to assess whether innate mechanisms (such as targeted induction of trained immunity) can be exploited for anti-pneumococcal protection.

1.4 Trained immunity

1.4.1 Evolutionary perspective and basic concepts

The term “immunological memory” describes the ability of our immune system to mount enhanced or accelerated responses against pathogens we have previously been exposed to. For the past decades, this feature was solely attributed to adaptive immune cells (T and B cells). However, this traditional paradigm was challenged by the evolving concept of “trained immunity”, i.e. the ability of innate immune cells to acquire memory characteristics. While this phenomenon gained substantial attention in recent years, earliest evidence for innate immune memory dates back to the early 20th century. In 1931, it was discovered that neonate vaccination with bacille Calmette-Guérin (BCG), an attenuated form of the bacterium *Mycobacterium bovid*, not only protected against tuberculosis, but also conferred heterologous protection against unrelated diseases, thus reducing overall childhood mortality (Bekkering *et al*, 2021). Yet, it took almost a century to understand that such non-specific effects can indeed be mediated by reprogramming of the innate immune system. Organisms which lack adaptive immunity (e.g. plants, invertebrates) are long known to possess innate memory characteristics that enable broad-spectrum resistance against secondary infections (Netea *et al*, 2011). Upon primary infection, plants develop so-called systemic acquired resistance, which is conferred by increased expression of PRRs and AMPs due to epigenetic rewiring (Bekkering *et al*, 2021). In *Drosophila melanogaster*, sublethal doses of *S. pneumoniae* were shown to protect against otherwise lethal reinfection via priming of macrophages (Pham *et al*, 2007).

Trained immunity (also referred to as innate memory) describes a stimulus-induced epigenetic and/or metabolic reprogramming of innate immune cells, which increases their reactivity to a subsequent homologous or heterologous challenge (s. Thesis figure 8). While the definition and mechanisms of this phenomenon were only defined in recent years, several earlier studies have described adaptive characteristics of innate immunity in vertebrates. Treatment with the fungal ligand β -glucan, for instance, was shown to protect against subsequent *Staphylococcus aureus* infection (Di Luzio & Williams, 1978), while muramyldipeptide (a peptidoglycan component) increased resistance against *S. pneumoniae* and *Toxoplasma gondii* (Krahenbuhl *et al*, 1981). Administration of CpG oligodioxynucleotides protected against experimental sepsis and *Escherichia coli* meningitis (Ribes *et al*, 2014), and exposure to flagellin was associated with an improved outcome of pneumococcal pneumonia (Munoz *et al*, 2010). Furthermore, BCG vaccination was shown to protect severe combined immunodeficiency (SCID) mice, which lack functional T and B cells, against lethal candidiasis (Bistoni *et al*, 1986).

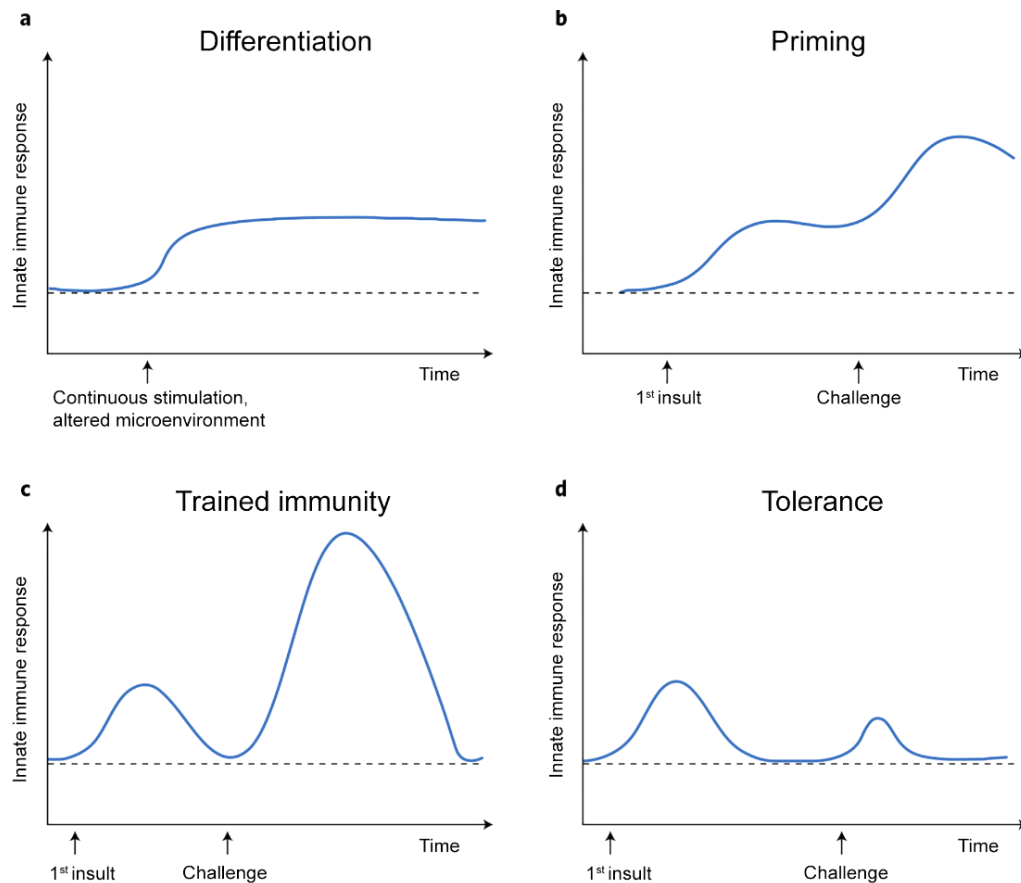


Thesis figure 8 - Basic concepts of trained immunity

Exposure to exogenous or endogenous compounds (described in chapter 1.4.2.) modulates the functional program of innate immune cells, leading to altered receptor expression, changes in chromatin accessibility and/or metabolic rewiring. This enables an increased reactivity (e.g. elevated cytokine production or phagocytosis) upon a subsequent homologous or heterologous challenge.

These studies collectively suggest that exposure to microbe-derived immunostimulatory agents may not only elicit specific protection against reinfection but can also modulate the outcome of non-related diseases, independently of adaptive immunity. However, it needs to be indicated that the underlying mechanisms of innate cross-protection may not be restricted to trained immunity, as innate immune cells can undergo different functional adaptations such as differentiation or priming (Divangahi *et al*, 2021). Therefore, it is crucial to clearly define the similarities and differences between these adaptations (s. Thesis figure 9). Immune cell differentiation (i.e. the transition of immature cells into mature cells; s. Thesis figure 9a) is accompanied by long-term functional and morphological changes, which are typically induced by alterations in the tissue environment or continuous stimulation (Lavin *et al*, 2014). Priming refers to a stimulus-induced modulation of a cell's functional state and immune status, which does *not* return to baseline levels before encountering a secondary challenge (s. Thesis figure 9b). Consequently, the altered reactivity of primed immune cells often results from additive or synergistic effects to the original priming stimulus (Divangahi *et al*, 2021).

During trained immunity, in contrast, the functional cellular program, which is modulated during primary exposure to a stimulus, returns to its baseline state after removal of the stimulus while epigenetic or metabolic reprogramming effects are maintained. This enables an increased immune response upon a subsequent homologous or heterologous challenge (s. Thesis figure 9c).



Thesis figure 9 - Schematic representation of innate adaptation programs

Primary exposure to a stimulus or insult can induce specific adaptations in innate immune cells, resulting in enhanced or repressed responsiveness upon a secondary challenge. The magnitude of the altered response is influenced by the concentration (low versus high dose) and duration (short versus long exposure) of the original stimulation.

Adapted from (Divangahi et al, 2021).

Innate immune tolerance (s. Thesis figure 9d) is considered as the opposite program of trained immunity as tolerized cells are unable to mount enhanced transcriptional responses during secondary stimulation. This is, for instance, observed upon repeated exposure to bacterial LPS, which enforces a tolerogenic epigenetic profile on macrophages, preventing the expression of inflammatory genes (Divangahi et al, 2021).

Trained immunity can be induced by a diverse range of stimuli (discussed in chapter 1.4.2) and was described for multiple innate cell types, including monocytes, macrophages, NK cells, and ILCs (discussed in chapter 1.4.4). The mechanisms and consequences of innate memory are influenced by multiple factors, including the investigated cell population, the type of inducing agent, as well as the experimental setup and disease setting. The most common experimental *in vitro* model, applied to study trained immunity, uses human peripheral monocytes which are exposed to an inducing agent (e.g. β -glucan) for approximately 24 h, followed by a resting period (five to seven days) and a subsequent challenge with a heterologous secondary stimulus (Divangahi *et al*, 2021).

In recent years, reprogramming of HSCs has gained a lot of attention as it provides an explanation for the longevity of innate training effects. In mice, this can be experimentally addressed by systemic administration of training agents (e.g. β -glucan, BCG), followed by homologous or heterologous *in vivo* challenge (Divangahi *et al*, 2021). In humans, BCG vaccination of healthy individuals was shown to elicit trained immunity in HSCs and circulating monocytes, resulting in enhanced responsiveness to various infectious agents (Netea *et al*, 2020).

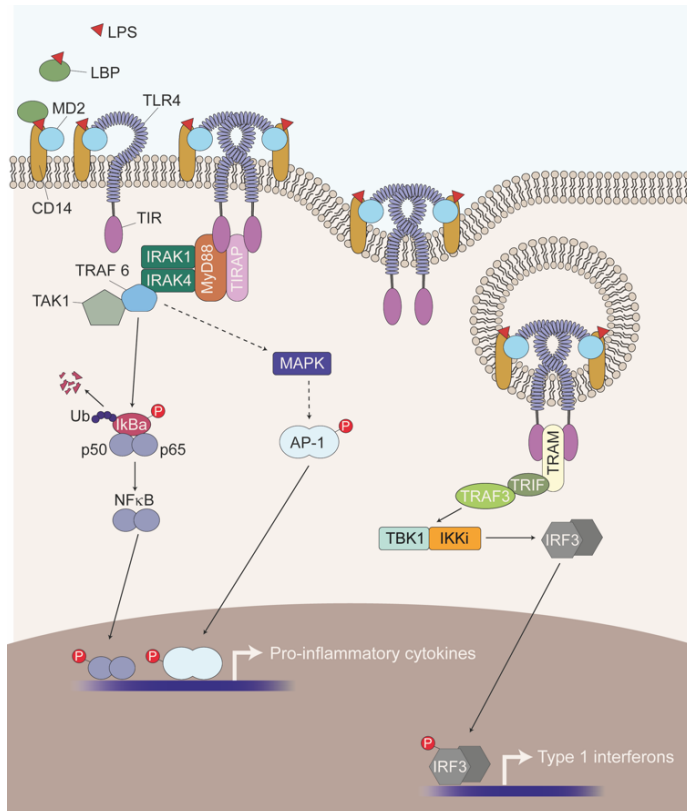
In the past decade, numerous studies identified broad benefits of innate memory for host defense, thus paving the path for novel therapeutic strategies. On the other hand, trained immunity may have a maladaptive impact on chronic inflammatory conditions as excessive immune activation can promote the progression of cardiovascular diseases, autoinflammatory syndromes and neurodegeneration (Bekkering *et al*, 2021). Potential pathological consequences of innate memory will be discussed in further detail in chapter 1.4.5.

1.4.2 Inducers of trained immunity

Trained immunity can be induced by various microbial and non-microbial stimuli, which can modulate secondary inflammatory responses with different intensity (Bekkering *et al*, 2021). BCG, β -glucan and LPS are three of the most frequently used microbe-associated training agents. Interaction of BCG with TLR2 and TLR4 initiates intracellular signaling cascades, leading to the activation of the Akt/mammalian target of rapamycin (mTOR) pathway and subsequent upregulation of glycolysis, OXPHOS and glutaminolysis (Arts *et al*, 2016c). In addition, the NOD2 pathway (activated upon TLR2/4 engagement) was shown to be critical in BCG-mediated training of monocytes as it induces IL-6, IL-1 β and TNF expression. On a mechanistic level, BCG-trained monocyte responses were associated with increased levels of histone 3 lysine 4 trimethylation (H3K4me3) near promoter regions of inflammatory gene loci (Bekkering *et al*, 2021).

The fungal cell wall component β -glucan binds to the dectin-1 receptor and, similar to BCG, initiates Akt/mTOR signaling. This leads to increased glycolysis, *decreased* OXPHOS, as well as accumulation of TCA cycle metabolites, which modulate the activity of histone-remodeling enzymes (e.g. inhibition of the histone demethylase KDM5) and thus alter chromatin accessibility (Arts *et al*, 2016b; Cheng *et al*, 2014).

The Gram-negative bacterial cell wall component LPS is recognized by TLR4 and triggers signaling via two different complexes (s. Thesis figure 10). In brief, engagement of the adaptor proteins TRIF and TRIF-related adapter molecule (TRAM) leads to the activation of interferon regulatory factor (IRF) 3, resulting in type 1 IFN production. On the other hand, signaling via MyD88, interleukin-1 receptor associated kinase (IRAK) family members and TNF receptor associated factor (TRAF) 6 induces MAPK signaling and activates the $\text{I}\kappa\text{B}$ kinase (IKK) complex. MAPK signaling culminates in the activation of activator protein 1 (AP-1), whereas IKK activation leads to phosphorylation, ubiquitination and proteosomal degradation of inhibitory $\text{I}\kappa\text{B}\alpha$, allowing for nuclear factor κ -light-chain-enhancer of activated B cells (NF- κB) dimerization, followed by its translocation to the nucleus. AP-1 and NF- κB subsequently induce the transcription of inflammatory genes (Seeley & Ghosh, 2017).



Thesis figure 10 - TLR4 signaling pathways

LPS binding protein (LBP) mediates the association between LPS and CD14, facilitating the interaction with MD2 and TLR4. Upon TLR4 oligomerization, adaptor molecules are recruited via Toll-interleukin-1 receptor (TIR) domains, resulting in MyD88-dependent or -independent signaling. The MyD88-dependent pathway ultimately leads to NF κ B phosphorylation and nuclear translocation, as well as activation of MAPK signaling, followed by induction of the transcription factor AP-1, which enables the expression of genes encoding proinflammatory cytokines. The MyD88-independent pathway leads to activation of TANK binding kinase 1 (TBK1) and inducible kinase IKKi, which promote the dimerization and translocation of IRF3, thus enabling expression type 1 IFN genes.

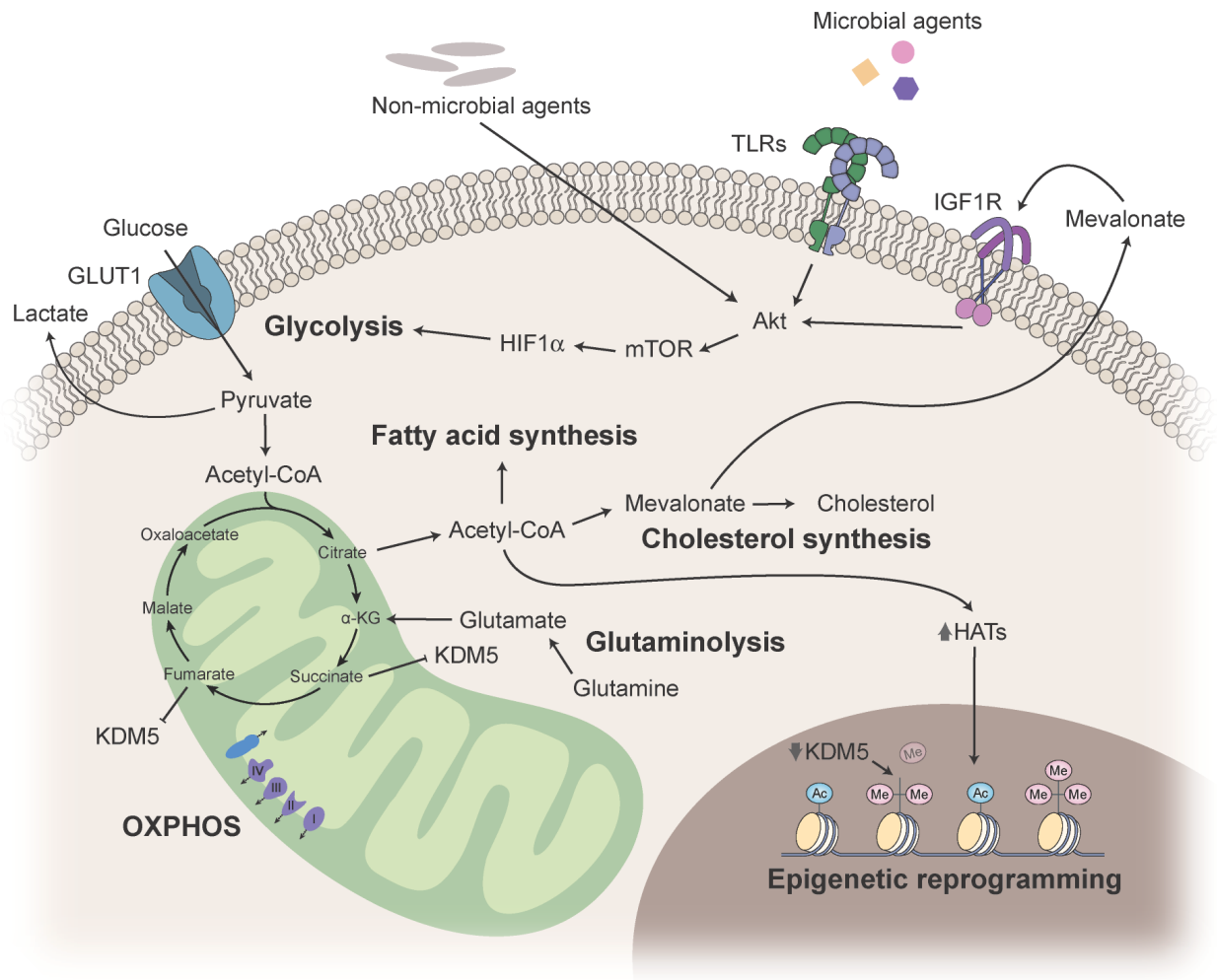
LPS was shown to modulate innate immune function in a dose- and context-dependent manner. Prolonged or high-dose exposure to LPS can result in the development of immune tolerance, whereas lower doses can induce trained immunity through regulation of transcription factor activity, which may cause or synergize with epigenetic rewiring (Bekkering *et al*, 2021). In addition to the above-mentioned microbial stimuli, several alternative training agents have been described. Oxidized low-density lipoprotein (oxLDL) was shown to modulate intracellular metabolism and cytokine expression in a manner similar to BCG. Other endogenous inducers of trained immunity include uric acid, aldosterone and interferons (Bekkering *et al*, 2021).

1.4.3 Mechanistic regulation of trained immunity

Trained immunity is mediated via epigenetic and metabolic reprogramming events, which occur during exposure to the training agent and result in hyperresponsiveness upon secondary challenge. These processes are closely intertwined and can activate different trained immunity programs, depending on the training stimulus, cell type and environmental context.

The key metabolic pathways involved in innate memory include glycolysis, OXPHOS, the TCA cycle and lipid metabolism (s. Thesis figure 11). Trained immunity is classically associated with a switch from OXPHOS to glycolysis, a phenomenon which was originally described in cancer cells (Warburg effect). While glycolysis is less efficient in generating adenosine triphosphate (ATP), it can be upregulated by multiple folds, resulting in faster ATP production compared to OXPHOS (Arts *et al*, 2016a). This switch can be promoted by Akt/mTOR signaling and results in the production and release of lactate. Importantly, several intermediate metabolites of this pathway can serve as cofactors for DNA and histone methyltransferases, while such enzymes can, in turn, regulate the expression of glycolysis-associated genes.

The TCA cycle, which occurs in the mitochondrial matrix, constitutes a central metabolic pathway, which is fuelled by acetyl-CoA and involves a series of redox reactions. During these reactions, nicotinamide adenine dinucleotide (NAD⁺) is converted into its reduced form NADH by gain of electrons. In addition, the cofactor flavin adenine dinucleotide (FAD) is reduced to FADH₂. Both, NADH and FADH₂, are used during OXPHOS, and thus ultimately contribute to mitochondrial ATP production. Trained immunity has been associated with a blunted TCA cycle, characterized by accumulation of intermediate substrates (Arts *et al*, 2016a), e.g. fumarate or citrate, which can in turn regulate epigenetic reactions. Fumarate, for instance, was reported to inhibit the lysine-specific histone demethylase KDM5, leading to increased histone methylation of inflammatory genes (Bekkering *et al*, 2021). Importantly, acetyl-CoA may serve as an acetyl donor for histone acetyl transferases (HATs), while Itaconate, another TCA metabolite, can inhibit trained immunity (Bekkering *et al*, 2021).



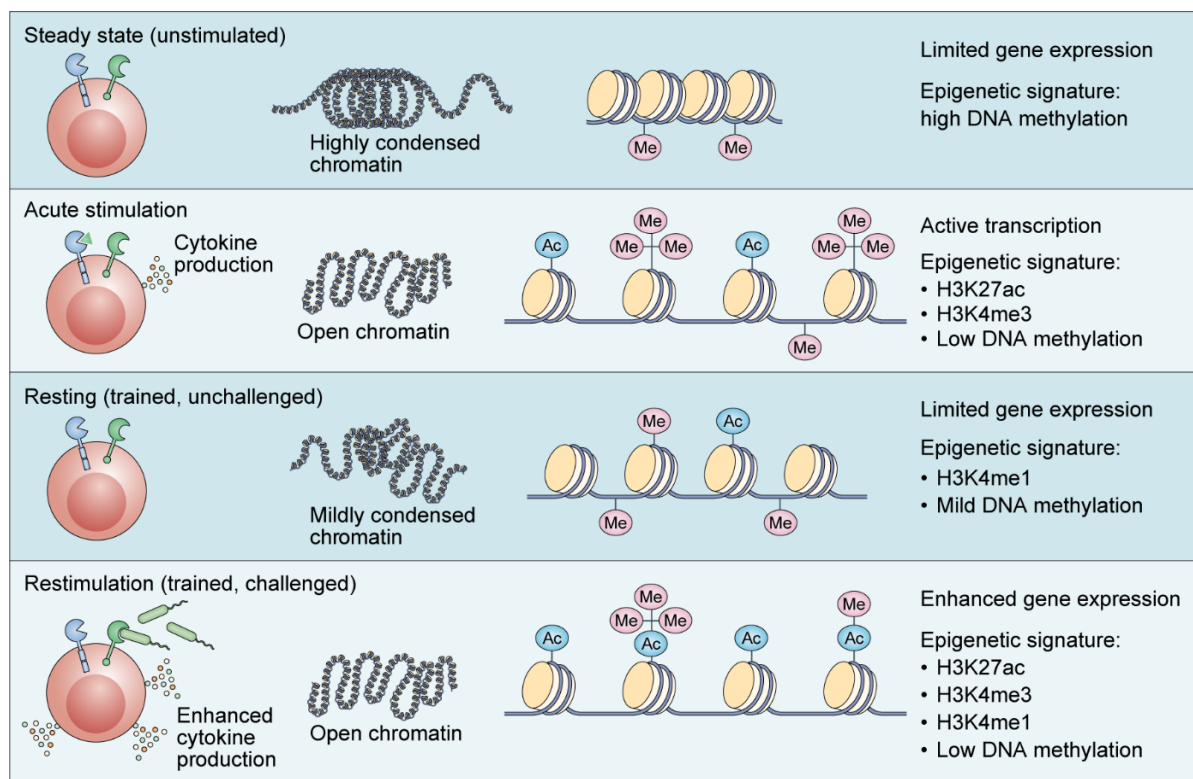
Thesis figure 11 - Metabolic regulation of trained immunity

Simplified illustration depicting the key metabolic pathways involved in trained immunity: glycolysis, the TCA cycle, OXPHOS, glutaminolysis (which can fuel the TCA cycle), and lipid synthesis. Acetyl-CoA constitutes a central element as it can enter the TCA cycle, provide acetyl groups to HATs or enter the mevalonate pathway to drive cholesterol synthesis. Accumulated intermediate metabolites of the TCA cycle may promote other metabolic pathways or modulate the activity of epigenetic enzymes. Abbreviations: Ac: acetylation; Me: methylation; KDM5: lysin-specific demethylase 5; HATs: histone acetyl transferases; OXPHOS: oxidative phosphorylation; α -KG: α -ketoglutarate; mTOR: mammalian target of rapamycin; HIF1 α : hypoxia-inducible factor 1 α ; GLUT1: glucose transporter 1.

Glutaminolysis, a central metabolic pathway which catabolizes glutamine to generate energy, was shown to promote innate memory induction via efficient replenishment of the TCA cycle (Arts *et al*, 2016b). Furthermore, accumulating evidence suggests that alterations of the cellular lipid metabolism are implicated in the establishment of trained immunity. While Arts *et al*. demonstrated a critical role of the cholesterol synthesis pathway in β -glucan-mediated training of monocytes (Arts *et al*, 2016b), Bekkering and colleagues found mevalonate (a metabolite used to generate the building blocks for cholesterol and steroid synthesis) - rather

than the synthesis of cholesterol itself - to be essential for memory induction, and demonstrated that mevalonate-induced monocyte training can be reversed by administration of statins (Bekkering *et al*, 2018).

In quiescent myeloid cells, the majority of inflammatory gene loci is in a repressed configuration, thus hindering access of the transcriptional machinery. Upon stimulation, epigenetic processes, e.g. DNA methylation or histone remodelling, facilitate chromatin unfolding and thereby promote gene expression (s. Thesis figure 12). Such exposures can leave a so-called “epigenetic scar” as these modifications are only partially removed upon cessation of the stimulus, thus changing the long-term responsiveness, which is central to trained immunity (Netea *et al*, 2020). The predominant epigenetic footprints associated with innate memory responses of myeloid cells are histone 3 lysine 27 acetylation (H3K27ac), which marks open chromatin regions and - in combination with histone 3 lysine 4 monomethylation (H3K4me1) - distant enhancers, and histone 3 lysine 4 trimethylation (H3K4me3), which can be found in the promoter regions of actively transcribed genes (Netea *et al*, 2020).



Thesis figure 12 - Epigenetic regulation of trained immunity

This illustration depicts the different chromatin states and epigenetic signatures associated with the induction of trained immunity. Abbreviations: Ac: acetylation; Me: methylation. Adapted from (Netea *et al*, 2020).

In a similar manner, changes in the DNA methylation status can induce a poised regulatory program by regulating chromatin accessibility. Recent studies suggested that changes in DNA methylation could discriminate between so-called “responders” (i.e. patients who can develop trained immunity) and “non-responders” in the context of BCG vaccination (Verma *et al*, 2017). Furthermore, microRNAs can play a role in the induction and/or regulation of these mechanisms. MiR-155, for example, was demonstrated to be involved in trained NK cell responses to murine cytomegalovirus (MCMV) infection (Netea *et al*, 2020). However, the precise processes of miRNA-mediated regulation warrant further investigations.

1.4.4 Cellular mediators of trained immunity

Innate memory properties have been ascribed to multiple cell types of the myeloid and lymphoid lineage (e.g. monocytes/macrophages, NK cells, ILCs) but were also identified in HSCs and structural cells (Hamada *et al*, 2018). Among these cell types, research has primarily focused on monocytes/macrophages and NK cells due to their historical association with LPS-induced tolerance (Netea *et al*, 2011). Indeed, some of the earliest evidence for innate reprogramming of macrophages came from a study describing how LPS can epigenetically silence a distinct set of inflammatory gene loci while priming loci coding for antimicrobial molecules (Foster *et al*, 2007). These findings were expanded by a publication demonstrating that β -glucan exposure can modulate the immune response of monocytes/macrophages upon challenge with various PAMPs (Quintin *et al*, 2012). Despite their short lifespan, trained monocyte responses were shown to last for at least three months, indicating that the underlying reprogramming events might occur within their progenitor cells (Netea *et al*, 2011). Recent work has confirmed and substantiated this hypothesis, revealing that trained immunity may occur in bone marrow HSCs (referred to as “central trained immunity”), as well as in blood- and tissue-resident innate immune cells (referred to as “peripheral trained immunity”). In this context, trained immunity of TRMs may be established in a cell-intrinsic manner, or arise from reprogrammed monocytic progenitors that migrate to distal organs and differentiate into trained macrophages. Due to their continuous microbial exposure, mucosal surfaces are ideal sites for the induction of innate memory responses. In 2020, Feuerstein and colleagues demonstrated that staphylococcal skin infection induced an innate memory signature in dermal macrophages, which was reflected by increased expression of STAT1 and CXCL9, as well as improved bacterial killing upon secondary infection. However, this memory signature was eventually extinguished due to increased replenishment of the local macrophage pool by bone marrow-derived monocytes (Feuerstein *et al*, 2020). A study by Wendeln *et al*. reported that repeated, peripheral administration of LPS can modulate microglia immunity in a dose-dependent manner, leading to the

establishment of trained immunity (upon low dose LPS treatment) or tolerance (upon high dose LPS treatment), which resulted in the exacerbation or alleviation of cerebral β -amyloidosis respectively (Wendeln *et al*, 2018). Furthermore, Yao *et al.* discovered that T-cell derived IFN- γ , produced upon adenoviral infection, can prime lung resident macrophages for enhanced reactivity upon secondary *S. pneumoniae* infection (Yao *et al*, 2018).

Accumulating evidence suggests that NK cells are able to acquire memory-like properties upon cytokine stimulation (e.g. during combined exposure to IL-12 and IL-18), viral infection or hapten sensitization (Netea *et al*, 2016), resulting in boosted proliferation, degranulation and/or IFN- γ production. During murine CMV infection, NK cells can undergo rapid expansion, and may mount an antigen-specific memory response upon reinfection with the same virus. In contrast, *unspecific* NK cell memory was reported in the context of BCG vaccination as NK cells isolated from vaccinated individuals produced more pro-inflammatory mediators upon *ex vivo* challenge with unrelated pathogens (Netea *et al*, 2016). Of note, BCG was also suggested to induce neutrophil training via reprogramming of HSC precursors, an effect which was shown to be significantly involved in the specific and unspecific protective effects of the vaccine (Acevedo *et al*, 2021).

Similar to NK cells, ILCs may mediate antigen-specific or unspecific memory responses. Liver-resident ILC1s were shown to expand and persist after murine CMV infection, mounting an antigen-specific protective response during secondary CMV challenge (Weizman *et al*, 2019). In the lung, IL-33 or fungal allergen-experienced ILC2s were found to be more proinflammatory upon secondary *in vivo* challenge with papain, leading to severe allergic inflammation (Martinez-Gonzalez *et al*, 2016). Furthermore, a recent publication demonstrated that ILC3s, critical mediators of intestinal homeostasis, developed protective trained immunity upon *Citrobacter rodentium* infection, which was characterized by metabolic changes, increased proliferation and enhanced IL-22 production upon reinfection (Serafini *et al*, 2022).

Recent work has shown that murine DCs, isolated after infection with the fungal pathogen *Cryptococcus neoformans*, mounted an increased cytokine response upon *ex vivo* challenge with the same fungus, an effect which appeared to be dependent on epigenetic remodeling (Hole *et al*, 2019).

Non-immune cells play a central role in host defense and have recently been suggested to acquire memory-like properties, which is sometimes referred to as “expanded trained immunity” (Bekkering *et al*, 2021). In 2016, Liu and colleagues found that adipose mesenchymal stem cells develop a short-term memory response upon exposure to LPS or TNF- α . This effect was mediated by microRNAs and changes in DNA methylation, and provided a therapeutic benefit in a rat model of diabetes (Liu *et al*, 2016). Furthermore,

intravenous (as opposed to subcutaneous) BCG administration was shown to modulate the transcriptional profile of HSCs and multipotent progenitor cells in the bone marrow, which promoted myelopoiesis and gave rise to trained monocytes/macrophages with enhanced antimycobacterial activity (Kaufmann *et al*, 2018).

In the skin, epithelial stem cells are able to memorize chemical or mechanical insults as well as microbial stimuli, resulting in improved healing capacity (Bekkering *et al*, 2021). Similarly, bronchial epithelial cells of the respiratory tract can acquire memory properties during allergic inflammation or flagellin exposure (Bekkering *et al*, 2021). In endothelial cells, *in vitro* incubation with high concentrations of glucose can induce persistent hyperinflammation and modulate their transcriptional response during a subsequent normoglycemic period (Bekkering *et al*, 2021). Additionally, oxidized phospholipids were recently shown to reprogram endothelial cell metabolism, thereby inducing a pro-atherogenic phenotype (Bekkering *et al*, 2021). Finally, fibroblasts can become persistently activated via epigenetic remodeling, which may have a negative impact on rheumatoid arthritis. However, such memory properties appear to be restricted to certain classes of fibroblasts and require future investigations (Bekkering *et al*, 2021).

1.4.5 Therapeutic targeting of trained immunity

While trained immunity likely evolved as a primitive form of immune cell memory, serving to protect the host against reinfections, innate reprogramming may result in hyperinflammation or immunosuppression if dysregulated. The hyper-IgD syndrome (HIDS), an autoinflammatory disorder with attacks of sterile inflammation, represents an example of excessive trained immunity. In HIDS patients, mevalonate accumulates due to defects in the mevalonate kinase, leading to continuous activation of the Akt/mTOR pathway and glycolysis in circulating monocytes (Mulder *et al*, 2019). Furthermore, chronic inflammatory conditions or autoimmunity may increase the susceptibility to atherosclerosis by establishing a maladaptive functional program in innate immune cells. In this context, it was demonstrated that oxLDL triggers inflammatory cytokine production and foam cell formation by eliciting trained immunity in human monocytes (Bekkering *et al*, 2014). Christ *et al.* reported western diet-induced metabolic reprogramming of myeloid precursor cells via inflammasome activation, suggesting potentially deleterious effects of trained immunity for inflammatory diseases, such as type 2 diabetes or systemic lupus erythematosus (Christ *et al*, 2018; Mulder *et al*, 2019).

In contrast, a defective myeloid activation program may drive immune paralysis (e.g. in LPS-induced sepsis) or promote cancer progression (Mulder *et al*, 2019).

The underlying mechanisms of trained immunity are amenable for therapeutic approaches. Epigenetic enzyme classes that promote innate memory may, for instance, be targeted by

selective epigenetic inhibitors, such as bromodomain and extraterminal domain inhibitors (BETis). These hinder the recognition of acetylated histone modifications and as such might prevent the induction of trained immunity to ameliorate chronic inflammatory conditions (Bekkering *et al*, 2021).

As enhanced Akt/mTOR signaling and glycolysis are activated by a variety of training agents, these pathways represent interesting candidates for therapeutic applications. Indeed, (partial) *in vivo* inhibition of glycolysis (e.g. via 3-PO, which abolishes 6-phosphofructo-2-kinase activity) was shown to reduce the development of atherosclerosis in mice (Bekkering *et al*, 2021). In addition, rapamycin-loaded high-density cholesterol (HDL)-nanoparticles were found to specifically inhibit Akt/mTOR signaling in innate immune cells and prevent training-induced allograft rejection (Bekkering *et al*, 2021). In contrast, *reversal* of trained immunity might require different therapeutic approaches as statins were unable to erase innate memory phenotypes in patients suffering from hypercholesterolemia (Bekkering *et al*, 2019).

Other potential strategies for the suppression of trained immunity include inhibition of the NLR family pyrin domain containing 3 (NLRP3) inflammasome, which can blunt IL- β release and inflammation, or inhibition of enzymes involved in cholesterol synthesis (Mulder *et al*, 2019). However, it needs to be mentioned that the therapeutic exploitation of inhibitory molecules is hampered by potential adverse reactions, toxic properties and limited bioavailability (Mulder *et al*, 2019). Proposed future strategies for therapeutic targeting of innate memory include antibodies (e.g. anti-IL-1 β), RNA interference (RNAi) therapeutics and, in particular, nano-immunotherapy. In addition, combination strategies, that enhance or synergize with such approaches, could further enhance their therapeutic specificity and durability. In this light, future research should focus on dissecting cell type-, tissue- and disease-specific aspects of trained immunity to optimally exploit innate memory responses for the treatment of patients.

1.5 Aims of the thesis

The concept of trained immunity has substantially expanded our understanding of immune cell memory, a feature which had traditionally been considered an exclusive hallmark of the adaptive immune system. While recent studies have identified cellular mediators and mechanistic aspects of innate memory responses, we still lack knowledge about *in vivo* features and consequences of trained immunity.

Due to their unique location in the alveoli of the lungs, AMs are at the front line of innate host defense and possess distinctive cellular properties. Thus, they represent interesting candidates to explore innate memory in a tissue- and disease-specific context.

The main purpose of this study was to investigate whether naturally occurring, environmental microbial compounds can elicit trained immunity in AMs. Furthermore, we sought to unravel the cellular mechanisms and *in vivo* impact of AM training in the context of pneumococcal pneumonia.

In particular, we aimed to:

- I) investigate whether pulmonary exposure to ambient LPS concentrations can alter AM reactivity to a secondary, bacterial challenge by inducing trained immunity.
- II) characterize the genetic, epigenetic and metabolic profile of trained AMs.
- III) dissect the mechanisms of LPS-induced AM memory.
- IV) determine whether LPS-trained AMs have the potential to modulate the outcome of bacterial pneumonia.
- V) assess the physiological consequences of pulmonary LPS exposure on a subsequent pneumococcal infection.

Results

Trained immunity of alveolar macrophages requires metabolic rewiring and type 1 interferon signaling

Sophie Zahalka^{1,2}, Philipp Starkl¹, Martin L. Watzenboeck^{1,2}, Asma Farhat^{1,2}, Mariem Radhouani^{1,2}, Florian Deckert^{1,2}, Anastasiya Hladik¹, Karin Lakovits¹, Felicitas Oberndorfer³, Caroline Lassnig^{4,5}, Birgit Strobl⁴, Kristaps Klavins^{2,6}, Mai Matsushita⁷, David E. Sanin⁷, Katarzyna M. Grzes⁷, Edward J. Pearce^{7,8}, Anna-Dorothea Gorki^{1,2*} & Sylvia Knapp^{1*}

¹Research Laboratory of Infection Biology, Department of Medicine I, Medical University of Vienna, Austria; ²CeMM, Research Center for Molecular Medicine of the Austrian Academy of Sciences, Vienna, Austria; ³Department of Pathology, Medical University of Vienna, Austria; ⁴Institute of Animal Breeding and Genetics, Department of Biomedical Sciences, University of Veterinary Medicine Vienna, Austria; ⁵Biomodels Austria, Department of Biomedical Sciences, University of Veterinary Medicine Vienna, Austria; ⁶Institute of General Chemical Engineering, Riga Technical University, Riga, Latvia; ⁷Department of Immunometabolism, Max Planck Institute of Immunobiology and Epigenetics, Freiburg, Germany; ⁸The Bloomberg-Kimmel Institute for Cancer Immunotherapy at Johns Hopkins, Johns Hopkins University, Baltimore, MD, USA.

*contributed equally

Disclosure: All authors declare no conflict of interest.

Correspondence:

Sylvia Knapp, MD, PhD

Research Laboratory of Infection Biology, Department of Medicine I

Medical University of Vienna

Waehringer Guertel 18-20, 1090 Vienna, Austria

Phone: +43-1-40400-51390, Fax: +43-1-40400-51670

E-mail: sylvia.knapp@meduniwien.ac.at

2.1 Abstract

Environmental microbial triggers shape the development and functionality of the immune system. Alveolar macrophages (AMs), tissue-resident macrophages of the lungs, are in constant and direct contact with inhaled particles and microbes. Such exposures likely impact AM reactivity to subsequent challenges by immunological imprinting mechanisms referred to as trained immunity. Here, we investigated whether a ubiquitous microbial compound has the potential to induce AM training *in vivo*. We discovered that intranasal exposure to ambient amounts of lipopolysaccharide (LPS) induced a pronounced AM memory response, characterized by enhanced reactivity upon pneumococcal challenge. Exploring the mechanistic basis of AM training, we identified a critical role of type 1 interferon signaling and found that inhibition of fatty acid oxidation and glutaminolysis significantly attenuated the training effect. Notably, adoptive transfer of trained AMs resulted in increased bacterial loads and tissue damage upon subsequent pneumococcal infection. In contrast, intranasal pre-exposure to LPS promoted bacterial clearance, highlighting the complexity of stimulus-induced immune responses, which likely involve multiple cell types and may depend on the local immunological and metabolic environment. Collectively, our findings demonstrate the profound impact of ambient microbial exposure on pulmonary immune memory and reveal tissue-specific features of trained immunity.

2.2 Introduction

Our immune system is invariably shaped by microbial encounters and exposure to environmental pathogen-associated molecular patterns (PAMPs). Such interactions can result in long-term functional changes of innate immune cells, which enable an increased responsiveness to secondary challenges (Netea *et al*, 2011). This phenomenon, referred to as trained immunity, has broadened our understanding of innate immunity and represents a critical component of immune cell memory (Netea *et al*, 2011). Trained immunity can be induced by endogenous or exogenous compounds (e.g. β -glucan, oxLDL, cytokines) and has been described for a wide range of cell types, including monocytes, macrophages and NK cells, as well as hematopoietic stem cells and multipotent progenitor cells (Kar & Joosten, 2020). While the molecular basis of trained immunity is not yet fully understood, it is known that innate memory responses mechanistically depend on a complex interplay between epigenetic regulation and cellular metabolism (Netea *et al*, 2020).

The lungs are continually exposed to particles and microbes from the external environment (Bals, 2005), which may impact local immune responses and induce innate memory.

Lipopolysaccharide (LPS), the major component of Gram-negative bacterial cell walls, is a ubiquitously present PAMP that can be detected in airborne particles, such as organic dust and cigarette smoke (Vernooy *et al*, 2002), and initiates a proinflammatory response upon recognition by the innate immune system (Mazgaeen & Gurung, 2020). There are considerable variations in the amount of personal, ambient LPS exposure. Urban LPS concentrations are generally below 10 inhalable endotoxin units (EU)/m³ (Rolph *et al*, 2018), whereas ranges of 300 to 6600 EU/m³ have been reported for endotoxin-rich environments, such as livestock farming (Basinas *et al*, 2015), corresponding to 0.15 – 3.3 EU per breath (assuming 0.5 L human tidal volume (Hallett *et al*, 2022)). While the consequences of LPS inhalation are diverse and complex, recent epidemiological studies have demonstrated a protective effect of environmental endotoxin exposure on the development of allergic diseases (Pivniouk *et al*, 2020).

Being located at the interface of the airways and the environment, alveolar macrophages (AMs) constitute the first line of innate cellular defense against inhaled microbes (Rubins, 2003) and are in direct contact with airborne allergens, environmental agents and PAMPs, including LPS. Given their unique location, AMs exhibit a distinctive cellular profile that tightly regulates their activation state to avoid excessive inflammatory responses (Bain & MacDonald, 2022). As such, they display limited plasticity and exhibit only moderate transcriptional and functional changes following severe insults such as bleomycin-induced fibrosis or influenza infection (Kulikauskaite & Wack, 2020). Furthermore, AMs are metabolically adapted to the low glucose levels of the alveolar space and depend on oxidative phosphorylation while maintaining only minimal glycolytic activity in homeostatic and inflammatory conditions (Woods *et al*, 2020). Despite their hyporesponsive state, AMs are key players in the innate pulmonary defense during respiratory infections and eliminate invading pathogens by processes such as phagocytosis or secretion of antimicrobial peptides, while playing an equally important role in the restoration of homeostasis (Rubins, 2003). AM-mediated initiation and resolution of inflammation have been shown to be particularly relevant during bacterial pneumonia, which is most commonly caused by the Gram-positive bacterium *Streptococcus pneumoniae* (Byrne *et al*, 2015). Due to their unique cellular properties, AMs are interesting candidates to study tissue-specific aspects of trained immunity. Yet, our current knowledge about innate memory responses of AMs and the underlying cellular mechanisms is limited.

In this study, we investigated whether exposure to ambient amounts of LPS can modulate AM function by inducing trained immunity. We applied a combination of genetic, epigenetic and metabolic analyses to uncover the unique cellular properties of AM memory and assessed the consequences of LPS training in the context of pneumococcal infection.

2.3 Results

2.3.1 LPS exposure induces trained immunity in alveolar macrophages

The respiratory tract is continuously exposed to airborne microbial products, which modulate the pulmonary immune system. Due to their strategic location in the alveoli of the lungs, AMs are in direct contact with inhaled particles and microbes, and thus represent potential candidates to develop trained immunity. To investigate whether ambient concentrations of ubiquitous airborne compounds can elicit AM memory, we administered 1 ng LPS (~ 0.5 EU/mouse; an amount in relation potentially inhaled by humans (Basinas *et al*, 2015)) or endotoxin-free saline intranasally (i.n.) to wild type C57BL/6J mice (Fig. 1A). This treatment induced an acute inflammatory response, characterized by a transient influx of neutrophils after 24 h (Fig. 1B). Six days later, neutrophils were no longer detectable in the BAL fluid (BALF; Fig. 1C), and post-lavage lung immune cell numbers were comparable to the control group, except for dendritic cell and B cell numbers, which remained moderately elevated in LPS-exposed lungs (Fig. S1A-C). These data support the transient nature of LPS-triggered effects, and exclude overt signs of persisting lung inflammation. To assess whether LPS exposure modulates AM immunity, we isolated AMs by BAL six days after i.n. LPS treatment and challenged the cells *ex vivo* with heat-inactivated *S. pneumoniae* (HISP, Fig. 1A). LPS-exposed AMs produced higher amounts of multiple cytokines and chemokines, including C-X-C Motif Chemokine Ligand (CXCL)-1, interleukin (IL)-1 β , IL-10, IL-12p40 and IL-6 compared to control (saline-exposed) AMs (Fig. 1D, Fig. S2A), indicating an innate memory effect. Taking absolute concentrations and log₂ fold changes into account (Fig. 1D), we selected IL-6, a cytokine critically involved in host immunity (Uciechowski & Dempke, 2020), as the most stable readout and decided to use it as a surrogate for LPS-induced AM memory in subsequent experiments. In support of this choice, we continued to observe elevated IL-6 responses by AMs two and six weeks after intranasal LPS treatment (Fig. 1E), indicating long-lasting cellular reprogramming following ambient LPS exposure.

Given that phagocytosis and efferocytosis are key effector functions of AMs, we next decided to investigate whether these processes are modulated six days after *in vivo* training. To analyze AM-mediated phagocytosis, AMs were isolated by BAL and incubated with FITC-labeled HISP, followed by FACS analysis. These experiments revealed that the phagocytic capacity of trained AMs was enhanced in comparison to saline-treated controls (Fig. 1F). AM-mediated efferocytosis was assessed after intratracheal transfer of CFSE-labeled apoptotic thymocytes on day six after training (Fig. S2B) and did not reveal any differences between the groups (Fig. S2C and D).

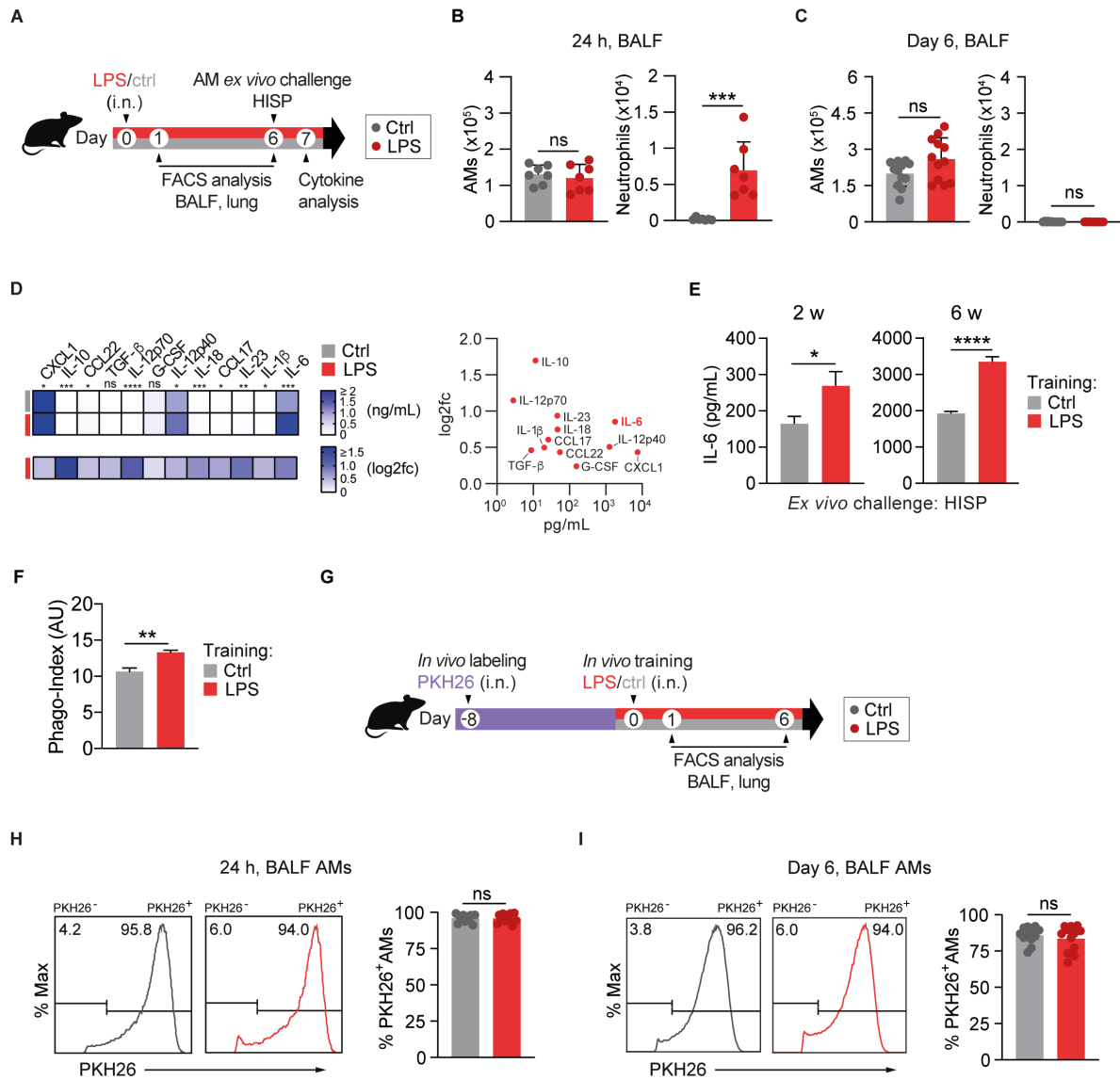


Figure 1 - LPS exposure induces trained immunity in alveolar macrophages.

(A) Experimental setup for i.n. LPS (1ng/mouse) or saline exposure, followed by FACS analysis (BALF, lung) or AM cytokine analysis upon ex vivo bacterial challenge. (B, C) Absolute numbers of BALF AMs and neutrophils, measured by flow cytometry 24 h (B) and six days (C) after *in vivo* treatment. (D) LEGENDplex analysis of LPS-exposed and control AMs upon ex vivo HISP-challenge (16 h). Absolute cytokine levels (top heat map) and log₂ fold change (log₂fc) of LPS-exposed AMs versus means of control AMs (bottom heat map) are shown. The right panel compares absolute levels and log₂fc of trained AMs. (E) IL-6 levels of LPS-exposed and control AMs upon ex vivo bacterial challenge two or six weeks after treatment. (F) Phagocytosis index (AU: arbitrary units) of trained and control AMs, isolated on day six after *in vivo* training, followed by ex vivo stimulation with FITC-labeled HISP and FACS analysis. (G) Experimental setup for PKH26 labeling eight days prior to *in vivo* training. (H, I) Representative histograms of PKH26 MFI (gated on CD11c⁺ Siglec F⁺ AMs) and percentage of PKH26⁺ AMs 24 h (H) and six days (I) after training. Graphs show means + SD of 7 (B) or 11-12 (C, H, I) biological replicates, means of 7-8 biological replicates (D) or means + SD of 3-5 technical replicates (E, F). Data (B, C, E, F) are representative of two independent experiments. Statistical analysis: student's t-test. ns, not significant. *p ≤ 0.05, **p ≤ 0.01, ***p ≤ 0.001, ****p ≤ 0.0001.

However, we noticed that LPS-exposed AMs showed elevated surface expression of MerTK (Fig. S2E) and Axl (Fig. S2F), two TAM family receptors known to promote apoptotic cell removal (Ranta & Kumar, 2020).

AMs are predominantly of embryonic origin and self-maintain locally with minimal contribution of circulating monocytes under steady-state conditions (Ginhoux & Jung, 2014). However, upon infection or severe lung injury, the alveolar niche can be replenished by monocytes, which get recruited to the lungs and acquire an AM profile under the influence of the local microenvironment (Kulikauskaite & Wack, 2020). In order to determine whether the transient inflammatory response to LPS inhalation induced replenishment of tissue-resident AMs by monocytes, we labeled resident AMs by i.n. administration of the fluorescent dye PKH26 (Maus et al, 2001) eight days prior to LPS treatment (Fig. 1G). Frequencies of PKH26⁺ and PKH26⁻ AMs were determined 24 h and six days after training. The dye selectively labeled lung-resident CD11c⁺ Siglec F⁺ AMs while CD11b⁺ Ly6C⁺ monocytes remained PKH26⁻ negative (Fig. S2G). Of note, the percentage of PKH26⁺ CD11c⁺ Siglec F⁺ AMs in BALF (Fig. 1H and I) and post-lavage lung tissue (Fig. S2H) was comparable between LPS-treated and control mice at both timepoints investigated. This indicates that the resident AM population was not replenished by inflammatory monocytes upon *in vivo* training. In conclusion, we showed that i.n. LPS exposure trains the local AM pool for increased cytokine production and phagocytosis following secondary bacterial challenge.

2.3.2 AM training depends on type 1 interferon signaling

LPS-mediated signaling is accompanied by the production of type 1 interferons (IFNs; e.g. IFN- β) (Vadiveloo *et al*, 2000) and type 2 IFNs (IFN- γ) (Varma *et al*, 2002), which have the capacity to modulate immune responses. Yao *et al*. reported that IFN- γ , produced by T-cells during respiratory adenoviral infection, primes AMs for enhanced immune activity upon secondary pneumococcal challenge (Yao *et al*, 2018). To test whether IFN- γ - or T cell-mediated responses contribute to LPS-induced AM memory, we applied our training model (*in vivo* training, followed by *ex vivo* AM challenge) to IFN- γ -receptor-deficient (Ifn γ r1^{-/-}) and Rag2-deficient (Rag2^{-/-}) mice, respectively. These experiments showed that the enhanced IL-6 response of LPS-exposed AMs occurred independently of IFN- γ -receptor signaling (Fig. S3A) and adaptive immunity (Fig. S3B).

LPS is a potent inducer of type 1 IFNs, which can in turn potentiate LPS-mediated immune responses (Goritzka *et al*, 2014). To investigate whether type 1 IFN signaling plays a role in LPS-induced AM memory, we trained type 1 IFN-receptor-deficient (Ifnar1^{-/-}) and control mice, and analyzed AM IL-6 production upon *ex vivo* HISP challenge six days later. Interestingly,

AMs retrieved from LPS-exposed *Ifnar1*^{-/-} mice were unable to mount a trained response (Fig. 2A), suggesting that type 1 IFN signaling plays an important role in the establishment of AM memory. Of note, this effect was not restricted to IL-6, as IL-12p40 and IL-12p70 responses were similarly diminished upon *Ifnar1* deficiency (Fig. S3C and D). Based on these findings, we aimed to dissect whether type 1 IFNs promote AM training in a direct or indirect manner. Using *Ifnar1*^{ΔCD169} and *Ifnar1*^{fl/fl} control mice, we found that macrophage-specific deficiency of type 1 IFN receptor expression abolished AM memory (Fig. 2B), indicating that AMs need to directly sense type 1 IFNs during LPS-mediated training.

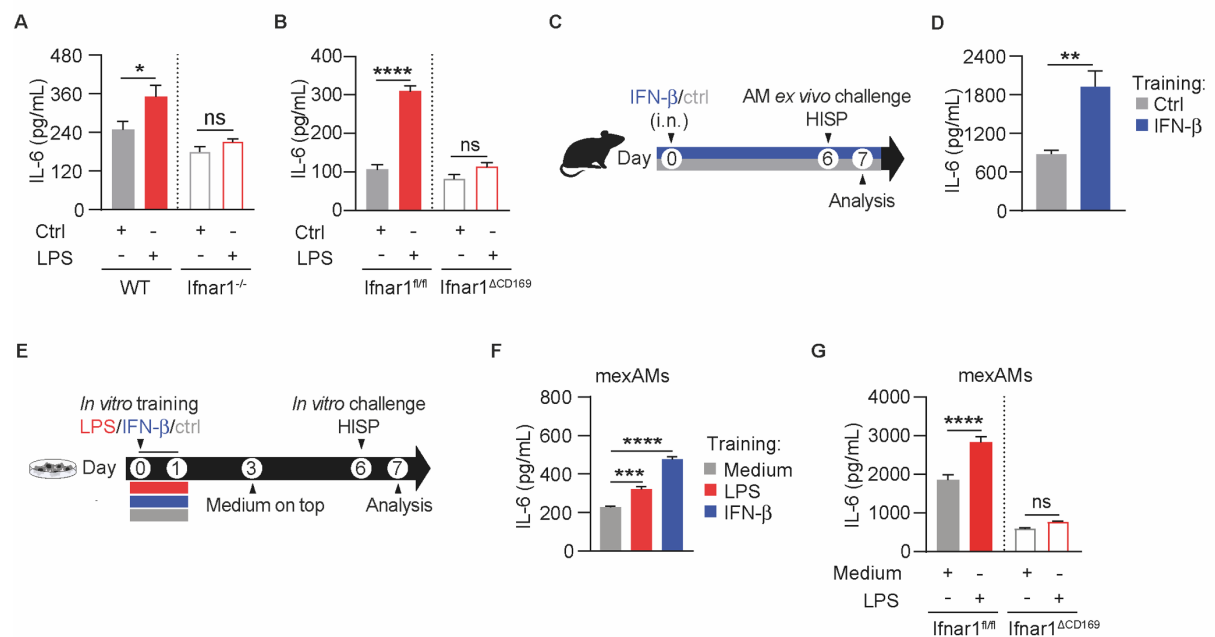


Figure 2 - LPS-induced AM training is driven by type 1 interferon signaling.

(A, B) IL-6 levels of HISP-challenged (16 h) LPS-trained and control AMs, isolated six days after *in vivo* training (performed as described in Fig. 1) of *Ifnar1*^{-/-} and WT control mice (A) or *Ifnar1*^{ΔCD169} and *Ifnar1*^{fl/fl} control mice (B). (C) Experimental setup for i.n. treatment with IFN-β (2000 U/mouse) or saline (control). AMs were isolated on day six, followed by ex vivo challenge with HISP (16 h). (D) IL-6 levels of IFN-β-trained and control AMs after ex vivo restimulation. (E) Experimental setup for *in vitro* LPS (10 ng/mL)- or IFN-β (800 U/ mL)- training of mexAMs, followed by *in vitro* HISP challenge (16 h) six days later. (F) IL-6 levels of control, LPS-trained and IFN-β-trained WT mexAMs after HISP challenge. (G) IL-6 levels of LPS-trained and control *Ifnar1*^{ΔCD169} and *Ifnar1*^{fl/fl} mexAMs after HISP challenge. Graphs show means + SEM of 4-5 technical replicates. In (A-D), four biological replicates per group were pooled and seeded as technical replicates for stimulation. Data are representative of two independent experiments. Statistical analysis: two-way ANOVA (factor 1: training; factor 2: genotype) (A, B, G), student's t-test (D) or one-way ANOVA (F). ns, not significant. *p ≤ 0.05, **p ≤ 0.01, ***p ≤ 0.001, ****p ≤ 0.0001.

This prompted us to investigate whether local administration of type 1 IFNs has the potential to induce trained immunity in AMs. For this purpose, we treated wild type mice i.n. with IFN-β or saline and examined the responsiveness of AMs six days later (Fig. 2C). Similar to LPS-

training, IFN- β exposure increased the IL-6 production by AMs upon secondary, bacterial challenge, indicating an innate memory effect (Fig. 2D). Given that type 1 IFNs act downstream of TLR4 signaling and can affect cellular immunity via autocrine signaling (Moorlag *et al*, 2018), we went on to explore whether AM memory can be induced in a cell-autonomous manner and generated murine *ex vivo* cultured AMs (mexAMs) (Gorki *et al*, 2022) from primary wild type AMs. Following *in vitro* expansion, mexAMs were stimulated for 24 h with LPS, IFN- β or medium, allowed to rest for five days, and subsequently challenged with HISP on day six after training (Fig. 2E). Similar to *in vivo* AM training, LPS- or IFN- β -exposed mexAMs produced increased amounts of IL-6 upon bacterial challenge (Fig. 2F), indicating that these stimuli have the potential to *directly* induce AM memory. Applying the same regimen to *Ifnar1* ^{Δ CD169} and *Ifnar1*^{fl/fl} control mexAMs, we could further demonstrate that autocrine type 1 IFN signaling can mediate LPS-induced *in vitro* training (Fig. 2G).

Collectively, our data suggest that type 1 IFNs play an important role in the establishment of LPS-mediated AM memory.

2.3.3 Trained AMs exhibit an altered transcriptional profile upon secondary bacterial challenge

Trained immunity is defined as the altered reactivity to a secondary trigger induced by prior exposure to a training stimulus (Divangahi *et al*, 2021). In contrast to primed immune responses, this phenomenon is characterized by the return to a baseline state after initial activation (Divangahi *et al*, 2021). Mechanistically, trained immunity has been associated with epigenetic remodeling and metabolic reprogramming, two processes that serve as the molecular basis for altered gene expression upon secondary challenge (Netea *et al*, 2020). To identify transcriptional changes of LPS-exposed and control AMs at baseline and upon subsequent bacterial stimulation, AMs were isolated six days after training and incubated for 3 h with medium or HISP (Fig. 3A). Principal component analysis (PCA) of RNA-seq results revealed a high similarity between trained and control AMs (Fig. 3B and C), and only 10 differentially expressed genes (DEGs) at baseline (Table S1). In contrast, transcriptional profiles clustered according to the preceding training stimulus upon bacterial challenge (Fig. 3B and C), which correlated with 165 upregulated and 27 downregulated genes identified in LPS-trained compared to control AMs (Table S2). DEGs detected upon HISP challenge mapped to different KEGG (Kyoto Encyclopedia of Genes and Genomes) pathways (Fig. 3D), with “cytokine-cytokine receptor interaction” and “chemokine signaling” pathways being most differentially regulated. Among on these pathways, signaling-related genes (*Prkcd*, *Nfkb1*, *Raf1*) as well as genes encoding chemokines of CC (*Ccl22*, *Ccl3*) and CXC (*Cxcl2*, *Cxcl3*) subfamilies were differentially expressed upon HISP stimulation (Fig. 3E).

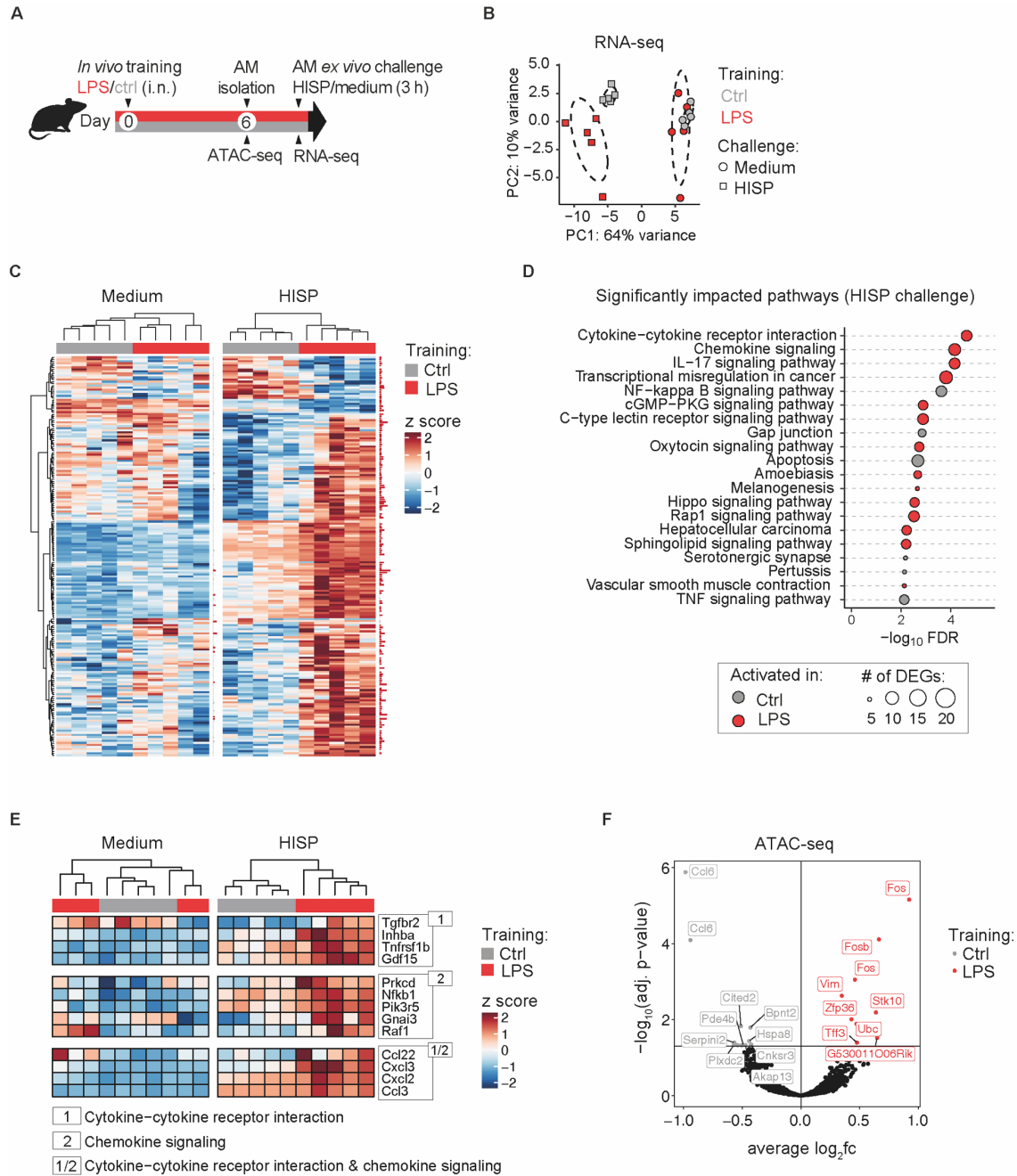


Figure 3 - LPS-trained AMs display an altered gene expression profile upon ex vivo challenge. (A) Experimental setup for ATAC-seq and RNA-seq analysis of AMs isolated on day six after *in vivo* training. (B) Principal component analysis of normalized gene expression data obtained from *in vivo* trained AMs upon 3 h ex vivo HISP-challenge (squares) or medium (circles). (C) Heatmap depicting DEGs in trained and control AMs upon medium or HISP challenge. Samples are clustered by unsupervised clustering. Data are *rlog* transformed, followed by z-score scaling. Cutoff: adjusted p-value ≤ 0.1 ; red horizontal bars adjacent to heatmaps indicate statistical significance. (D) Top 20 KEGG pathways in HISP-challenged trained and control AMs. Circle size indicates to the number of DEGs associated with the respective pathway. (E) Heatmaps depicting DEGs identified in the top two differentially regulated pathways in trained and control AMs upon medium or HISP challenge. Data are *rlog* transformed, followed by z-score scaling. (F) Volcano plot displaying differentially accessible regions (DARs; $\text{padj} \leq 0.05$) of trained versus control AMs identified by ATAC-seq analysis six days after *in vivo* training. Labels indicate top 10 DARs per group.

In accordance, CXCL1 protein levels were markedly increased upon *ex vivo* challenge of trained AMs (Fig. S2A).

To assess whether the altered transcriptional responsiveness of LPS-exposed AMs was associated with persistent epigenetic changes reflected by altered chromatin accessibility, BAL AMs were processed for Assay for Transposase-Accessible Chromatin (ATAC)-seq analysis on day six after *in vivo* training (Fig. 3A). In total, we identified 24 differentially accessible regions (DARs; Fig. S4A and Table S3; FDR ≤ 0.05), nine of which were more accessible in the trained group (Fig. 3F). Among these, three DARs were annotated to the genes *Fos* (2 DARs) or *Fosb* (1 DAR), which are associated with transcriptional regulation of multiple biological processes, including cell migration, differentiation and inflammation (Bejjani *et al*, 2019). Next we considered the possibility that accelerated gene expression upon secondary challenge may result from altered baseline deposition of permissive histone marks, such as H3K4 methylation or H3K27 acetylation (Yan & Boyd, 2006). To test whether AM training depends on methylation- or acetylation events established during LPS exposure, we trained WT mexAMs in presence of the methyltransferase inhibitor 5'-deoxy-5'-methylthioadenosine (Ifrim *et al*, 2014) (MTA), the acetyltransferase inhibitor anacardic acid (Sun *et al*, 2006) or DMSO. After 24 h, cells were washed and allowed to rest in medium until bacterial challenge (Fig. S4B). Neither of the inhibitors influenced the trained IL-6 response (Fig. S4C), suggesting that the targeted epigenetic enzymes do not contribute to LPS-induced AM memory.

Collectively, trained and control AMs displayed similar gene expression levels and few changes in chromatin accessibility at baseline, but mounted an augmented transcriptional response upon secondary, bacterial challenge.

2.3.4 Secondary metabolic AM responses are modulated by prior LPS exposure

Recent research highlighted the critical impact of cellular metabolism on the functional state of immune cells, including the induction, maintenance and regulation of trained immunity (Arts *et al*, 2016a). Importantly, metabolic pathways do not only provide energy and macromolecular building blocks, but can directly influence the epigenetic machinery by providing intermediate metabolites that serve as substrates or cofactors (Riksen & Netea, 2021). In monocytes and macrophages, glycolysis, glutaminolysis and cholesterol synthesis have been described to play crucial roles in the induction of trained immunity, with increased glycolysis defined as hallmark of trained macrophages (Arts *et al*, 2016a; Riksen & Netea, 2021). AMs, however, are unique tissue-resident immune cells that are metabolically adapted to the remarkably low glucose concentration of the alveolar space, and primarily utilize oxidative phosphorylation to meet their energy demands (Woods *et al*, 2020). We therefore speculated that the metabolic

characteristics of trained AMs may differ from those classically associated with trained monocytes and macrophages. To investigate the baseline metabolism of AMs six days after *in vivo* training, we performed Seahorse analyses (Fig. 4A and B).

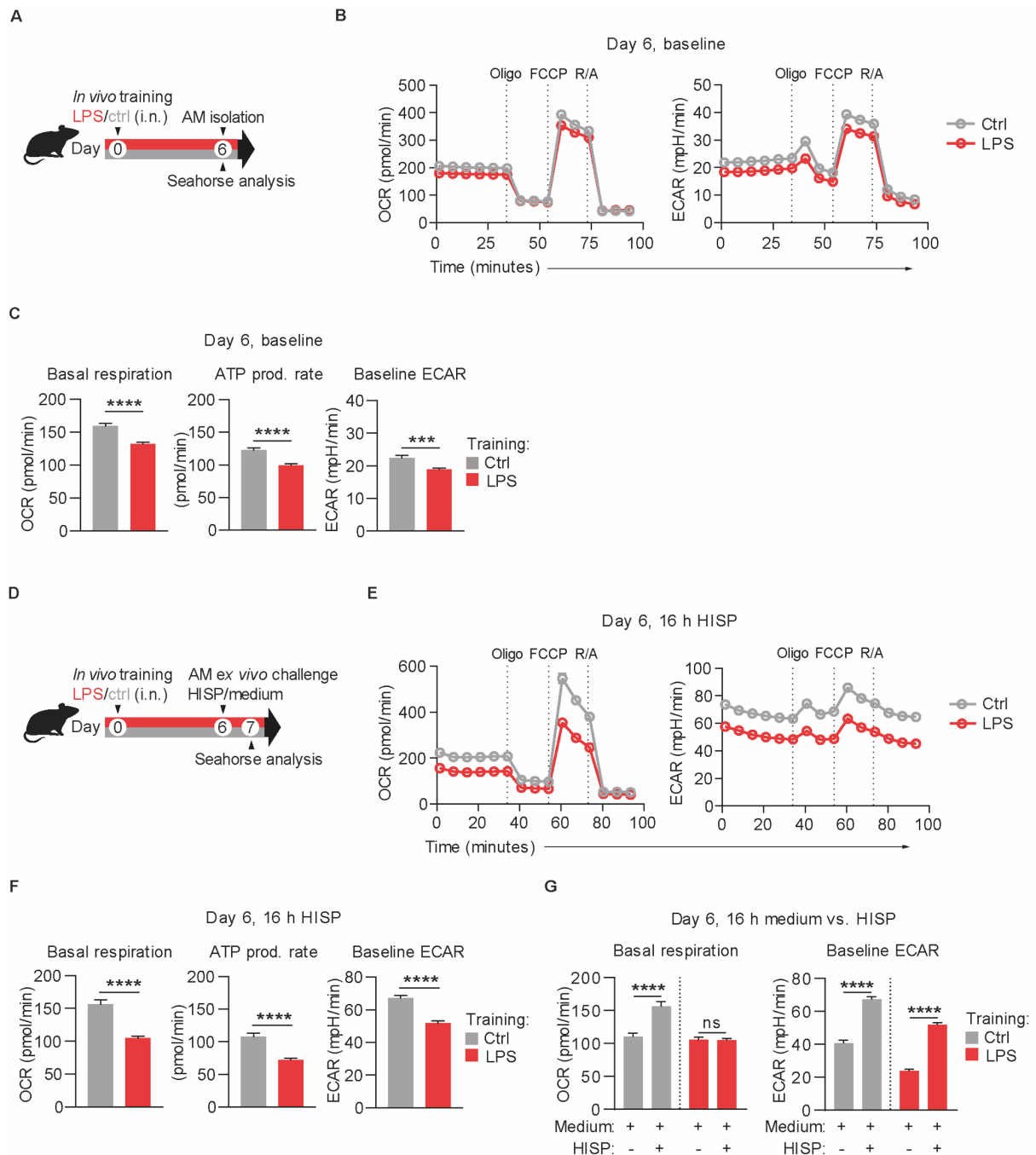


Figure 4 - LPS exposure persistently alters the metabolic state and responsiveness of AMs.

(A) Experimental setup for Seahorse analyses of AMs on day six after *in vivo* training with LPS/saline. (B) OCR and ECAR of trained and control AMs, measured at baseline and after sequential treatment with oligomycin (Oligo), FCCP and rotenone/antimycin A (R/A). (C) Quantification of baseline OCR (basal respiration), ATP production rate and baseline ECAR. (D) Experimental setup for Seahorse analyses of AMs upon *ex vivo* HISP- or medium challenge (16 h) on day six after training. (E) OCR and

ECAR of trained and control AMs, 16 h after HISP stimulation, measured at baseline and after sequential treatment with indicated drugs. **(F)** Quantification of basal respiration, ATP production rate and baseline ECAR 16 h after HISP challenge. **(G)** Quantification of baseline OCR and ECAR 16 h after stimulation with HISP in medium versus medium only. Graphs show means + SEM of 10-11 technical replicates from pooled biological replicates (n=5-8). Data are representative of two independent experiments. Statistical analysis: student's t-test. ns, not significant. *** $p \leq 0.001$, **** $p \leq 0.0001$; OCR, oxygen consumption rate; ECAR, extracellular acidification rate; FCCP, carbonyl cyanide-4-(trifluoromethoxy)phenylhydrazone.

Compared to control AMs, LPS-exposed AMs displayed a reduced basal metabolic activity, reflected by a decreased oxygen consumption rate (OCR) and extracellular acidification rate (ECAR) (Fig. 4C). Sequential inhibition of selected electron transport chain (ETC) components further revealed a reduced ATP production rate of trained AMs (Fig. 4C), while maximum respiratory capacity and spare respiratory capacity (SRC) were unaltered (Fig. S5A). To assess how prior LPS exposure affects AM metabolism upon secondary, bacterial challenge, we performed Seahorse analyses of trained and control AMs 16 h after incubation with HISP (Fig. 4D and E). Interestingly, basal OCR and ECAR, ATP production (Fig. 4F), as well as maximum and spare respiratory capacity (Fig. S5B) were significantly decreased in trained cells. While saline-exposed AMs exhibited an increased OCR upon bacterial stimulation (16 h; compared to incubation with medium only), trained AMs displayed similar OCR levels in presence or absence of HISP (Fig. 4G). Although both trained and control cells increased their ECAR upon bacterial challenge (Fig. 4G), the absolute ECAR of trained AMs was lower than that of control AMs at the investigated time point.

In summary, these experiments demonstrate that ambient LPS exposure rewires AM metabolism, which further impacts the metabolic response to subsequent bacterial challenge.

2.3.5 LPS training induces changes in AM metabolite and lipid composition

Based on these findings, we went on to investigate the effects of LPS training on the metabolite and lipid composition of AMs. CD11c⁺ Siglec F⁺ AMs were FACS-sorted six days after LPS administration and subjected to LC-MS/MS-based analyses (Fig. 5A; Fig. S6A). Targeted metabolomic analysis revealed that trained AMs contained increased amounts of S-adenosyl-methionine (SAM; Fig. 5B), an essential metabolite synthesized from methionine and ATP (Parkhitko *et al*, 2019). In accordance, intracellular amino acid profiles (Fig. S6B) showed a trend for increased methionine concentrations in trained AMs compared to control cells (Fig. S6C). SAM acts as a universal methyl group donor for RNA, DNA, lipids and proteins and was reported to drive a proinflammatory macrophage phenotype in the context of LPS-induced inflammation (Yu *et al*, 2019).

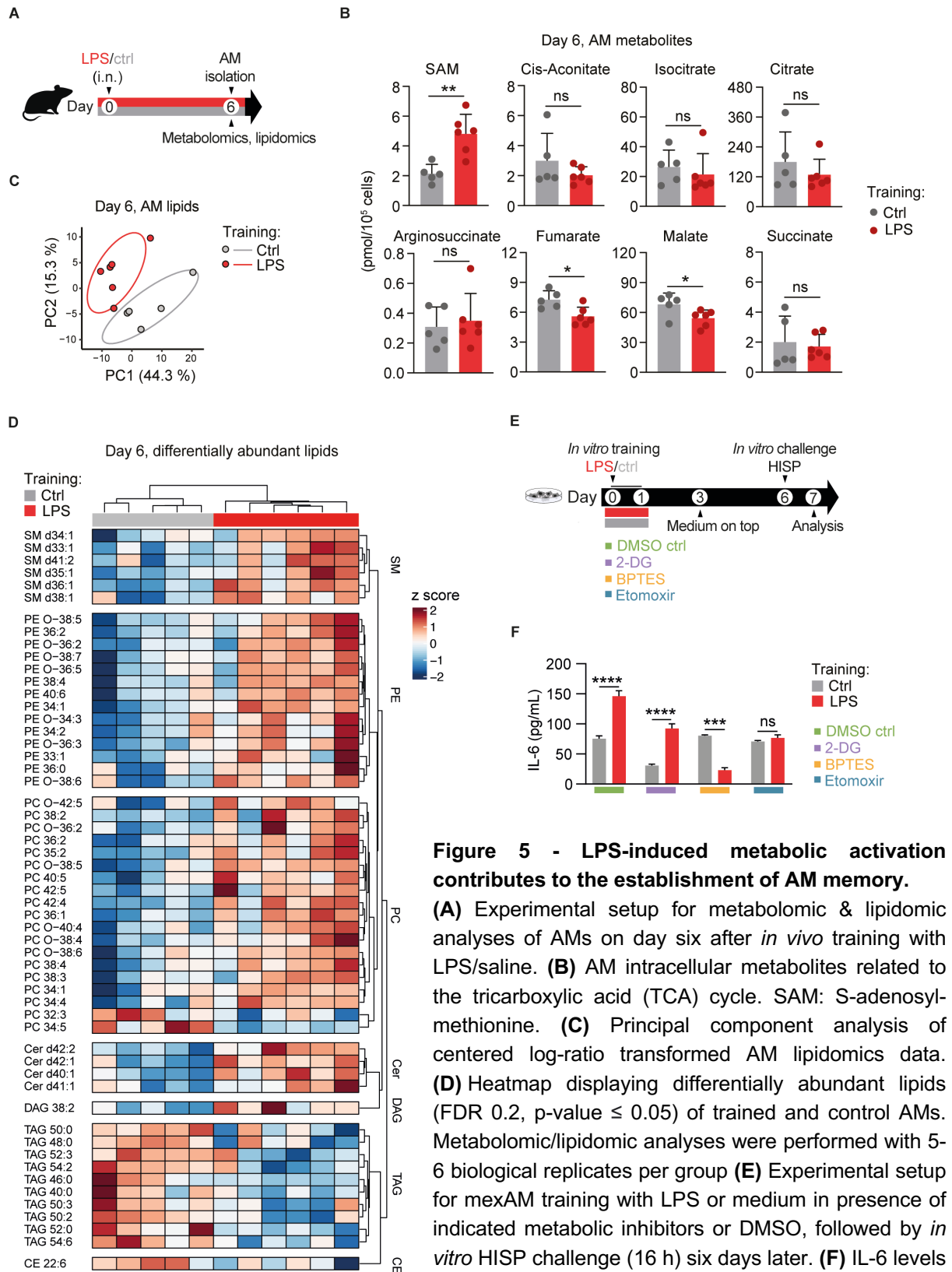


Figure 5 - LPS-induced metabolic activation contributes to the establishment of AM memory.

(A) Experimental setup for metabolomic & lipidomic analyses of AMs on day six after *in vivo* training with LPS/saline. (B) AM intracellular metabolites related to the tricarboxylic acid (TCA) cycle. SAM: S-adenosyl-methionine. (C) Principal component analysis of centered log-ratio transformed AM lipidomics data. (D) Heatmap displaying differentially abundant lipids (FDR 0.2, p-value ≤ 0.05) of trained and control AMs. Metabolomic/lipidomic analyses were performed with 5-6 biological replicates per group (E) Experimental setup for mexAM training with LPS or medium in presence of indicated metabolic inhibitors or DMSO, followed by *in vitro* HISP challenge (16 h) six days later. (F) IL-6 levels of mexAMs stimulated as described in (E). Data are representative of two independent experiments. Graphs show means + SD of 5-6 biological replicates (B) or means + SEM of 4-5 technical replicates (F). Statistical analysis: student's t-test (B) and two-way ANOVA (F) (factor 1: training; factor 2: inhibitor). ns, not significant. * $p \leq 0.05$, ** $p \leq 0.01$, *** $p \leq 0.001$, **** $p \leq 0.0001$. Cer: ceramides; DAG: diacylglycerols; PE: phosphatidylethanolamines; SM: sphingomyelins; PC: phosphatidylcholines; CE: cholesterol esters; TAG: triacylglycerols.

In addition, LPS exposure modulated metabolites of the tricarboxylic acid (TCA) cycle, with fumarate and malate being significantly reduced compared to control AMs (Fig. 5B). Interestingly, lipidomic analysis identified profound differences between LPS- and saline-exposed AMs on day six after training (Fig. 5C). Trained AMs contained substantially higher amounts of selected ceramides (Cer), phosphatidylethanolamines (PE), sphingomyelins (SM) and phosphatidylcholines (PC), essential membrane lipids that can directly or indirectly impact membrane receptor signaling (Sunshine & Iruela-Arispe, 2017). In contrast, triacylglyceride (TAG) levels were strongly reduced in trained compared to control AMs (Fig. 5D). TAGs serve as cellular energy stores that fuel cell intrinsic ATP production in the mitochondria by providing free fatty acids for β -oxidation (Castoldi *et al*, 2020). In summary, these findings imply that *in vivo* LPS exposure profoundly modulates the metabolite and lipid composition of AMs.

2.3.6 LPS-induced rewiring of AM metabolism is critical for memory induction

Tissue-resident AMs predominantly rely on oxidative phosphorylation (OXPHOS) to meet their metabolic demands (Khaing & Summer, 2020). This process is tightly linked to the TCA cycle, which serves as the main electron donor for the mitochondrial ETC. Substrates fueling the TCA cycle can be generated by multiple processes, including fatty acid oxidation (FAO), glutaminolysis and oxidation of amino acids or pyruvate (Martinez-Reyes & Chandel, 2020). Based on the altered metabolite and lipid composition of LPS-exposed AMs, we speculated that the initial metabolic activation evoked by the training stimulus might be critical for the altered reactivity observed upon secondary challenge. To test this hypothesis, we applied selective metabolic inhibitors during *in vitro* mexAM training and determined the consequences on the trained IL-6 response exerted upon bacterial challenge. 2-deoxyglucose (2-DG), bis-2-(5-phenylacetamido-1,3,4-thiadiazol-2-yl)ethyl sulfide (BPTES) and etomoxir were used to inhibit glycolysis, glutaminolysis or FAO, respectively (Fig 5E). While glycolysis appeared to be dispensable for the establishment of mexAM memory, inhibition of FAO and glutaminolysis abrogated the trained IL-6 response of LPS-exposed cells (Fig. 5F), suggesting that LPS-mediated metabolic rewiring is critical for the establishment of AM memory.

2.3.7 LPS training modulates pneumonia outcome

AM activation represents an ambiguous balancing act, which serves to promote pathogen clearance while maintaining tissue integrity. Consequently, malfunction, hypo- or hyperactivation of AMs can have detrimental consequences for the host (Bain & MacDonald, 2022; Hetzel *et al*, 2021). To investigate whether LPS-trained AMs can modulate the outcome of a subsequent pneumococcal infection, we isolated AMs five days after *in vivo* training

(Fig.S7A-C) and transferred them intratracheally (i.t.) into naïve recipients (Fig. S7D), followed by i.n. *S. pneumoniae* infection ("in vivo challenge") 24 h later (Fig. 6A).

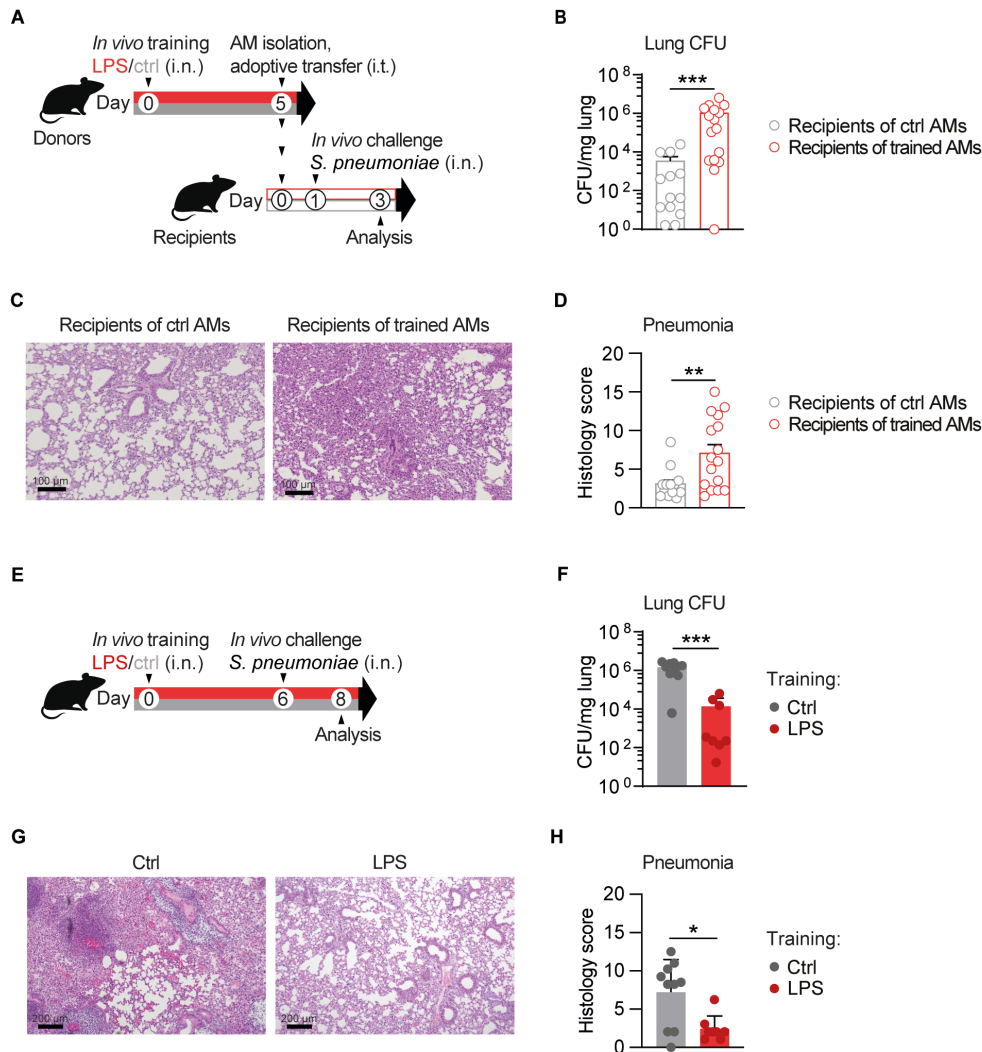


Figure 6 - LPS exposure modulates pneumonia outcome in a context-dependent manner.

(A) Experimental setup for adoptive transfer of LPS-trained or control donor AMs, followed by i.n. *S. pneumoniae* infection (in vivo challenge). Donor AMs were isolated by BAL five days after in vivo training and transferred intratracheally (i.t.) to naïve WT mice. Recipients were i.n. infected with *S. pneumoniae* 24 h after cell transfer. (B) Lung bacterial loads of recipients, determined 48 h after infection. (C, D) Representative histology images (C) and pneumonia score (D) of H&E-stained lung tissue 48 h after infection; scale bars: 100 µm. Graphs show means + SEM of two pooled experiments with 6-8 biological replicates each (total n = 12-16). (E) Experimental setup for in vivo training, followed by infection with *S. pneumoniae* (in vivo challenge) on day six. (F) Lung bacterial loads, 48 h after infection. (G, H) Representative histology images (G) and pneumonia score (H) of H&E-stained lung tissue, 48 h after infection; scale bars: 200 µm. Graphs show means + SD of 8-10 biological replicates. Data are representative of two independent experiments. Statistical analysis: Mann-Whitney-U test. *p ≤ 0.05, **p ≤ 0.01, ***p ≤ 0.001.

Recipients of trained AMs displayed increased bacterial loads (Fig. 6B) and lung inflammation (Fig. 6C and D), indicating that adoptive transfer of LPS-experienced AMs impairs host defense against bacterial pneumonia. Considering that LPS-mediated effects on other (i.e. non-AM) cell populations are omitted in a transfer setup, we next addressed the impact of LPS training in a physiologically more relevant setting and infected mice with *S. pneumoniae* six days after LPS exposure (Fig. 6E).

These experiments revealed that LPS-pretreated animals displayed enhanced bacterial clearance (Fig. 6F) and reduced lung tissue inflammation (Fig. 6G and H) 48 h after infection. While LPS-exposed animals demonstrated increased recruitment of inflammatory cells early upon infection (6 h; Fig. S7E-G), monocyte and neutrophil numbers were decreased after 48 h (Fig. S7H), indicating accelerated initiation and resolution of inflammation.

Overall, our results highlight the necessity to investigate the physiological consequences of environmental exposures as they may be influenced by multiple cellular players and tissue-specific parameters.

2.4 Discussion

Continuous exposure to environmental microbial triggers poses a strong impact on the education and maturation of our immune system, affecting human health and disease susceptibility (MacGillivray & Kollmann, 2014). Due to their unique location at the interphase of the airways and our environment, AMs are in direct contact with inhaled substances and thus represent potential candidates to develop mucosal-associated trained immunity. Yet, our current knowledge about the tissue-specific properties and consequences of AM memory remains very limited. In this study we discovered that pulmonary exposure to ambient amounts of LPS (corresponding to an inhaled endotoxin concentration of ~ 0.5 EU) induces a robust AM memory response, characterized by increased phagocytic activity and cytokine production upon secondary, bacterial challenge. Our RNA-seq and protein analyses collectively revealed that LPS-experienced AMs, being transcriptionally similar to control AMs at baseline, produced elevated amounts of multiple cytokines (e.g. IL-6, IL12-p40 and IL-1 β) following subsequent pneumococcal challenge. Given that some of these factors (CXCL1, CXCL2 and CXCL3) are powerful neutrophil chemoattractants that play a prominent role in host defense (Cai *et al*, 2010; Fillion *et al*, 2001), LPS-induced AM memory may potentially impact the immune response and outcome of infectious challenges by modulating pulmonary inflammation and/or neutrophil recruitment. While AM memory was overall associated with increased production of pro-inflammatory cytokines, we also observed an upregulation of

IL-10. This anti-inflammatory mediator was reported to play an ambivalent role in host defense against *S. pneumoniae* as it prevented exacerbated neutrophil influx while favoring bacterial dissemination (Penaloza *et al*, 2015). In this context, future studies will be required to investigate a potential immunomodulatory effect of trained IL-10 production during pneumococcal infection.

Innate memory responses have mechanistically been linked to epigenetic reprogramming events induced upon exposure to the training stimulus (Fanucchi *et al*, 2021). However, this evidence is primarily based on studies investigating trained immunity in the context of cellular differentiation. For instance, it was reported that systemic administration of Bacille Calmette-Guérin (BCG) promotes bone marrow myelopoiesis by inducing transcriptional changes in hematopoietic stem cells, which give rise to epigenetically modified, trained macrophages (Kaufmann *et al*, 2018). Additionally, β -glucan-trained murine monocytes were shown to differentiate into epigenetically altered macrophages, which confer protection against *Candida albicans* infection (Quintin *et al*, 2012). In this study, we characterized the epigenetic profile of AMs upon *in vivo* training and discovered few changes in chromatin accessibility six days after LPS exposure. In a recent publication, Aegerter *et al.* demonstrated that tissue-resident AMs displayed minimal changes in chromatin accessibility following an infectious lung insult, whereas monocyte-derived AMs readily maintained an open chromatin conformation (Aegerter *et al*, 2020). While our data support the notion that AMs exhibit limited epigenetic plasticity, it remains to be investigated whether differential regulation of the identified chromatin loci plays a mechanistic role in the establishment of AM memory. Exploring the possibility that altered baseline deposition of histone marks could mediate AM training, we further demonstrated that selective inhibition of methyl- and acetyltransferase activity did not diminish the training effect. While these findings collectively suggest that chromatin remodeling is no major driving factor of LPS-induced AM memory, it remains to be investigated whether other epigenetic mechanisms (e.g. modulation of gene expression by micro RNAs) or other enzyme classes are critical for AM training.

Despite their limited inflammatory potential at steady state, AMs constitute the front line of cellular host defense against respiratory pathogens and play an important role in the initiation of the inflammatory response (Rubins, 2003). Due to their continuous exchange with the environment, they represent ideal candidates to investigate trained immunity at mucosal sites. Yao *et al.* demonstrated that respiratory adenoviral infection induces AM memory via CD8⁺ T cell-derived IFN- γ (Yao *et al*, 2018). However, while IFN- γ -exposed AMs showed enhanced responsiveness upon subsequent *S. pneumoniae* challenge, the cells did not return to a baseline state following adenoviral infection, which was illustrated by elevated glycolysis and

increased transcriptional activity 28 days after adenoviral exposure. These findings imply that the increased reactivity of memory AMs upon secondary challenge may possibly be a consequence of prior IFN- γ -priming rather than innate training. While IFN- γ -priming constitutes a well-established concept and reportedly alters macrophage immunity by promoting a proinflammatory phenotype (Hayes *et al*, 1995; Mosser & Edwards, 2008; Wu *et al*, 2014), we showed that LPS-induced AM training occurs *independently* of IFN- γ -receptor signaling and adaptive immunity, and, instead, identified a novel mechanistic regulation of pulmonary macrophage memory. We discovered that type1 IFN deficiency profoundly diminishes AM training and extended our findings by showing that i.n. administration of IFN- β can replicate the training effect of pulmonary LPS exposure. While type 1 IFNs possess potent antiviral and immunostimulatory properties, mistimed, inappropriate or excessive type 1 IFN responses can impair anti-bacterial immunity, and thus facilitate secondary bacterial superinfections, e.g. via suppression of Th17 responses (Kudva *et al*, 2011; Lee *et al*, 2015) or impairment of neutrophil recruitment (Navarini *et al*, 2006). Notably, our experimental model differs from settings of viral-bacterial superinfections in important aspects, such as the extent and duration of type 1 IFN exposure, as well as the timing of *S. pneumoniae* infection. As we have not investigated a potential impact of i.n. IFN- β treatment on pneumonia outcome in this study, future research will be required to assess potential consequences of exogenous IFN- β administration on pneumococcal clearance.

Recent research has highlighted the critical impact of cellular metabolism on immune cell activation and regulation of innate memory responses (Riksen & Netea, 2021). Along these lines, multiple studies provide evidence for a key role of glycolytic metabolism in trained monocytes (Arts *et al*, 2016a). In addition to glycolysis, glutaminolysis has been reported to be essential for the induction of BCG-induced innate memory (Arts *et al*, 2016b) and both pathways have been shown to be closely intertwined with epigenetic regulation. While these studies have highlighted a critical role of metabolic regulation in trained immunity *in vitro*, we lack knowledge about tissue-specific metabolic reprogramming of innate immune cells.

The pulmonary niche constitutes a unique mucosal environment, which is characterized by remarkably low glucose availability (Baker *et al*, 2007). Being metabolically adapted to these conditions, AMs display limited glycolytic activity and rely on mitochondrial oxidative phosphorylation (Khaing & Summer, 2020; Woods *et al*, 2020). A recent study by Svedberg *et al*. demonstrated that impaired glycolysis of AMs limits their responsiveness during type 2 inflammation (Svedberg *et al*, 2019), suggesting a functional implication of this metabolic constraint. We here identified a critical role of glutaminolysis and FAO in the establishment of LPS-induced AM memory and provide evidence that glycolytic activation is dispensable for this process. Of note, the altered metabolic profile of AMs was not reflected on a gene

expression level, which might potentially be explained by different temporal dynamics of metabolic and genetic responses. To our knowledge, this study is the first to describe a metabolic dependency of AM memory, and to report a role of FAO in trained immunity of tissue-resident macrophages. Furthermore, these data emphasize that the cellular characteristics of AM memory reflect their unique immunological and metabolic properties.

In recent years, several epidemiological and experimental studies have identified a protective role of trained immunity due to heterologous protection against unrelated pathogens (Arts *et al*, 2018; Ciarlo *et al*, 2020; Quintin *et al*, 2012). However, innate memory responses may also be maladaptive in conditions of chronic inflammation, such as atherosclerosis, neurodegeneration and autoimmunity (Bekkering *et al*, 2021). In this study, we found that adoptive transfer of trained AMs resulted in increased lung inflammation and impaired bacterial clearance following *S. pneumoniae* infection (compared to recipients of control AMs). In contrast, i.n. exposure to LPS, a scenario in which LPS-mediated reprogramming can potentially affect any lung-resident cell population, improved pneumonia outcome. Based on these findings, and disregarding the inherent limitations of cell transfer experiments due to concomitant inflammation, we speculate that i.n. LPS treatment not only induces AM training but likely imprints other (non-AM) cell populations (e.g. resident structural, myeloid or lymphoid cell types), thereby altering their responsiveness to *S. pneumoniae* challenge. Such additional reprogramming events might be crucial to prevent excessive inflammation and promote anti-bacterial immunity. Similarly, LPS-induced modulations of the local immune and metabolic environment (e.g. altered availability of soluble mediators or metabolites) may critically influence the outcome of subsequent infectious challenges. While our data indicate that trained AMs can exert a significant impact on pneumococcal clearance in a transfer setting, the experimental set up did not enable us to delineate whether and how AMs contribute to the protective effect following intranasal LPS exposure. These findings may therefore represent two independent observations. However, they collectively underline the complexity of biological systems and illustrate that a single cell population may not be sufficient to dictate the ultimate outcome of host defense.

Several epidemiological studies have demonstrated that exposure to a microbe-rich, diverse environment is linked to a decreased prevalence of allergies, a phenomenon commonly referred to as the “farm effect” (Pivniouk *et al*, 2020). A remarkable example for this effect is offered by a study showing that house dust from traditional farming environment decreases asthma prevalence and development by engaging and modulating innate immunity (Stein *et al*, 2016). We here demonstrated that inhalation-exposure to ambient endotoxin levels significantly improves the outcome of bacterial pneumonia. While these findings underline the

immunomodulatory potential of environmental agents, future studies will be required to dissect the underlying cellular mechanisms of this observation. Furthermore, it remains to be investigated whether LPS-induced reprogramming of AMs plays a role in allergic airway inflammation and other respiratory diseases.

Altogether, our data highlight the necessity to investigate trained immunity in a tissue-specific context and emphasize that the mechanisms and consequences of innate memory are influenced by the local microenvironment and disease setting.

2.5 Materials and Methods

Additional methodological details on cell isolation and flow cytometry, phagocytosis/efferocytosis assays, RNA-seq, ATAC-seq and LC-MS/MS sample preparation and data analysis, mexAM culture, histological evaluation and study design can be found in the Supplementary Materials.

Mice

Age-matched, 8-10-week-old male mice were used throughout the study. Mice were housed at the Medical University of Vienna (MUW, Austria), at the Institute of Molecular Biotechnology (IMBA, Vienna, Austria), at the Vienna BioCenter (VBC, Austria) or at the Max Planck Institute (MPI) of Immunobiology and Epigenetics (Freiburg, Germany). C57BL/6J mice were purchased from Janvier (in-house maintenance breeding at MUW) or from the Jackson Laboratory (maintenance at MPI). Rag2^{-/-} mice (Hao & Rajewsky, 2001) (originally ordered from Jackson), Ifnar^ΔCD169 and Ifnar^{fl/fl} control mice were bred at IMBA. Ifnar1^{-/-} (Muller *et al*, 1994), Ifngr1^{-/-} (Huang *et al*, 1993), and respective C57BL/6N wild type control mice were bred at the VBC. All mice were housed in a specific pathogen-free environment according to the Federation of European Laboratory Animal Science Associations (FELASA) guidelines and were matched for sex, age and genetic background in individual experiments. All mouse experiments were approved by and performed in accordance with the Austrian Federal Ministry of Science and Research (BMWF-66.009/0363-WF/V/3b/2017; 2020-0.009.488) and the Regierungspraesidium Freiburg, Germany (35-9185.81/G-18/65).

In vivo training

Mice received 50 µL endotoxin-free saline (Braun) containing 1 ng LPS (Sigma; E.coli O55:B5) or 2000 U mouse IFN-β (pbl assay science) or saline only i.n. under light isoflurane

anaesthesia (2% isoflurane, 2 L/min O₂) or after intraperitoneal (i.p.) injection of Ketazol (100 mg/kg; OGRIS Pharma) and Rompun (10 mg/kg; Bayer).

Ex vivo challenge of AMs

On day six after *in vivo* training, AMs were isolated by BAL as described (s. Supplementary Materials). Cells were resuspended in RPMI medium (10% FCS, 1% penicillin-streptomycin [PS; Sigma]), counted and seeded at a density of 5×10^4 cells per well in a TC-treated 96 well plate (Corning). After 2 h, non-adherent cells were washed off with PBS. Subsequently, trained and control AMs were challenged with heat-inactivated *S. pneumoniae* (HISP; ATCC6303, MOI [multiplicity of infection] 100) in RPMI medium (3% FCS, 1% PS) or with medium only for 3 h (RNA-seq analysis) or 16-24 h (cytokine analysis, Seahorse experiments). IL-6 levels were quantified by ELISA (BioLegend) or LEGENDplex (BioLegend). Levels of CXCL1, TGF- β 1, G-CSF, IL-18, IL-23, CCL22, IL-10, IL-12p40, IL-6, TNF- α , CCL17 and IL-1 β were measured using the LEGENDplex Mouse Macrophage/Microglia Panel (BioLegend) according to the manufacturer's instructions. Data analysis was performed using the LEGENDplex data analysis software.

In vivo labeling of tissue-resident AMs

Tissue-resident AMs were labeled by i.n. treatment with PKH26 (Sigma) eight days prior to *in vivo* training. The dye was prepared according to the manufacturer's instructions and administered at 10 μ M in a volume of 50 μ L. At indicated time points, BALF and post-lavage lung AMs were analyzed by flow cytometry to determine frequencies of PKH26⁺ and PKH26⁻ cells.

Seahorse analysis

AMs were isolated by BAL six days after *in vivo* training. Biological replicates were pooled by experimental group and seeded in technical replicates in XF-96 cell culture plates (Agilent) at a density of 8×10^4 cells/well in 80 μ L RPMI medium (3% FCS, 1% PS). To remove non-adherent cells, the plate was incubated for 2 h at 37°C and cells were washed twice either with PBS (followed by subsequent *ex vivo* challenge, performed as described) or XF assay medium (Seahorse XF RPMI medium, pH 7.4, 10 mM Glucose, 1 mM Pyruvate, 2 mM L-Glutamine [all from Agilent], 3% FCS). Prior to analysis, cells were incubated under non-CO₂ conditions in XF assay medium for 1 h. Oxygen consumption rate (OCR) and extracellular acidification rate (ECAR) of AMs were analyzed using a Seahorse XF-96 Extracellular Flux Analyzer (Agilent). Where indicated, 1 μ M oligomycin, 1.5 μ M carbonyl cyanide p-trifluoromethoxyphenylhydrazone (FCCP) or 100 nM rotenone plus 1 μ M antimycin A (all from

Sigma) were injected to assess mitochondrial function. Means of R/A values (non-mitochondrial respiration) were subtracted from OCR raw data for quantification of mitochondrial parameters. ECAR data represent raw values.

Murine pneumonia model

Pneumonia was induced by i.n. infection with 10^4 CFUs mid-logarithmic-stage *S. pneumoniae* serotype 3 (ATCC6303) as previously described (Rijneveld *et al*, 2001). Lungs were harvested 48 h after infection. Right lobes were collected for determination of bacterial counts, the left lobe was collected for histological analysis. Bacterial growth was quantified by plating 10-fold serial dilutions of lung homogenates on blood agar plates.

Adoptive AM transfer

For adoptive AM transfer experiments, donor AMs were isolated by BAL on day five after *in vivo* training with LPS or saline. BALF samples were pooled by experimental group and centrifuged for 5 min (4°C, 300 g). Cells were resuspended in PBS, counted and diluted to a concentration of 10^7 cells/mL. Subsequently, 3×10^5 cells were transferred intratracheally to naïve wild type recipients in a volume of 30 µL. Twenty-four hours after transfer (i.e. six days after donor training), recipients were i.n. infected with 10^4 CFU *S. pneumoniae*.

Statistical analysis

Differences in values obtained from two experimental groups were assessed by student's t-test (unpaired) or Mann-Whitney test (non-parametric). One-way-ANOVA or two-way ANOVA analysis followed by Šídák's multiple comparisons test was used to determine differences between multiple groups. Data were analyzed using GraphPad Prism 8.0 and are presented as mean +SD or mean + SEM for experiments performed with biological or technical replicates, respectively.

Data availability

Raw and processed sequencing data (RNA-seq and ATAC-seq) are available in the NCBI Gene Expression Omnibus database (accession number GSE184684). Raw and processed LC-MS/MS data are available in the MetaboLights database (accession number MTBLS3151).

2.6 Supplementary Methods

Cell isolation and flow cytometry (BAL, lung)

BAL fluid was collected as previously described with minor modifications (Rijneveld *et al*, 2001). In brief, after exposure and midline incision of the trachea, mouse airways were flushed with a total of 5 mL endotoxin-free saline by instillation of 0.5 mL aliquots via a sterile 18-gauge tracheal cannula (Venflon, BD). Prior to staining, BALF samples were pelleted by centrifugation (4°C, 300g) and resuspended in PBS 1% BSA. Post-lavage lungs were weighed, and tissue homogenization was performed using a gentleMACS™ Tissue Dissociator (Miltenyi Biotec) following the manufacturer's protocol with minor adaptations. Briefly, after primary homogenization (program m_lung_01_02), lungs were digested for 35 min on a shaker (37°C, 180 rpm) in RPMI medium supplemented with 5% FCS (Sigma), DNase I (12 U/ mL, Sigma) and Collagenase I (160U/ mL, Gibco). Subsequently, suspensions were homogenized (program m_lung_02_01), filtered over 70 µm strainers (Miltenyi Biotec) and centrifuged for 5 min (4°C, 300 g). Erythrocytes were lysed on ice in ACK lysis buffer (150 mM NH₄Cl, 10 mM KHCO₃, 0.1 mM Na₂EDTA, pH 7.2 – 7.4; all chemicals from Sigma), cell suspensions were filtered over 30 µm strainers and resuspended in PBS 1% BSA. BALF and lung cell suspensions were incubated with viability dye (eBioscience) and anti-mouse CD16/32 (eBioscience), followed by fluorescently labeled monoclonal antibodies (Table S4). Stained cells were washed with PBS and fixed for 30 min using Fix&Perm Fixation Medium A (Nordic Mubio) unless indicated otherwise. Samples were acquired on an LSR Fortessa flow cytometer (BD) and analyzed using FlowJo software (FlowJo LLC). For LC-MS/MS analysis, CD11c⁺ Siglec F⁺ AMs were flow-sorted on a FACS Aria™ Fusion flow cytometer (BD).

Phagocytosis assay

AM phagocytosis was assessed on day six after *in vivo* training with LPS or saline. AMs were isolated by BAL, seeded at equal numbers and left to adhere in RPMI medium (10% FCS, 1% PS). After 2 h, cells were washed with PBS and incubated with FITC-labeled HISP (MOI 100) in RPMI medium (3% FCS, 1% PS) at 37°C or 4°C (negative control) for 45 min. Thereafter, cells were washed again and treated with proteinase K (50 µg/mL; Roche) for 10 min at 4°C to remove residual adherent bacteria. After washing, samples were processed for flow cytometry as described and incubated with fluorescently labeled monoclonal antibodies (anti-CD45, anti-CD11c and anti-Siglec F; Table S4) to allow identification of AMs. Cells were analyzed by flow cytometry without prior fixation. The phagocytosis index was calculated as $[(37^{\circ}\text{C } \% \text{FITC}^{+} \text{ AMs}) \times (37^{\circ}\text{C } \text{FITC MFI of FITC}^{+} \text{ AMs})] - [(4^{\circ}\text{C } \% \text{FITC}^{+} \text{ AMs}) \times (4^{\circ}\text{C } \text{FITC MFI of FITC}^{+} \text{ AMs})]$.

Adoptive transfer of CFSE-labeled apoptotic thymocytes (efferocytosis assay)

For efferocytosis assays, thymocytes were isolated from 4-week old wild type mice, seeded at a density of 1.8×10^7 cells/well in a non-coated 12-well plate (CytoOne) and incubated in RPMI medium (10% FCS, 1% PS) containing dexamethasone ($1 \mu\text{M}$, Sigma). After 24 h, the apoptotic cells were collected by centrifugation (2500 rpm, 7 min, 4°C), washed twice with PBS, diluted to a concentration of 1×10^7 cells/mL and incubated with CFSE ($5 \mu\text{M}$, Invitrogen) for 20 min at RT. Subsequently, labeled cells were washed twice and resuspended at a concentration of 1×10^8 cells/mL in PBS. WT mice received 3×10^6 CFSE-labeled apoptotic thymocytes in 30 μL PBS (or PBS only) intratracheally (i.t.) on day six after i.n. LPS/saline treatment. Two hours after transfer, AMs were isolated by BAL, processed for flow cytometry as described and incubated with fluorescently labeled monoclonal antibodies (anti-CD45, anti-CD11c, anti-Siglec F, anti-MerTK, anti-Axl and Ter119; Table S4). Cells were analyzed by flow cytometry without prior fixation.

RNA isolation & Quant-seq analysis

RNA-seq analysis was performed on day six after *in vivo* training. AMs were isolated and challenged as described. Three hours after *ex vivo* challenge, cells were washed twice with cold PBS and lysed in RLT buffer (Qiagen) containing 1% 2-mercaptoethanol (Sigma). Total RNA was isolated using the RNeasy Micro kit (Qiagen). QuantSeq libraries were prepared using the QuantSeq 3' mRNA-Seq Library Prep Kit (FWD) for Illumina in combination with the PCR Add-on Kit for Illumina and the UMI Second Strand Synthesis Module for QuantSeq FWD (all from Lexogen), following the manufacturers' instructions. Libraries were prepared with 150 ng total RNA input and 15 amplification cycles. Sample quality was assessed on a Bioanalyzer 2100 (Agilent Technologies). Subsequently, 65 bp single-end sequencing was performed by the Biomedical Sequencing Facility (BSF, Center of Molecular Medicine and Medical University of Vienna) on a HiSeq3000/4000 instrument (Illumina).

Quant-seq data processing and bioinformatic analysis

Raw sequencing data were processed using the QuantSeq data analysis pipeline (Lexogen) hosted on the BlueBee Genomics Platform (Bluebee), as recommended by the manufacturer. In brief, unique molecular identifier (UMIs) were added to the read identifiers and trimmed from the reads using the *umi2index* process. Next, reads were quality- and adapter-trimmed using *Bbduk* and aligned to the mouse reference genome (mm10) using STAR aligner with modified ENCODE settings. To remove PCR duplicates, reads with identical UMIs and mapping were collapsed. Finally, reads mapping to genes were quantified using *HTSeq-count*. Differential gene expression was assessed using *DESeq2* (Love *et al*, 2014). Results were corrected for

multiple testing using independent hypothesis weighting (*ihw* R package) (Ignatiadis *et al*, 2016). Genes with an FDR-adjusted p-value of ≤ 0.1 were considered differentially expressed. Differentially activated KEGG pathways were assessed using Signaling Pathway Impact Analysis (SPIA) (Tarca *et al*, 2009).

Assay for transposase-accessible chromatin with sequencing (ATAC-seq)

To analyze chromatin accessibility, AMs were isolated six days after *in vivo* training by BAL. Differentially accessible regions of biological replicates were identified by ATAC-seq as previously described with some adaptations (Buenrostro *et al*, 2013; Corces *et al*, 2016). Briefly, 5×10^4 AMs were pelleted by centrifugation (4°C, 5 min, 500 g). Each pellet was lysed in 25 μ L transposase reaction mix (9.75 μ L RNase-free water, 12.5 μ L 2 x TD buffer [Illumina], 0.5 μ L 50x proteinase inhibitor cocktail [Roche], 2 μ L TDE1 [Illumina], 0.25 μ L 1% Digitonin [Promega]) and incubated at 37°C for 30 min. Subsequently, DNA was purified using the Qiagen MinElute kit and eluted in 12 μ L. The optimal number of amplification cycles was determined for each sample by qPCR [qPCR reaction mix per sample: 2.7 μ L RNase-free water, 0.2 μ L ROX reference dye (Invitrogen), 0.5 μ L index primer 1 noMX, 0.5 μ L index primer 2.1, 0.1 μ L 100x SYBR green (Sigma-Aldrich), 5 μ L NEBnext High-Fidelity 2x PCR master mix (New England Biolabs) and 1 μ L tagmented sample]. Subsequent library amplification was performed at the determined cycle numbers, using custom Nextera index primers (Buenrostro *et al*, 2013) (enrichment PCR reaction mix per sample: 10 μ L RNase-free water, 2.5 μ L index primer 1 noMX, 2.5 μ L barcoded index primer, 25 μ L NEBnext High-Fidelity 2x PCR master mix, 10 μ L tagmented sample). Enrichment was followed by SPRI (Beckman Coulter) size selection in order to exclude DNA fragments exceeding 1200 bp. DNA concentrations were determined using a Qubit fluorometer (Life Technologies), libraries were pooled at a final concentration of 4 nM and sequenced by the BSF (HiSeq 3000/4000, 50 bp single-end).

ATAC-seq data processing and bioinformatic analysis

Quality of raw fastq files was assessed using fastqc (v.0.11.8). Subsequently, raw reads were trimmed with trimmomatic (v.0.32) and aligned to the mouse reference genome (mm10) using bowtie (v.2.2.4; parameters: very sensitive, end-to-end). For further analysis, primary alignments with a mapping quality below 30 were discarded. Peak-calling was performed using MACS (v.2.1.0; parameters: nomodel, shift -100, extsize 200). Peak files were loaded into R (v.4.1.0) and filtered to only retain peaks which were confirmed by at least three samples within each treatment group (LPS or control). Next, a consensus peak set was computed by applying the function *reduce* of the GenomicRanges (v.1.42.0) package. Consensus peaks overlapping with blacklisted genomic regions were discarded (source:

<http://mitra.stanford.edu/kundaje/akundaje/release/blacklists/mm10-mouse/>).

Quantitative measurements were obtained by counting reads within consensus peaks using the function *featureCounts* of the Rsubread (v.2.4.3) package in R. The peak count matrix was filtered using the edgeR (v.3.32.1) function *filterByExpr* and peaks with a minimum of 100 counts in at least 75% of the samples of a treatment group were retained. Sample-specific quality weights were computed with the *voomWithQualityWeights* function of the limma (3.46.0) R package using the trimmed mean of M values (TMM). For each peak region, a linear model was fitted to the count data with *lmFit* and DARs were determined with *eBayes*. DARs with an adjusted p-value ≤ 0.05 were considered significant. Finally, peak regions were annotated to the org.Mm.eg.db reference using the ChIPseeker (v.1.5.1) function *annotatePeak*.

LC-MS/MS sample prep and analysis

For metabolomic and lipidomic analyses of trained and control AMs, CD11c⁺ Siglec F⁺ AMs were flow-sorted from BALFs six days after *in vivo* administration of LPS or saline (biological replicates). Each cell pellet was lysed in 310 μ L MetOH. After adding 10 μ L isotopically-labelled lipid internal standard mix (dissolved in MetOH) and 80 μ L isotopically-labelled metabolite internal standard mix (dissolved in ddH₂O), samples were vortexed and transferred to 1.5 mL HPLC glass vials. Subsequently, 640 μ L chloroform were added and samples were vortexed again. After addition of 240 μ L ddH₂O, samples were shaken on ice (10 min, 400 rpm) and centrifuged (4°C, 10 min, 1000 g). The upper water phase was collected and dried using a nitrogen evaporator. Samples were reconstituted in 50 μ L ddH₂O for LC-MS based metabolite measurements. The lower chloroform phase was collected and dried using speed vac. Samples were reconstituted in 20 μ L MetOH for LC-MS based lipid measurements. LC-MS metabolite analysis (detection of amino acids) was performed using a Vanquish UHPLC system coupled with an Orbitrap Q Exactive (Thermo Scientific) mass spectrometer. LC-MS/MS analysis (detection of TCA cycle metabolites) was performed on a Xevo TQ-MS (Waters) mass spectrometer using an Acquity UHPLC (Waters) system. LC-MS lipid analysis was performed using a Vanquish UHPLC system (Thermo Fisher Scientific) combined with an Orbitrap Fusion Lumos Tribrid mass spectrometer (Thermo Fisher Scientific). Data were processed using the TraceFinder software (ThermoFisher Scientific; Analysis of amino acids and lipids) and the MassLynx V4.1 software (Waters; Analysis of TCA cycle metabolites).

LC-MS/MS data processing and bioinformatic analysis

Bioinformatic analyses were performed in R (v. 3.4.1). For metabolite data analysis, individual metabolite concentrations were normalized to the total number of sorted cells. Differences

between groups were assessed using t-tests. Individual metabolites with p-values ≤ 0.05 and individual amino acids with p-values ≤ 0.05 and FDR ≤ 0.2 were considered statistically significant. For lipid data analysis, individual lipid species that were below detection limit in more than 66% of all samples were excluded from further analysis. For the remaining lipids, values below detection limit were imputed using the half minimum method. To account for differences in sorted cell numbers and potential variation induced by sample processing, lipid data were normalized by centered log-ratio transformation. Lipids significantly differing between groups were identified using t-tests, and individual lipid species with p-values ≤ 0.05 and FDR ≤ 0.2 were considered statistically significant.

Histological analysis

For histological analysis, lungs were fixed in 10% formaldehyde and embedded in paraffin. Lung sections were H&E-stained and examined by a trained pathologist (FO), blinded to experimental group assignments. Examined parameters included pleuritis, edema, bronchitis, endothelitis, interstitial inflammation and perivascular infiltrates. Each parameter was scored in the range of 0 to 3 points (0=absent, 1=mild, 2=moderate, 3=severe). The final histology score was calculated as the sum of all scores for the indicated parameters with additional 0.5 points added for every infiltrate covering 10% of total tissue area.

Generation and *in vitro* training of murine *ex vivo* cultured alveolar macrophages (mexAMs)

For generation of mexAM cultures, BAL AMs were obtained from adult wild type mice and expanded and cultured in mexAM medium (RPMI supplemented with 10% FCS, 1% PS, 30 ng/ mL murine GM-CSF [Peprotech], 10 ng/ mL human TGF- β [Peprotech] and 1 μ M rosiglitazone [Sigma]) as previously described (Gorki *et al*, 2022). For *in vitro* training, mexAMs (passage 15-25) were seeded in 6-well plates (Corning; 4×10^5 cells/well in 2 mL mexAM medium) and stimulated with 10 ng/ mL LPS (Sigma) or 400 U/ mL mouse IFN- β (pbl assay science) for 24 h. To address the role of metabolic and epigenetic regulation, cells were pre-incubated for 1 h in mexAM medium containing 1 mM 2-deoxyglucose (2-DG; Sigma), 10 μ M bis-2-(5-phenylacetamido-1,3,4-thiadiazol-2-yl)ethyl sulfide (BPTES; Sigma), 3 μ M etomoxir (Sigma), 1 mM 5'-deoxy-5'-methylthioadenosine (MTA; Cayman chemical), 10 μ M anacardic acid (Abcam) or DMSO, followed by incubation with LPS or medium in presence of inhibitors or DMSO for 24 h. After stimulation, cells were washed with PBS and maintained in mexAM medium. On day three, 0.5 mL fresh medium were added on top. On day six, cells were washed with PBS, detached by Lidocaine (Xylanaest purum; Gebro Pharma; 0.5% in PBS) treatment and seeded in a 96 well plate (Corning) in RPMI medium (3% FCS, 1% PS; 5×10^4

cells/well). After 2 h of adherence, cells were challenged with HISP (MOI 100 in RPMI medium) or medium only for 16 h.

Study design

The aim of this study was to investigate whether environmental LPS exposure alters AM reactivity to a subsequent bacterial challenge by inducing trained immunity. To this end, we i.n. administered LPS or saline (control) to male WT mice. LPS-mediated effects on secondary AM responses were assessed by ELISA/LEGENDplex and FACS analysis at baseline and upon *ex vivo* HISP challenge (day six after treatment). Flow cytometry-based *in vivo* labeling of resident AMs was conducted to evaluate a potential contribution of recruited monocytes to the trained AM pool. We investigated the role of adaptive immunity, interferon- α/β -receptor- and IFN- γ -receptor signaling in LPS-induced AM memory by applying our training model (*in vivo* training, followed by *ex vivo* AM challenge) to Rag2^{-/-}, Ifnar1^{-/-}, Ifnar1 ^{Δ CD169}, Ifngr1^{-/-} and respective control mice. Furthermore, we i.n. administered recombinant IFN- β and analyzed AM IL-6 production upon *ex vivo* HISP challenge. In order to characterize the genetic, epigenetic and metabolic profile of LPS-trained AMs, we performed RNA-seq, ATAC-seq, metabolomic/lipidomic and Seahorse analyses. The role of epigenetic regulation and metabolism was further evaluated using selective epigenetic or metabolic inhibitors respectively. To assess a potential impact of trained AMs on pneumonia outcome, we performed an adoptive intratracheal transfer of trained or control AMs into naïve recipients, which were subsequently infected with *S. pneumoniae*. Lastly, to investigate the physiological consequence of LPS inhalation, we i.n. administered LPS or saline (control) to wild type mice, followed by *S. pneumoniae* infection six days later. Throughout the study, mice were randomly distributed to experimental cages prior to treatment to avoid potential cage effects. To minimize confounding effects of animal housing/location, imported strains were maintained in the in-house mouse facility for a minimum of two weeks. For pneumonia experiments, termination criteria (BMWF-66.009/0363-WF/V/3b/2017; 2020-0.009.488) were established a priori. For remaining experiments, no a priori inclusion/exclusion criteria were set. Histological samples were evaluated by a trained pathologist (FO), blinded to experimental group assignments.

2.7 Supplementary Figures

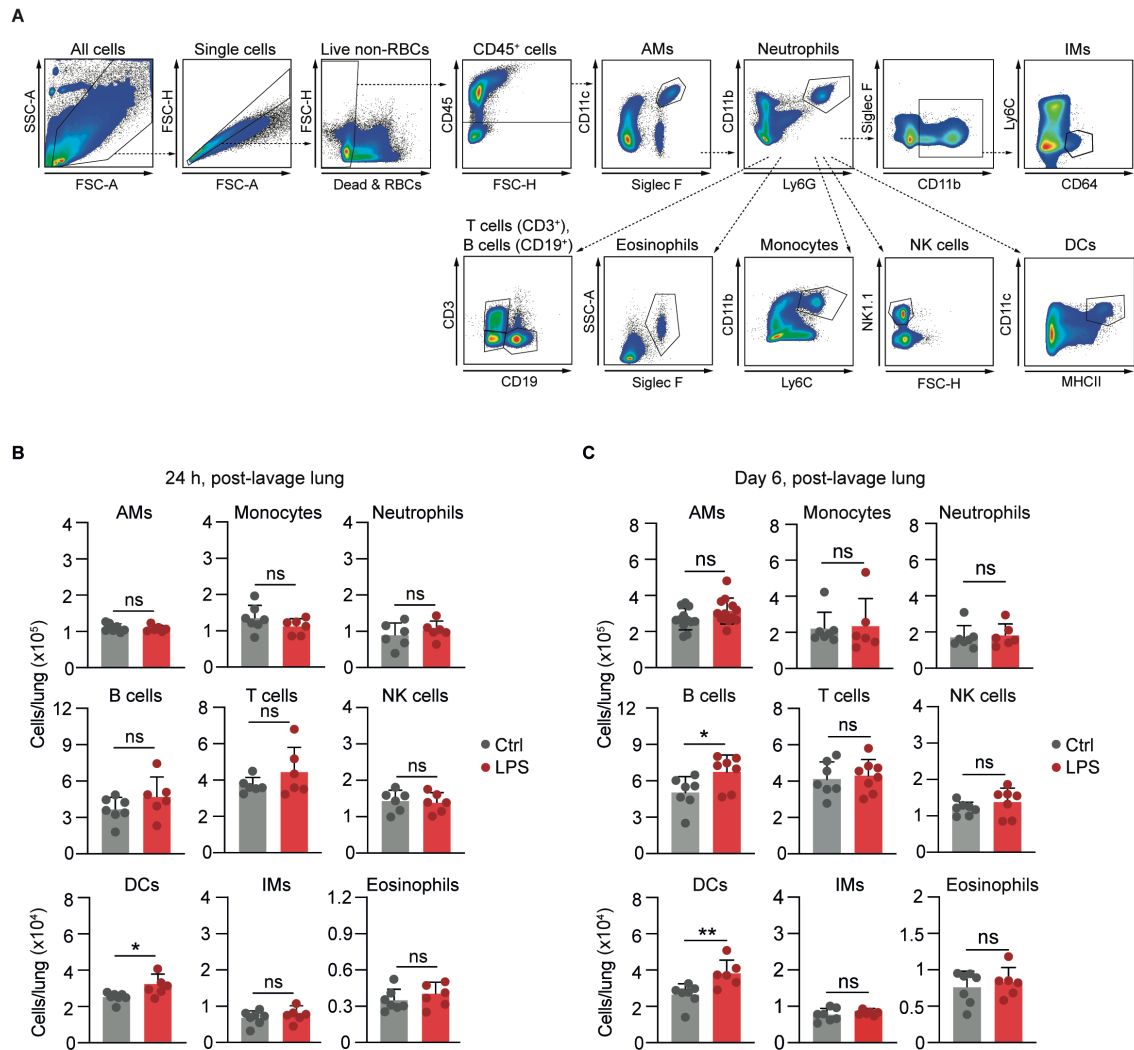


Figure S1 - FACS analysis of post-lavage lung tissue following LPS exposure.

Refers to Fig. 1. **(A)** Flow cytometry gating strategy for analysis of post-lavage lungs following i.n. LPS (1 ng/mouse) or saline exposure. **(B, C)** Cellular composition of post-lavage lungs, 24 h **(B)** and six days **(C)** after treatment. Graphs show means + SD of 6-12 biological replicates. Data are representative of two independent experiments. Statistical analysis: student's t-test. ns, not significant. * $p \leq 0.05$, ** $p \leq 0.01$.

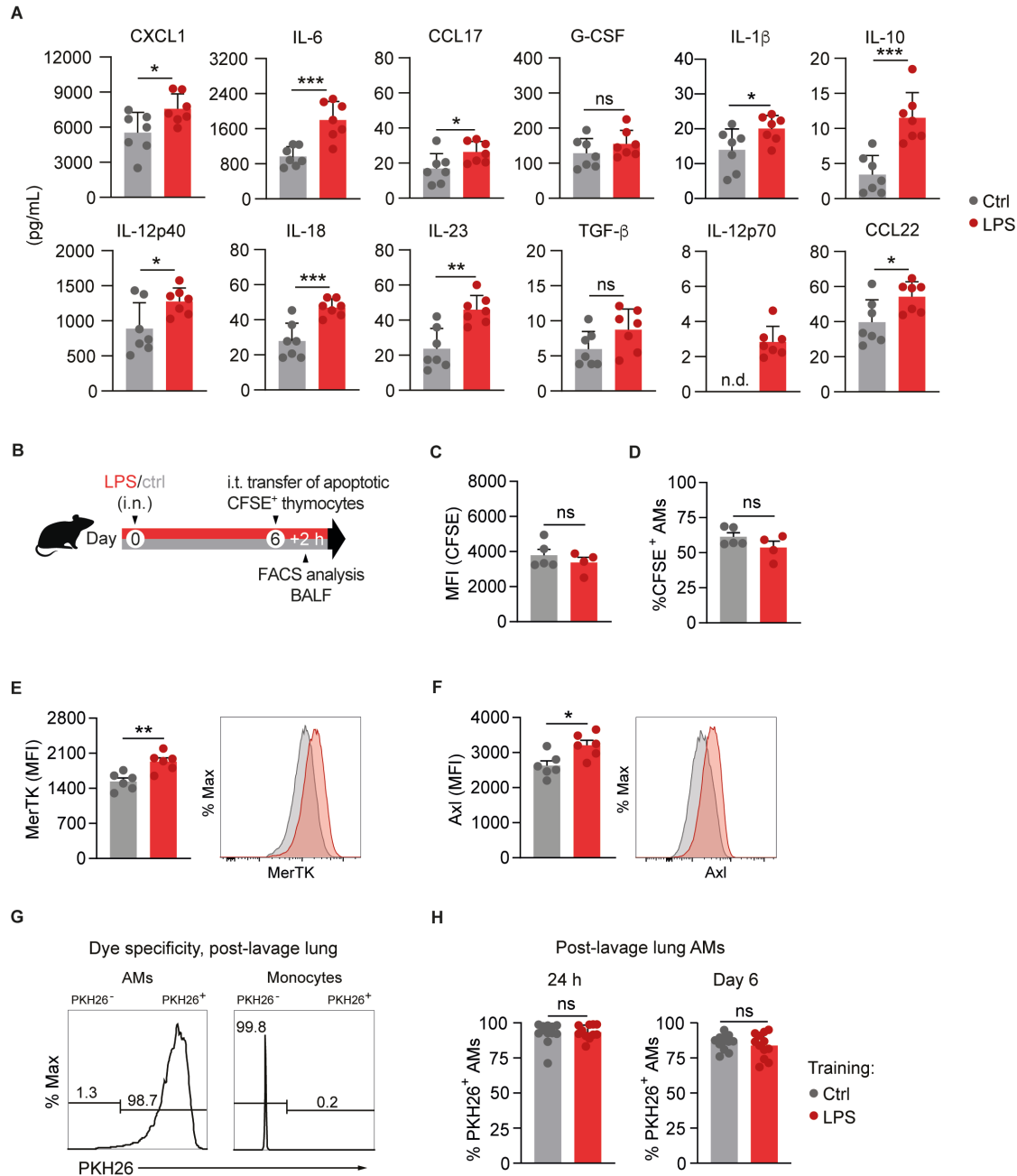


Figure S2 - Analysis of AM cytokines, efferocytosis and turnover following *in vivo* LPS exposure. Refers to Fig. 1. **(A)** Absolute cytokine levels of LPS-exposed and control AMs upon *ex vivo* HISP challenge (16 h), determined by LEGENDplex analysis. BAL AMs were isolated six days after *in vivo* treatment. **(B)** Experimental setup for analysis of AM efferocytosis. Six days after *in vivo* LPS/saline exposure, WT mice received 3×10^6 CFSE-labeled apoptotic thymocytes via intratracheal transfer. BALF was collected and subjected to FACS analysis 2 h after transfer. **(C, D)** CFSE mean fluorescence intensity (MFI) **(C)** and percentage of CFSE $^{+}$ cells **(D)**, pre-gated on CD11c $^{+}$ Siglec F $^{+}$ BALF AMs. **(E, F)** MerTK **(E)** and Axl **(F)** MFI of CD11c $^{+}$ Siglec F $^{+}$ BALF AMs following apoptotic thymocyte transfer. Representative histograms are displayed adjacent to bar graphs. Data are representative of two independent experiments. **(G)** Representative histograms depicting PKH26 MFI of CD11c $^{+}$ Siglec F $^{+}$ post-lavage lung AMs and CD11b $^{+}$ Ly6C $^{+}$ monocytes, 24 h after *in vivo* training. **(H)** Percentage of PKH26 $^{+}$ post-lavage lung AMs 24 h and six days after training. Graphs show means + SD of 7-8 **(A)**, 4-6 **(C-F)** or 11-12 **(H)** biological replicates. Statistical analysis: student's t-test. ns, not significant. *p \leq 0.05, **p \leq 0.01, ***p \leq 0.001.

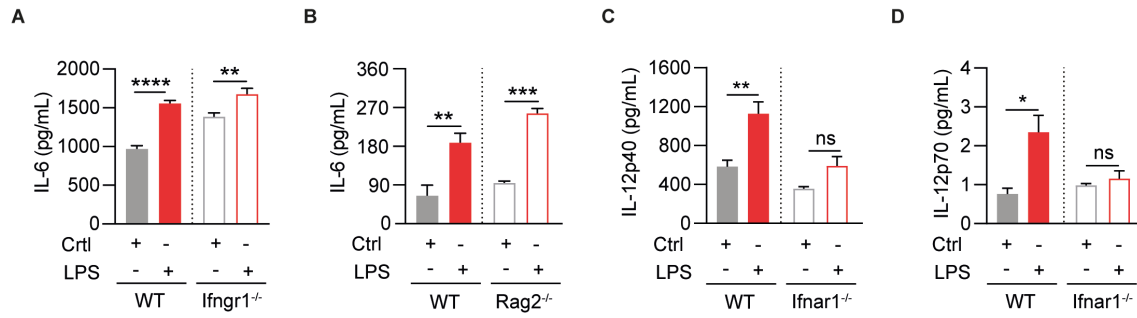


Figure S3 - Cytokine analysis of HISP-challenged Ifngr1^{-/-}, Rag2^{-/-} and Ifnar1^{-/-} AMs six days after *in vivo* training. Refers to Fig. 2. **(A, B)** IL-6 levels of HISP-challenged (16 h) LPS-exposed and control AMs, isolated six days after *in vivo* training of Ifngr1^{-/-} **(A)**, Rag2^{-/-} **(B)** and respective wild type control mice. **(C, D)** IL-12p40 **(C)** and IL-12p70 **(D)** levels of HISP-challenged LPS-exposed and control AMs, isolated six days after *in vivo* training of Ifnar1^{-/-} and WT control mice. Biological replicates (n=4) were pooled and seeded as technical replicates. Graphs represent means + SEM of 3-5 technical replicates. Data are representative of two independent experiments. Statistical analysis: 2-way ANOVA (factor 1: training; factor 2: genotype). ns, not significant. *p ≤ 0.05, **p ≤ 0.01, ***p ≤ 0.001, ****p ≤ 0.0001.

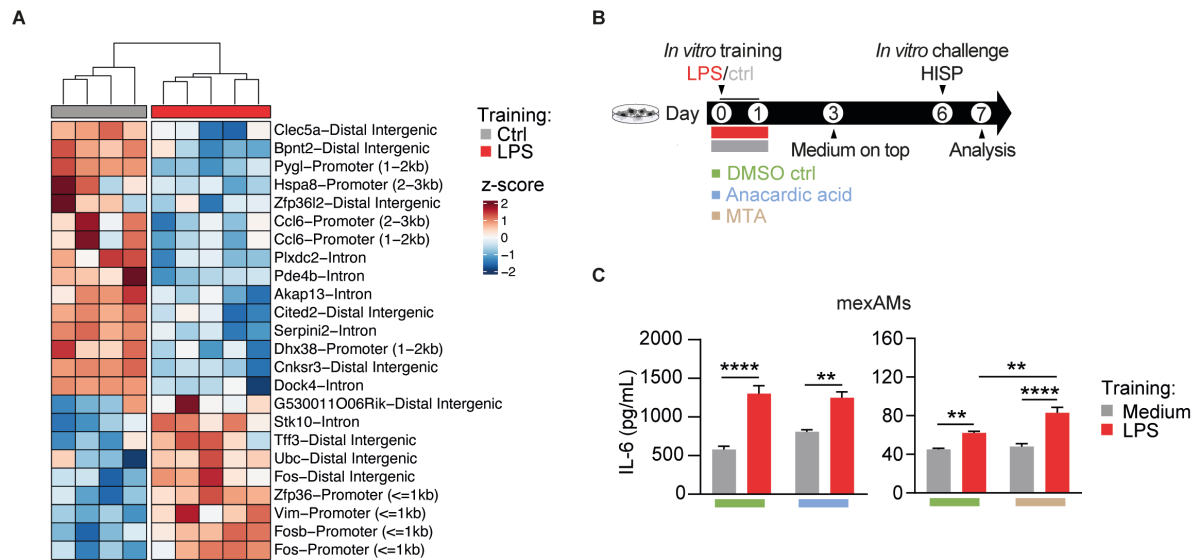


Figure S4 - AM ATAC-seq analysis and inhibition of epigenetic enzymes during mexAM training. Refers to Fig. 3. **(A)** Heatmap displaying differentially accessible chromatin regions (adjusted p-value ≤ 0.05) of LPS-trained and control AMs. Cells were isolated and processed for ATAC-seq analysis six days after *in vivo* training. Raw counts were log₂-transformed, followed by z-score scaling. **(B)** Experimental setup for mexAM training with LPS or medium in presence of anacardic acid, 5'-deoxy-5'-methylthioadenosine (MTA) or DMSO, followed by *in vitro* HISP challenge (16 h) six days later. **(C)** IL-6 levels of mexAMs stimulated as described in **(B)**. Graphs show means + SEM of 4-5 technical replicates. Data are representative of two independent experiments. Statistical analysis: 2-way ANOVA (factor 1: training; factor 2: inhibitor). **p ≤ 0.01 , ****p ≤ 0.0001 .

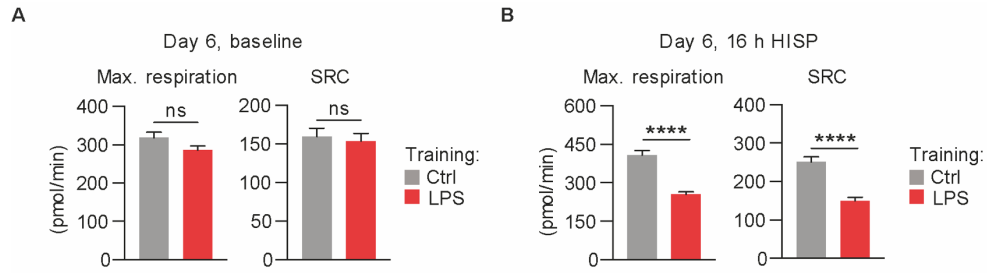


Figure S5 - Maximum and spare respiratory capacity of AMs on day six after *in vivo* training. Refers to Fig. 4. **(A, B)** Maximum respiratory capacity (max. respiration) and spare respiratory capacity (SRC) of LPS-trained and control AMs on day six after *in vivo* training at baseline **(A)** and after *ex vivo* HISP challenge (16 h) **(B)**. Biological replicates (n=5-8) were pooled and seeded as technical replicates. Graphs show means + SEM of 10-11 technical replicates. Statistical analysis: student's t-test. ns, not significant. ****p ≤ 0.0001.

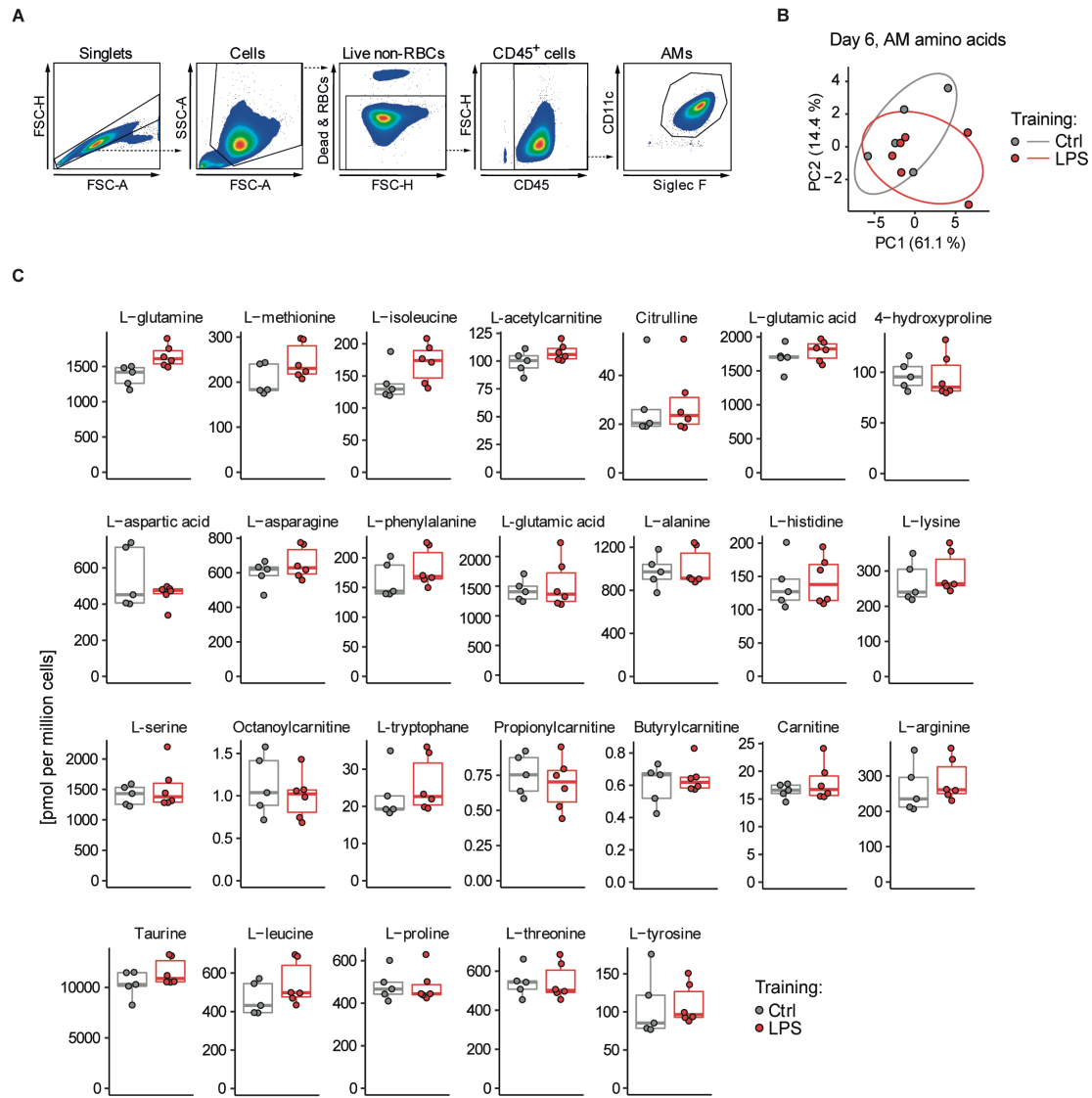


Figure S6 - AM amino acids six days after *in vivo* training.

Refers to Fig. 5. **(A)** Flow cytometry sorting strategy for isolation and LC-MS/MS analysis of CD11c⁺ Siglec F⁺ AMs on day six after *in vivo* training with LPS or saline. **(B, C)** Principal component analysis **(B)** and absolute concentration **(C)** of intracellular AM amino acids, detected six days after training. Graphs show medians and interquartile range of 5-6 biological replicates. Statistical analysis: student's t-test. Individual amino acids with p-values ≤ 0.05 and FDR ≤ 0.2 were considered statistically significant.

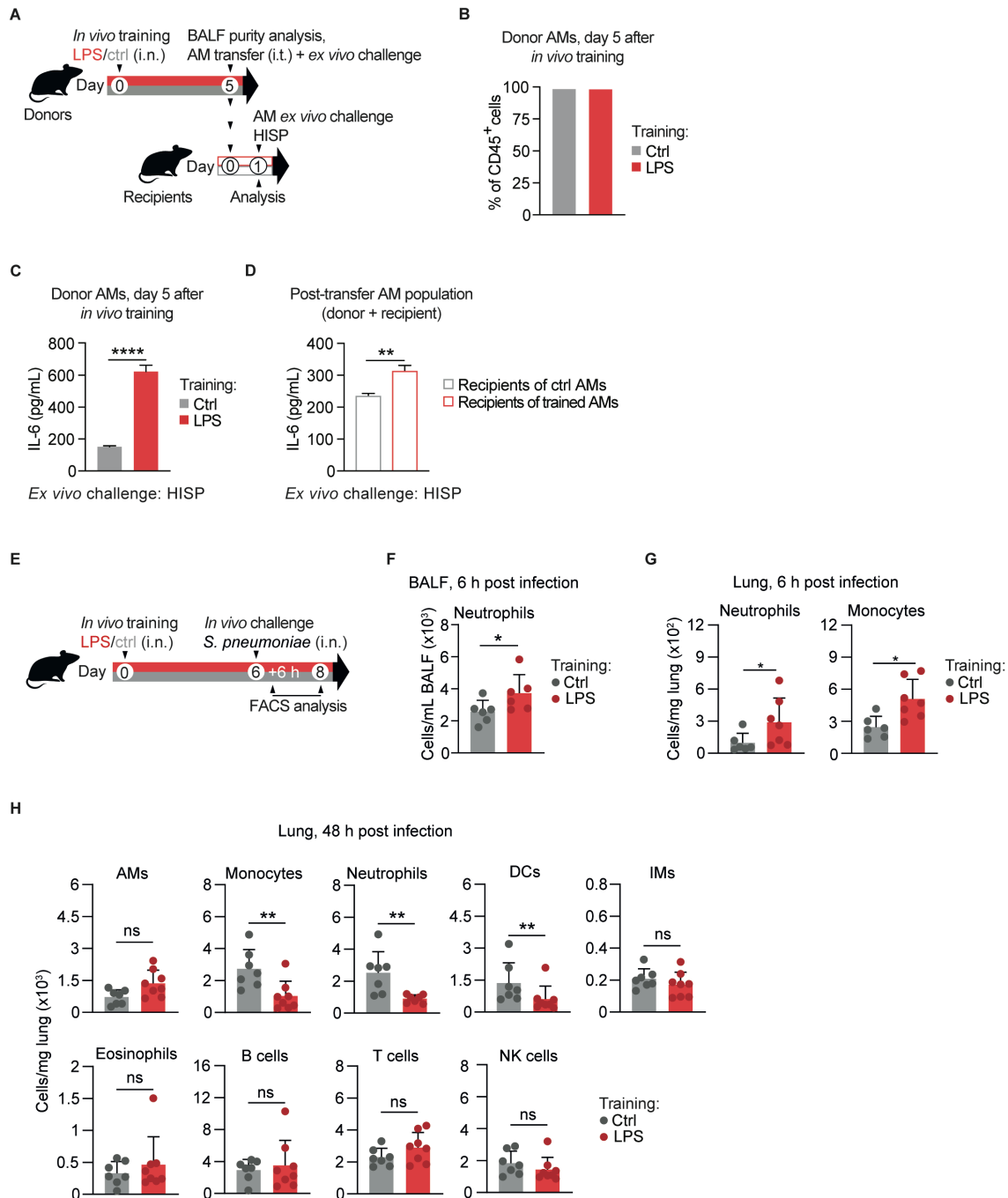


Figure S7 - Assessment of AM engraftment and post-infection FACS analysis after *in vivo* training. Refers to Fig. 6. **(A)** Experimental setup for adoptive transfer of trained and control AMs five days after *in vivo* training with LPS or saline. Donor BALF purity and successful establishment of donor AM memory were assessed by FACS analysis and *ex vivo* HISP challenge respectively. Donor cells were transferred intratracheally (i.t.) into naïve recipients. After 24 h, the chimeric AM population was isolated, followed by *ex vivo* HISP (16 h) challenge. **(B)** Frequencies of CD11c⁺ Siglec F⁺ donor AMs, day five after *in vivo* training. Biological replicates (n=5) were pooled by group for purity analysis. **(C, D)** IL-6 levels of HISP-challenged donor AMs isolated on day five after *in vivo* training **(C)** or of HISP-challenged AMs isolated from recipients 24 h after adoptive transfer (i.e. comprising recipient and donor AMs) **(D)**. Biological replicates (n=5) were pooled by group and seeded as technical replicates. **(E)** Experimental setup for *in vivo* training with LPS/saline, followed by *S. pneumoniae* infection (*in vivo* challenge) six days later. BALF and/or lung tissue samples were analyzed by flow cytometry 6 h and

48 h after infection. **(F)** BALF neutrophil numbers, 6 h after infection. **(G)** Lung monocyte and neutrophil numbers, 6 h after infection. **(H)** Cellular composition of LPS-exposed and control lungs, 48 h after infection. Data are representative of two independent experiments. Graphs show means + SEM of 5 technical replicates **(C, D)** or means + SD of 6-8 biological replicates **(F-H)**. Statistical analysis: student's t-test. ns, not significant. * $p \leq 0.05$, ** $p \leq 0.01$, **** $p \leq 0.0001$.

2.8 Supplementary Tables

Table S1

mean expr. (base)	log ₂ fc	p-value	adj. p-value	gene ID	gene symbol
168,465467	0,74240214	2,04676E-07	0,000619846	ENSMUSG00000025355	Mmp19
102,8197985	1,109822417	1,09315E-06	0,001655263	ENSMUSG00000096954	NA
47,48523992	-0,712048566	5,01717E-06	0,014246798	ENSMUSG00000019960	Dusp6
163,5240364	1,860895232	1,88174E-05	0,014246798	ENSMUSG00000029379	Cxcl3
1501,875586	0,655481284	1,87338E-05	0,021530591	ENSMUSG00000092341	Malat1
210,4886767	-0,401776284	3,1949E-05	0,030598925	ENSMUSG00000029915	Clec5a
96,35604795	0,669262572	5,27866E-05	0,043333708	ENSMUSG00000071076	Jund
125,841747	0,540465946	0,000140767	0,058214553	ENSMUSG00000054364	Rhob
151,8029916	0,506658614	0,000253344	0,058214553	ENSMUSG00000092274	Neat1
589,6807058	-0,242575364	0,000416294	0,086092111	ENSMUSG00000030654	Arl6ip1

Table S1 - Differentially expressed genes identified in AMs six days after *in vivo* training.

List of differentially expressed genes (DEGs) identified in LPS-trained and control AMs six days after *in vivo* training and 3 h after *ex vivo* incubation with medium (baseline). Genes are ordered by adjusted p-value (padj), from lowest to highest. DEGs with padj ≤ 0.1 were considered significant and are displayed. *To view the complete gene list, please refer to the online version of the publication.*

Table S2

mean expr.	log ₂ fc	p-value	adj. p-value	gene ID	gene symbol
163,5240364	2,794226664	2,22751E-13	7,5422E-10	ENSMUSG00000029379	Cxcl3
54,85177199	1,043734668	3,87235E-11	1,52006E-07	ENSMUSG00000021701	Plk2
19,82049382	1,920913479	1,57394E-11	1,52006E-07	ENSMUSG00000041324	Inhba
106,3942793	0,88197214	6,78405E-10	4,618E-07	ENSMUSG00000016319	Slc25a5
189,0528119	0,849704192	5,92737E-10	4,618E-07	ENSMUSG00000020077	Srgn
1348,806501	0,422053739	2,68448E-09	1,01264E-06	ENSMUSG00000020644	Id2
125,841747	0,792264054	2,25351E-09	1,09571E-06	ENSMUSG00000054364	Rhob
20,34945926	1,754426831	5,59778E-10	1,6905E-06	ENSMUSG00000033213	AA467197
172,1057704	1,685957087	2,89444E-08	7,27894E-06	ENSMUSG00000050370	Ch25h
83,45393785	0,881904148	4,0706E-08	1,05037E-05	ENSMUSG00000037072	Selenof
303,6939136	0,448279037	1,10654E-07	2,27677E-05	ENSMUSG00000015143	Actn1
168,465467	0,76358305	1,59075E-07	3,17698E-05	ENSMUSG00000025355	Mmp19
41,94008096	0,988134807	8,81956E-08	4,59494E-05	ENSMUSG00000035969	Rusc2
59,32361778	0,976147901	1,49229E-07	6,20292E-05	ENSMUSG00000019850	Tnfaip3
473,674776	0,540505286	4,46222E-07	8,71785E-05	ENSMUSG00000030142	Clec4e
26,06857086	1,531044237	6,77772E-08	8,71785E-05	ENSMUSG00000035900	Gramd4
97,66465677	0,603644365	6,46509E-07	8,71785E-05	ENSMUSG00000042622	Maff
83,17839751	0,737586482	4,63451E-07	8,71785E-05	ENSMUSG00000061731	Ext1
734,2954708	0,483778941	8,47942E-07	0,000101009	ENSMUSG00000019970	Sgk1
183,2604143	0,550229669	9,23348E-07	0,00011913	ENSMUSG00000026628	Atf3
83,68062054	0,720570269	7,76278E-07	0,000125815	ENSMUSG00000028381	Ugcg
106,6789254	0,854910776	8,19438E-07	0,000126116	ENSMUSG00000028517	Plpp3
1086,465153	0,352805394	2,19928E-06	0,000306634	ENSMUSG00000028367	Txn1
564,5051427	0,404587802	2,89126E-06	0,000306634	ENSMUSG00000030256	Bhlhe41
66,81901583	0,753613668	4,24284E-07	0,000306634	ENSMUSG00000033184	Tmed7
8,712886405	2,338433692	1,52791E-07	0,000325908	ENSMUSG00000034893	Cog3
314,4335461	0,564390284	3,14355E-06	0,000382117	ENSMUSG00000024659	Anxa1
274,9602538	0,480586901	4,40747E-06	0,000382117	ENSMUSG00000025290	Rps24
73,01915345	0,768591647	2,41708E-06	0,000455743	ENSMUSG00000016496	Cd274
462,697024	0,899437386	5,89508E-06	0,000455743	ENSMUSG00000038508	Gdf15
186,6477672	0,478127041	4,11156E-06	0,000455743	ENSMUSG00000046982	Tshz1
35,74503666	1,004132474	2,9444E-06	0,00053545	ENSMUSG00000017132	Cyth1
75,47738112	0,644407306	6,97825E-06	0,000545654	ENSMUSG00000020057	Dram1
227,6451595	0,543252414	1,12266E-05	0,000747337	ENSMUSG00000007458	M6pr
88,48391953	0,664643568	1,20163E-05	0,00077705	ENSMUSG00000043017	Ptgir
100,2978664	0,702299852	8,68975E-06	0,000821561	ENSMUSG00000029234	Tmem165
156,5603733	0,473613787	2,12115E-05	0,001373921	ENSMUSG00000054808	Actn4
296,9198649	0,392361001	3,95333E-05	0,002407022	ENSMUSG00000024335	Brd2
534,8388509	0,410064169	4,24454E-05	0,002407022	ENSMUSG00000056501	Cebpb
897,2583029	1,211645332	4,01743E-05	0,002407022	ENSMUSG00000058427	Cxcl2
233,3082133	-0,341676443	7,03922E-05	0,003885861	ENSMUSG00000004266	Ptpn6
223,3813832	0,513451472	6,8696E-05	0,003919895	ENSMUSG00000030103	Bhlhe40
84,42663249	1,290918264	7,49593E-05	0,004177813	ENSMUSG00000069662	Marcks

Table S2

mean expr.	log ₂ fc	p-value	adj. p-value	gene ID	gene symbol
180,1251056	0,382667659	8,89747E-05	0,004846252	ENSMUSG00000011884	Gltf
322,6752875	0,321060236	8,26519E-05	0,006251371	ENSMUSG00000035011	Zbtb7a
201,2328167	0,355672108	0,000138787	0,007230755	ENSMUSG00000051510	Mafg
63,15331931	-0,670997083	2,08013E-05	0,007996418	ENSMUSG00000050552	Lamtor4
53,66909308	1,75113593	6,05297E-05	0,008366591	ENSMUSG00000018293	Pfn1
396,7557741	0,344200983	0,000179534	0,008366591	ENSMUSG00000023010	Tmbim6
250,456474	0,548827899	0,000130971	0,008915361	ENSMUSG00000062515	Fabp4
1751,99083	-0,28221737	0,000134591	0,00893559	ENSMUSG00000026864	Hspa5
2507,063367	0,245588433	0,000206951	0,009537956	ENSMUSG00000060802	B2m
96,35604795	0,597627461	0,000150119	0,009590387	ENSMUSG00000071076	Jund
72,15943649	0,788540631	9,13587E-05	0,009845281	ENSMUSG00000034101	Ctnnd1
110,1615406	0,509690777	0,000248055	0,010207785	ENSMUSG00000025795	Rassf3
119,6873207	0,537339708	0,000169482	0,010247365	ENSMUSG00000029771	Irf5
166,1430635	0,405456538	0,000189569	0,010522406	ENSMUSG00000020023	Tmcc3
55,05281316	1,18123708	3,53883E-05	0,010522406	ENSMUSG00000021215	Net1
31,2891021	1,127362978	6,78235E-06	0,010522406	ENSMUSG00000029017	Pmpcb
197,592151	0,315878697	0,000181398	0,010522406	ENSMUSG00000031444	F10
119,497242	-0,500807705	0,000183725	0,010522406	ENSMUSG00000041515	Irf8
27,07379379	0,980656772	2,84566E-05	0,010580195	ENSMUSG00000034160	Ogt
65,10131421	0,767182351	0,000118958	0,010869679	ENSMUSG00000000441	Raf1
1153,576392	0,325415246	0,000205456	0,010869679	ENSMUSG00000020572	Nampt
360,5320373	0,363214625	0,000210175	0,011005329	ENSMUSG00000015839	Nfe2l2
1300,141013	0,330236812	0,000286619	0,011205861	ENSMUSG00000027737	Slc7a11
264,5382375	0,502894116	0,000292791	0,011276321	ENSMUSG00000036438	Calm2
92,77325708	0,49695158	0,000226464	0,011276321	ENSMUSG00000062203	Gspt1
600,3832837	0,321373348	0,000248713	0,012204682	ENSMUSG00000028599	Tnfrsf1b
72,40530623	0,628518764	0,000180786	0,013122854	ENSMUSG00000035725	Prkx
266,7375739	0,319053329	0,000388772	0,013122854	ENSMUSG00000063406	Tmed5
991,3484101	0,298876292	0,000292037	0,013733573	ENSMUSG00000032740	Ccdc88a
105,4896077	-0,440720033	0,000480634	0,014901783	ENSMUSG00000022270	Retreg1
53,25631101	0,825725353	6,92248E-05	0,016901846	ENSMUSG00000050148	Ubqln2
14,2070729	1,585462946	2,39747E-05	0,017817044	ENSMUSG00000022096	Hr
159,3652818	0,412122413	0,000524652	0,017817044	ENSMUSG00000032504	Pdcd6ip
868,1791817	0,319589629	0,000613538	0,018034221	ENSMUSG00000073411	H2-D1
61,29590383	-0,725412172	0,000119609	0,018058204	ENSMUSG00000020914	Top2a
255,2658443	-0,362091626	0,00046558	0,019324827	ENSMUSG00000022982	Sod1
317,0305635	0,29460298	0,000458126	0,019324827	ENSMUSG00000024639	Gnaq
290,668908	0,397802831	0,000655368	0,019324827	ENSMUSG00000031596	Slc7a2
197,2504913	0,421023288	0,000457476	0,019324827	ENSMUSG00000043131	Mob1a
461,5714655	0,289345126	0,000726305	0,019805583	ENSMUSG00000028634	Hivep3
113,6267083	0,411043369	0,000662035	0,020336978	ENSMUSG00000020594	Pum2
45,33501878	0,632156992	0,00029845	0,02043263	ENSMUSG00000003382	Etv3
128,2290828	0,403212144	0,000797215	0,02098087	ENSMUSG00000024949	Sf1
620,0131516	0,260776099	0,000764179	0,021050765	ENSMUSG00000037242	Clic4

Table S2

mean expr.	log ₂ fc	p-value	adj. p-value	gene ID	gene symbol
351,8334676	0,277858468	0,000805178	0,021850287	ENSMUSG00000020152	Actr2
23,41049966	1,169811284	2,07782E-05	0,021850287	ENSMUSG00000038803	Ost4
327,7193647	0,399751816	0,00086962	0,02186924	ENSMUSG00000064351	mt-Co1
50,67454619	0,573742178	0,000301985	0,022231796	ENSMUSG00000015312	Gadd45b
46,76632257	0,670151118	0,000172734	0,022231796	ENSMUSG00000032096	Arcn1
35,96449659	0,675104355	0,000403198	0,022333337	ENSMUSG00000030199	Etv6
109,3251224	0,409806911	0,000830228	0,02279052	ENSMUSG00000046223	Plaur
95,81192099	0,520621805	0,000912985	0,023032025	ENSMUSG00000024190	Dusp1
181,3077497	0,338046518	0,000962261	0,024022258	ENSMUSG00000005506	Celf1
116,76091	0,423352511	0,000973974	0,024063988	ENSMUSG00000034957	Cebpa
98,36689049	0,424555683	0,000977935	0,025749499	ENSMUSG00000055239	Kcmf1
136,5249019	0,348874576	0,001085265	0,026015437	ENSMUSG00000025239	Limd1
295,883959	-0,405248131	0,001028363	0,026015437	ENSMUSG00000026360	Rgs2
435,0005009	-0,28094848	0,00109936	0,026015437	ENSMUSG00000026600	Soat1
260,0821248	0,379778955	0,001088098	0,026015437	ENSMUSG00000030162	Olr1
138,8125192	0,358251399	0,001185615	0,026052704	ENSMUSG00000028165	Cisd2
85,89897865	0,561784374	0,000804381	0,026324706	ENSMUSG00000040128	Pnrc1
21,01796357	1,090811013	0,000122293	0,026613699	ENSMUSG00000031555	Adam9
67,64996381	0,533495391	0,000484774	0,026613699	ENSMUSG00000075700	Selenot
54,36437398	0,5258964	0,000555845	0,026760114	ENSMUSG00000037553	Zdhc18
76,83363748	0,462985552	0,001304398	0,027335869	ENSMUSG00000026466	Tor1aip1
150,43266	0,465959569	0,001342326	0,02778067	ENSMUSG00000000001	Gnai3
71,85877711	-0,56922496	0,000169134	0,02778067	ENSMUSG00000045969	Ing1
42,36481495	0,64660794	0,000612949	0,028445874	ENSMUSG00000028760	Eif4g3
439,3481069	0,230743792	0,001331422	0,030674835	ENSMUSG00000026473	Glul
88,51151682	0,465352943	0,001351977	0,030872756	ENSMUSG00000050812	Ecpas
589,6807058	-0,228261917	0,001084665	0,032383628	ENSMUSG00000030654	Arl6ip1
237,0876069	0,257939289	0,001105658	0,032441257	ENSMUSG00000034120	Srsf2
4674,080348	0,2228031	0,001568504	0,032441257	ENSMUSG00000064341	mt-Nd1
279,6472562	-0,362940175	0,00164003	0,033593703	ENSMUSG00000023004	Tuba1b
255,4015456	-0,336070495	0,001191786	0,034197444	ENSMUSG00000026202	Tuba4a
87,66995738	0,507795084	0,001590977	0,034498608	ENSMUSG00000031309	Rps6ka3
39,28708751	-0,698000594	0,00023466	0,035069163	ENSMUSG00000027227	Sord
130,6222697	0,347003654	0,001644471	0,035069163	ENSMUSG00000055065	Ddx17
96,21063382	0,421754435	0,001302425	0,036146842	ENSMUSG00000028163	Nfkb1
379,5988976	0,285968131	0,001354469	0,037479931	ENSMUSG00000040659	Efh2
131,4997742	0,505117311	0,002239801	0,040882199	ENSMUSG00000026107	Nabp1
1147,725319	0,187710914	0,001523084	0,041256394	ENSMUSG00000000290	Itgb2
107,9128967	0,378473695	0,002413926	0,04336105	ENSMUSG00000022125	Cln5
22,58317761	-0,985659742	0,000237834	0,044890323	ENSMUSG00000026605	Cenpf
28,90898195	0,814216475	0,000259845	0,044890323	ENSMUSG00000038175	Myliip
789,3386593	0,252687119	0,001760084	0,046197784	ENSMUSG00000037902	Sirpa
37,8630924	-0,777794591	0,000336836	0,046814409	ENSMUSG00000034165	Ccnd3
115,357186	0,360326288	0,001817541	0,046977553	ENSMUSG00000026276	Septin2

Table S2

mean expr.	log ₂ fc	p-value	adj. p-value	gene ID	gene symbol
64,70207959	0,677876111	0,00055638	0,049636933	ENSMUSG00000022018	Rgcc
77,81325314	0,409314815	0,002589176	0,050233636	ENSMUSG000000102037	Bcl2a1a
306,1492266	-0,255262085	0,002922271	0,052264616	ENSMUSG000000013974	Mcomp1
11,9027188	1,288332041	0,000129283	0,055135197	ENSMUSG000000047454	Gphn
167,4410217	0,305617495	0,003319882	0,05524974	ENSMUSG000000021770	Samd8
44,7085403	0,70446977	0,000420388	0,055441353	ENSMUSG000000056629	Fkbp2
138,8087742	0,508910415	0,00227462	0,055809391	ENSMUSG000000059248	Septin9
130,2091953	0,373762141	0,002353052	0,057205572	ENSMUSG000000027878	Notch2
77,46681288	0,469177546	0,002351583	0,057205572	ENSMUSG000000032440	Tgfr2
127,5696178	-0,349816489	0,002488431	0,059585858	ENSMUSG000000024691	Fam111a
113,0371164	0,331818104	0,003724035	0,059585858	ENSMUSG000000031591	Asah1
296,2899169	-0,320526282	0,002516528	0,059585858	ENSMUSG000000043091	Tuba1c
468,6352458	0,240636775	0,003910176	0,061243107	ENSMUSG000000005610	Eif4g2
32,8919244	0,766253715	9,48826E-05	0,061243107	ENSMUSG000000021890	Eaf1
302,85577	0,590689875	0,003557183	0,062869212	ENSMUSG000000000805	Car4
36,94450637	0,708811941	0,000822469	0,065888402	ENSMUSG000000072704	Smim10l1
307,0098821	0,235205675	0,004391326	0,067155315	ENSMUSG000000027366	Sppl2a
133,5830672	-0,33734089	0,004597677	0,068542083	ENSMUSG000000002778	Kdelr1
372,7686411	0,351255846	0,004603143	0,068542083	ENSMUSG000000026193	Fn1
948,7339044	0,231436698	0,004272053	0,068542083	ENSMUSG000000032786	Alas1
928,2524412	0,256143034	0,004296975	0,068542083	ENSMUSG000000032802	Srxn1
49,61287119	0,524834875	0,001809846	0,06883703	ENSMUSG000000025337	Sbds
244,8872764	0,539134114	0,003175592	0,070184109	ENSMUSG000000000982	Ccl3
18,15223359	1,132637128	0,000117266	0,070353508	ENSMUSG000000044674	Fzd1
2866,462168	0,260981796	0,003230128	0,070353508	ENSMUSG000000064370	mt-Cytb
101,1383107	0,354103557	0,00429576	0,070603311	ENSMUSG000000028191	Bcl10
112,4845052	0,395886969	0,003388888	0,072623586	ENSMUSG000000009376	Met
208,6247537	0,30757223	0,004850464	0,073110243	ENSMUSG00000001687	Ubl3
109,4032207	0,41539262	0,003482503	0,073696876	ENSMUSG000000020300	Cpeb4
240,0630077	0,387678596	0,004981808	0,074134144	ENSMUSG000000024030	Abcg1
41,22324283	-0,560918697	0,002331394	0,074134144	ENSMUSG000000024660	Incenp
88,31835588	0,385859675	0,003627242	0,074821663	ENSMUSG000000021930	Spryd7
14,13000657	1,122253383	0,000217793	0,074821663	ENSMUSG000000039062	Anpep
61,55777011	0,501485297	0,002113128	0,074821663	ENSMUSG000000040028	Elavl1
319,0206438	-0,241918856	0,005229455	0,075498853	ENSMUSG000000024608	Rps14
120,5335623	0,294506927	0,005010478	0,075630755	ENSMUSG000000020901	Pik3r5
462,93734	0,230644362	0,005630526	0,075630755	ENSMUSG000000021948	Prkcd
82,21961106	0,699121074	0,003764159	0,075630755	ENSMUSG000000025283	Sat1
539,4237542	0,205825134	0,003769456	0,075630755	ENSMUSG000000029994	Anxa4
95,21587203	0,339778935	0,00539638	0,075630755	ENSMUSG000000037236	Matr3
43,35185123	0,598846078	0,001127855	0,077220353	ENSMUSG000000031875	Cmtm3
186,9998546	0,300427473	0,003986715	0,078433926	ENSMUSG000000058835	Abi1
3576,73717	-0,22907666	0,004067613	0,079077734	ENSMUSG000000007891	Ctsd
193,2637561	-0,276618818	0,004065907	0,079077734	ENSMUSG000000026374	Tsn

Table S2

mean expr.	log ₂ fc	p-value	adj. p-value	gene ID	gene symbol
14,87225545	-1,201607022	0,000247223	0,080871581	ENSMUSG00000023015	Racgap1
7,405265927	1,613460985	0,000277288	0,083506147	ENSMUSG00000042079	Hnmpf
206,6191234	0,291466982	0,005810934	0,083990189	ENSMUSG00000032350	Gclc
13,30169445	1,285900732	0,000271088	0,083990189	ENSMUSG00000032487	Ptgs2
139,5422309	0,282052091	0,005983926	0,08578243	ENSMUSG00000063273	Naa15
254,462173	0,270442772	0,006910698	0,086415127	ENSMUSG00000056851	Pcbp2
47,52974773	-0,519490878	0,003107772	0,087962055	ENSMUSG00000021591	Glrx
205,3296084	0,292077939	0,004816446	0,08911548	ENSMUSG00000021036	Sptlc2
183,5257227	-0,259546492	0,006908888	0,089987536	ENSMUSG00000032046	Abhd12
12,65489607	1,165288659	0,00031175	0,09345588	ENSMUSG00000050567	Maml1
188,6586671	0,559219782	0,006830827	0,094764352	ENSMUSG00000019804	Snx3
38,11078899	0,589238194	0,001532545	0,095618521	ENSMUSG00000007659	Bcl2l1
13,30256372	1,168670941	0,000317122	0,095618521	ENSMUSG00000031779	Ccl22
74,59512152	0,420642156	0,003121934	0,095618521	ENSMUSG00000038866	Zcchc2
263,9692792	0,34886742	0,007575676	0,095618521	ENSMUSG00000045763	Basp1
567,1974445	0,567569207	0,005375946	0,095797982	ENSMUSG00000072596	Ear2
166,8082335	0,283216587	0,007150286	0,096096343	ENSMUSG00000061244	Exoc5

Table S2 - Differentially expressed genes identified in HISP-challenged AMs six days after *in vivo* training. List of differentially expressed genes (DEGs) identified in LPS-trained and control AMs six days after *in vivo* training and 3 h after *ex vivo* incubation with HISP. Genes are ordered by adjusted p-value (padj), from lowest to highest. DEGs with padj ≤ 0.1 were considered significant and are displayed. *To view the complete gene list, please refer to the online version of the publication.*

Table S3

region start	region end	avlog2fc	avlog2cpm	pvalue	padj	annotation	gene symbol
83585564	83586919	-0,9851	5,5794474	7,39E-11	1,32E-06	Promoter	Ccl6
85478163	85479210	0,92243	5,0026885	7,81E-10	6,97E-06	Distal Intergenic	Fos
19307880	19309095	0,65742	5,3033304	1,25E-08	7,44E-05	Promoter	Fosb
83587118	83587976	-0,9428	4,9694355	1,82E-08	8,10E-05	Promoter	Ccl6
85473415	85474613	0,46013	6,2800261	2,49E-07	0,000888	Promoter	Fos
13573323	13575896	0,34864	7,5617546	7,92E-07	0,002355	Promoter	Vim
32540769	32541695	0,63939	4,5192145	2,55E-06	0,006486	Intron	Stk10
28378677	28379549	0,43131	5,8029168	4,42E-06	0,009862	Promoter	Zfp36
125381857	125383880	0,4725	5,9209313	6,51E-06	0,012893	Distal Intergenic	Ubc
17484811	17486016	-0,5123	4,9740976	8,30E-06	0,014807	Distal Intergenic	Cited2
5203184	5204165	-0,4301	5,5599215	9,96E-06	0,016141	Distal Intergenic	Bpnt2
90737681	90739223	0,6499	5,4362517	2,03E-05	0,030144	Distal Intergenic	G530011O06Rik
40806640	40808548	-0,4428	5,7524552	2,67E-05	0,036605	Promoter	Hspa8
31121300	31122363	0,47732	5,0968488	3,16E-05	0,040263	Distal Intergenic	Tff3
75276277	75277012	-0,569	4,3057845	3,41E-05	0,040524	Intron	Serpini2
7117861	7118838	-0,4234	5,1373864	4,09E-05	0,045576	Distal Intergenic	Cnksr3
75666688	75667810	-0,4731	4,8592239	4,79E-05	0,046962	Intron	Akap13
16550183	16551479	-0,5728	4,3454549	4,65E-05	0,046962	Intron	Plxdc2
102514775	102515536	-0,4916	4,7214302	5,53E-05	0,046962	Intron	Pde4b
109563765	109564452	-0,5454	4,437817	5,32E-05	0,046962	Promoter	Dhx38
40594676	40595659	-0,5695	4,3413758	5,15E-05	0,046962	Distal Intergenic	Clec5a
70225507	70226277	-0,4294	4,9969669	6,12E-05	0,047482	Promoter	Pygl
40745933	40746771	-0,54	4,354137	6,12E-05	0,047482	Intron	Dock4
84178774	84180097	-0,5062	5,3526392	6,43E-05	0,047748	Distal Intergenic	Zfp36l2

Table S3 - Differentially accessible chromatin regions identified in AMs on day six after *in vivo* training. List of differentially accessible regions (DARs) identified by ATAC-seq in LPS-trained and control AMs six days after *in vivo* training. Regions are ordered by adjusted p-value (padj), from lowest to highest. DARs with $\text{padj} \leq 0.05$ were considered significant and are displayed. Values in column “avlog2cpm” indicate average read counts of DARs expressed as \log_2 -transformed cpm (counts per million reads). *To view the complete table, which contains additional information on region width, chromosome number, gene start, gene end, gene length, strand, distance to transcription start site and ENSEMBL IDs, please refer to the online version of the publication.*

Table S4a - Reagents, disposables and antibodies.

Material	Company	Catalogue number
ATAC-seq		
TDE1 Tagment DNA Enzyme	Illumina	15027865
TD Buffer	Illumina	15027866
Tagment DNA Enzyme and Buffer Small Kit	Illumina	20034197
Digitonin	Promega	G9441
Qiagen MinElute kit	Qiagen	28004
ROX reference dye	Invitrogen	12223-012
Nextera DNA library prep Kit	Nextera	15028212
SYBR Green nucleic acid gel stain	Sigma	S9430
NEBnext High-Fidelity 2x PCR master mix	New England Biolabs	M0541S
Cell culture		
96 well tissue-culture treated multiple well plate	Corning	3585
12 well flat bottom plate, non-treated	CytoOne	CC7672-7512
Penicillin-Streptomycin (solution)	Sigma	P4333
RPMI-1640 Medium with L-glutamine and sodium bicarbonate	Sigma	R8758
Fetal bovine serum heat- inactivated	Sigma	F9665
Dulbecco's Phosphate Buffered Saline (without calcium chloride and magnesium chloride)	Sigma	D8537
6 well tissue-culture treated multiple well plate	Corning	3506
Trypan Blue solution	Sigma	T8154
Xylanaest® purum 2%	Gebro Pharma	
Cytokine analysis		
ELISA MAX™ Standard Set Mouse IL-6	BioLegend	431301
LEGENDplex mouse macrophage/microglia panel	BioLegend	740846
LEGENDplex data analysis software	BioLegend	N/A
In vivo labeling		
Red Fluorescent Phagocytic Cell Linker Kit	Sigma	PKH26PCL
CellTrace CFSE Cell Proliferation Kit	Invitrogen	C34554
Quant-seq		
RLT buffer	Qiagen	79216
2-mercaptoethanol	Sigma	M3148
RNeasy Micro kit	Qiagen	74034
Quantseq 3' mRNA-Seq Library Prep Kit (FWD) for Illumina	Lexogen	015.96
PCR Add-on Kit for Illumina	Lexogen	020.96
UMI Second Strand Synthesis Module for QuantSeq FWD (Illumina, Read1)	Lexogen	081.96

Table S4a - Reagents, disposables and antibodies.

Material	Company	Catalogue number
Seahorse		
Seahorse XF RPMI Medium, pH 7.4	Agilent	103576-100
Seahorse XF Glucose 1M solution	Agilent	103577-100
Seahorse XF Pyruvate 100 mM solution	Agilent	103578-100
Seahorse XF L-glutamine 200 mM solution	Agilent	103579-100
Oligomycin A	Sigma	75351
Fluoro-carbonyl cyanide phenylhydrazine	Sigma	C2920
Rotenone	Sigma	R8875
Antimycin A	Sigma	A8674
Seahorse XF96 cell culture microplate	Agilent	101085-004
Seahorse XFe96 FluxPak	Agilent	102416-100
Organ collection and processing		
18G Venflon	BD Biosciences	391457
BD Connecta™	BD Biosciences	394602
NaCl 0.9%	B. Braun	3570130
MACS® SmartStrainers 70µm	Miltenyi Biotec	130-110-916
GentleMACS™ C Tubes	Miltenyi Biotec	130-096-334
Fix&Perm Fixation Medium A	Nordic Mubio	GAS-002A-1
MACS® SmartStrainers 30µm	Miltenyi Biotec	130-110-915
Bovine Serum Albumin	Carl Roth	8076.3
DNAse I	Sigma	DN25
Collagenase I	Gibco	17100-017
NH ₄ Cl	Sigma	A9434
KHCO ₃	Sigma	237205
Na ₂ EDTA	Sigma	E4884
Cytokines & inhibitors		
Mouse IFN-β	pbl assay science	12405-1
5'-deoxy-5'-methylthioadenosine	Cayman chemical	15593
Anacardic acid	Abcam	ab120892
2-deoxyglucose	Sigma	D8375
bis-2-(5-phenylacetamido-1,3,4-thiadiazol-2-yl)ethyl sulfide	Sigma	SML0601
Etomoxir	Sigma	E1905
Murine GM-CSF	Peprtech	315-03
Human TGF-β	Peprtech	100-21
Rosiglitazone	Sigma-Aldrich	R2408
Heat-inactivated <i>S. pneumoniae</i> ATCC6303	N/A	N/A
FITC-labeled heat-inactivated <i>S. pneumoniae</i> ATCC6303	N/A	N/A

Table S4a - Reagents, disposables and antibodies.

Material	Company	Catalogue number
LPS E.coli O55:B5	Sigma	2880
Dexamethasone	Sigma	D883
cryo-sure DMSO	WAK-Chemie Medical GmbH	WAK-DMSO-10
Bacterial culture		
Todd Hewitt Bouillon	Carl Roth	X936.1
Anaesthesia		
Rompun	Bayer	Approval nr. 14840
Ketasol	OGRIS Pharma	Approval nr. 8-00173

Table S4b - Flow cytometry antibodies.

Epitope	Fluorophore	Company	Catalogue nr.	Clone	Dilution
anti-mouse TER-119	APC/Cy7	BioLegend	116223	TER-119	1:200
fixable viability dye	eFluor 780	eBioscience	65-0865-14	N/A	1:1000
anti-mouse CD16/32	N/A	eBioscience	14-016-82	93	1:500
anti-mouse CD45	BV510	BioLegend	103138	30-F11	1:100
anti-mouse CD45	PerCP Cy5.5	BioLegend	109827	104	1:200
anti-mouse CD45	PE-Cy7	BioLegend	109830	104	1:200
anti-mouse Siglec F	AF647	BD	562680	E50-2440	1:200
anti-mouse Siglec F	PerCP Cy5.5	BD	565526	E50-2440	1:200
anti-mouse CD11c	AF700	eBioscience	56-0114-82	N418	1:200
anti-mouse CD11c	PE	BD	557401	HL3	1:200
anti-mouse CD11c	APC	BioLegend	117310	N418	1:200
anti-mouse CD11b	Pacific Blue	BioLegend	101224	M1/70	1:200
anti-mouse CD11b	AF700	eBioscience	56-0112-80	M1/70	1:200
anti-mouse CD11b	BV605	BioLegend	101237	M1/70	1:200
anti-mouse Ly6C	BV605	BioLegend	128036	HK1.4	1:200
anti-mouse Ly6G	FITC	BioLegend	127605	1A8	1:200
anti-mouse Ly6G	PE-Cy7	BioLegend	127617	1A8	1:200
anti-mouse Ly6G	BV510	BioLegend	127633	1A8	1:200
anti-mouse CD3	PE-Cy7	BioLegend	100319	145-2C11	1:200
anti-mouse CD3	FITC	BioLegend	100204	17A2	1:200
anti-mouse NK1.1	APC	BioLegend	108709	PK136	1:200
anti-mouse MHCII	Pacific Blue	eBioscience	48-5321	M5/114.15.2	1:200
anti-mouse CD19	BV605	BioLegend	115540	6D5	1:200
anti-mouse CD64	PE-Cy7	BioLegend	139313	X54-5/7.1	1:200
anti-mouse Axl	APC	Thermo Fisher	17-1084-82	MAXL8DS	1:200
anti-mouse MerTK	PE-Texas Red	BioLegend	151523	2B10C42	1:100

Table S4c - Instruments.

Qubit fluorometer (Life Technologies)
HiSeq 3000/4000 (Illumina)
FACSAria™ Fusion
Bioanalyzer 2100 (Agilent Technologies)
Orbitrap Q Exactive (Thermo Scientific)
Vanquish UHPLC system (Thermo Fisher Scientific)
Orbitrap Fusion™ Lumos™ Tribrid™ mass spectrometer (Thermo Fisher Scientific)
XF-96 Extracellular Flux Analyzer (Seahorse Biosciences)

3

Extended discussion

The concept of trained immunity has broadened our understanding of the innate immune system, thereby challenging the classical dogma that the formation of an immunological memory is restricted to adaptive immune cells. Research of the past decade identified a vast diversity of cell types capable of developing trained immunity, and demonstrated the complexity of its underlying mechanisms. Furthermore, it moved the impact of experimental models and disease settings into focus. However, while *in vitro* studies allowed us to gain insights into inducing agents, signaling pathways and mechanistic aspects of trained immunity, our current knowledge about the induction, regulation and consequences of mucosal innate memory remains very scarce.

Our lungs are continuously exposed to airborne environmental compounds, including house dust mite, cigarette smoke, microbe-associated compounds and pathogenic agents (Brunekreef, 2018). Being located at the interface of the airways and the lungs (Aberdein *et al*, 2013), AMs are prone to encounter such stimuli and thus may be particularly susceptible to develop an innate immune memory. In 2018, Yao and colleagues demonstrated that respiratory adenoviral infection leads to the induction of “memory AMs”, that self-maintained independently of incoming monocytes and produced increased amounts of chemoattractants upon secondary challenge with *S. pneumoniae* (Yao *et al*, 2018). The induction (but not maintenance) of this phenotype was dependent on CD8⁺ T-cell derived IFN- γ and resulted in enhanced protection against pneumococcal pneumonia due to enhanced AM-mediated neutrophil recruitment (Yao *et al*, 2018). While this study clearly illustrates that innate reprogramming of AMs can have a significant impact on lung immunity, certain aspects should be considered with regards to the conceptual definition of trained immunity. It is known that IFN- γ can enhance the immunological reactivity and microbicidal activity of macrophages, a concept termed “IFN- γ priming” (Wu *et al*, 2014). As discussed in chapter 1.4.1., primed (as opposed to trained) immune responses do not return to baseline following primary stimulation. In the above-mentioned publication, IFN- γ -experienced AMs were characterized by increased transcriptional and glycolytic activity at baseline, four weeks after adenoviral exposure. Therefore, the described phenotype might be a consequence of IFN- γ priming rather than innate training.

We here discovered that exposure to a ubiquitous microbial agent, LPS, can elicit trained immunity in AMs and demonstrated that AM training occurred independently of IFN- γ and T cells. Instead, we found that type 1 IFN receptor signaling was critical for AM memory induction and provide evidence that this process may occur via autocrine regulation.

Upon TLR4-mediated recognition of LPS, the MyD88-independent signaling cascade culminates in the dimerization and translocation of IRF3, enabling the production of type 1 IFNs, which are released and bind to the heterodimeric type 1 IFN receptor in an autocrine or paracrine manner (Chang *et al*, 2007). In the canonical pathway, this activates the receptor-associated kinases JAK1 and tyrosine kinase 2 (TYK2), which phosphorylate STAT1 and STAT2 molecules, enabling their dimerization, nuclear translocation and binding to IRF9 (McNab *et al*, 2015). Together, these components form the interferon-stimulated gene (ISG) factor 3 (ISGF3) complex, which binds to IFN-stimulated response elements within the promoter regions of ISGs, enabling their transcriptional activation and, thereby, the induction of an antiviral cellular program (McNab *et al*, 2015). In addition, non-canonical signaling can occur via activation of STAT1 homodimers, STAT3, STAT4 or STAT5, allowing for transcription of a broad range of genes (McNab *et al*, 2015).

Using CD169Cre *Ifnar1*^{fl} mice, we could show that AM-specific *Ifnar1* deficiency abrogated the trained IL-6 response of LPS-exposed AMs. These findings suggest that type 1 IFNs, produced as a consequence of intranasal LPS administration, may *directly* act on AMs to induce trained immunity. In addition, we provided evidence that AM training can occur via autocrine sensing of type 1 IFNs in an *in vitro* setting. Considering that type 1 IFNs can be produced by a multitude of cell types (e.g. pDCs, macrophages, B cells, epithelial cells), it remains to be investigated, which cell population(s) serve(s) as the major source of type 1 IFNs during *in vivo* LPS training.

While we demonstrated that exogenous administration of IFN- β can train AMs similarly to LPS, it needs to be indicated that the mechanistic basis of IFN- β -mediated AM training may differ from that of LPS-induced AM memory. Of note, type 1 IFNs are able to modulate the core metabolic program of innate immune cells (Wu *et al*, 2016). In murine plasmacytoid DCs, autocrine sensing of type 1 IFNs (following stimulation with the TLR9 agonist CpG) reportedly increased FAO and OXPHOS (Wu *et al*, 2016). In our study, we identified a critical role of cellular metabolism in LPS-induced mexAM training. In this context, it might be possible that AM-derived IFN- β contributes to the acute metabolic activation of AMs during LPS exposure, thus enabling the enhanced production of proinflammatory mediators upon subsequent bacterial challenge.

Research of the past years has highlighted the impact of cellular metabolism on immune cell activity and function. Trained immunity is commonly associated with elevated glycolytic activity, which is sometimes accompanied by a decrease in OXPHOS (Arts *et al*, 2016a). However, the metabolic demands and dependencies of innate immune cells can depend on the availability of nutrients specific for their tissue environment. AMs are metabolically adapted to the low glucose concentration and lipid-rich milieu of the lungs (Ogger & Byrne, 2021), and demonstrate limited glycolytic activity in response to LPS (Woods *et al*, 2020). Instead, they preferably engage OXPHOS and express high levels of PPAR- γ , which regulates the accumulation of lipids and promotes FAO in order to sustain energy production via OXPHOS (Ogger & Byrne, 2021). We found that LPS-induced AM training occurred independently of glycolysis, while glutaminolysis and FAO, two central metabolic pathways that can fuel the TCA cycle, were critical drivers of this process. Additionally, LPS-exposed AMs were characterized by decreased TAG levels on day six after training. TAGs are crucial to for the maintenance of energy homeostasis (Wang *et al*, 2017) and store large amounts of fatty acids that are covalently linked to the trivalent alcohol glycerol via ester bonds (Grabner *et al*, 2021). Upon TAG hydrolysis, free fatty acids are released and may feed into mitochondrial FAO to generate acetyl-CoA, a key metabolite of the TCA cycle (Grabner *et al*, 2021). Based on our findings, it could be speculated that cytoplasmic TAGs (which are commonly located in lipid droplets) are lysed upon LPS exposure, thus allowing the release and usage of stored fatty acids for FAO. LPS-mediated AM training was further characterized by increased levels of different phosphatidylcholines, which constitute major components of biological membranes. These lipid classes might potentially promote AM receptor expression and receptor-mediated signaling via membrane remodelling, allowing for faster recognition and translation of secondary stimuli. Along these lines, future experiments will be required to fully understand whether and how lipid metabolism contributes to the development of AM memory.

Our metabolomic analysis further revealed that trained AMs contained reduced levels of two TCA cycle intermediates – fumarate and malate. Conversely, β -glucan-induced trained immunity of macrophages reportedly led to accumulation of citrate, succinate, fumarate, malate and 2-hydroxyglutarate, as these metabolites were replenished via glutaminolysis (Arts *et al*, 2016b). Further, increased levels of succinate and fumarate can promote glycolysis by stabilizing HIF1 α , and may antagonize histone- and DNA demethylation (Arts *et al*, 2016a). Considering that AMs display a unique metabolic phenotype, it appears plausible that the metabolic features of AM memory may differ from those reported for monocytes or other macrophage populations. In addition, it needs to be noted that metabolomic analysis represents a snapshot of the cellular metabolic profile at the investigated timepoint of sample

collection. Metabolic tracing of isotopically labelled substrates may serve to fully understand the metabolic circuits of LPS-induced AM memory in the future.

Interestingly, LPS-exposed AMs displayed a reduced oxygen consumption rate (OCR) and extracellular acidification rate (ECAR) on day six after *in vivo* training and during bacterial *ex vivo* challenge. These findings are in sharp contrast to the increased glycolytic activity classically associated with innate memory, which might possibly be explained by the distinct metabolic profile and dependencies of AMs. Although seahorse measurements enable real-time assessment of metabolic rates, the obtained results might depend on the investigated timepoint. In order to characterize the metabolic state of LPS-exposed AMs at the time of enhanced cytokine production, we performed respective measurements 16 h after bacterial restimulation. While both OCR and ECAR were significantly decreased at this timepoint, we did not dissect whether the metabolic activity of trained AMs is increased *early* upon bacterial challenge. Furthermore, a potential inter-connection or co-dependency of cellular metabolism and cytokine production is difficult to assess and speculate about, as transcriptional regulation and metabolic activity do not necessarily correlate due to differences in temporal dynamics.

Apart from metabolic rewiring, epigenetic regulation serves as a fundamental mechanistic basis of trained immunity. Epigenetic modifications, established during primary exposure to the training agent, can modulate the accessibility of chromatin, which facilitates (or hinders) transcription upon a secondary challenge. In this study, we found that LPS-exposed AMs displayed a limited number of differentially accessible regions six days after *in vivo* training. The reduced plasticity of AMs has been proposed to result from their prolonged tissue residency and may have been favoured throughout evolution in order to preserve tissue homeostasis at steady state and following inflammatory insults (Guilliams & Svedberg, 2021). Recruited monocytes, on the contrary, maintain a plastic epigenetic profile as they are able to differentiate into TRMs during inflammation. After prolonged residency within the tissue-specific niche of the lungs, however, they are imprinted by the local environment and acquire an AM-like phenotype (Guilliams & Svedberg, 2021).

At steady state, AM activation is dampened via various mechanisms (s. chapter 1.2.2.) to prevent excessive inflammation. Considering that AMs are continuously exposed to - potentially pathogenic - compounds from the external environment, their restricted epigenetic memory might enable a fast return to baseline. However, this ability likely depends on the intensity and duration of such insults. Roquilly et al. reported that AMs acquire a tolerized epigenetic profile during primary pneumonia (induced by *E. coli* or influenza A virus infection), which leads to impaired phagocytosis and enhanced susceptibility to secondary pneumonia (*E. coli* or *S. aureus*) four weeks after initial infection (Roquilly et al, 2020). Further, the authors

showed that upregulation of SIRP α during the early phase of primary pneumonia promoted an immuno-suppressive environment, which led to the induction of AM paralysis (Roquilly *et al*, 2020). This study highlights that preceding inflammatory responses can modulate the local microenvironment of the lungs, thus altering the reactivity of AMs to a subsequent infectious challenge. Furthermore, the authors' findings indicate that the tissue-specific context constitutes a major determinant of AM functionality, and thus point out the necessity to address the *in vivo* consequences of AM imprinting.

While our ATAC-seq data suggest that AMs maintain a small number of epigenetic changes following LPS exposure, there are a few important aspects that need to be considered. As we did not address the possibility that *in vivo* training might not affect the entire AM population, but instead induce and/or reprogram specific AM subsets, it is possible that potential differences in chromatin accessibility are under-represented by bulk ATAC-seq analysis. Of note, the same consideration applies to bulk RNA-seq approaches. Single-cell analysis of epigenetic and gene expression profiles may serve as an elegant tool to fully elucidate whether LPS training results in the formation of AM subpopulations.

Our ATAC-seq analysis revealed that multiple regions associated with the transcription factor Fos were more accessible in LPS-trained compared to control AMs. Fos proteins are able to form heterodimers with Jun proteins (i.e. transcription factors of the Jun family), leading to the formation of the AP-1 complex, a master regulator of multiple biological processes, including proliferation, differentiation, survival and apoptosis (Gazon *et al*, 2017). In this context, it can be speculated that increased availability of Fos could, in turn, promote increased AP-1 levels and consequently accelerate signal transduction during secondary bacterial challenge. Future experiments will be required to test this hypothesis.

Epigenetic processes are often closely intertwined with cellular metabolism. On day six after *in vivo* training, LPS-exposed AMs contained increased levels of S-adenosyl-methionine (SAM), a global methyl group donor, which may potentially influence epigenetic processes by serving as a donor for histone or DNA methylation. Addressing this possibility, we trained mexAMs in presence of the methyltransferase inhibitor MTA and found that the trained IL-6 response was *augmented*. SAM was reported to inhibit LPS-induced TNF production and iNOS expression while promoting IL-10 production (Hevia *et al*, 2004). During polyamine synthesis, decarboxylated SAM (which is originally synthesized from L-methionine and ATP) is converted into MTA. As MTA was observed to retain many of the effects ascribed to SAM, it is possible that SAM-mediated processes may be, at least partially, attributed to its conversion into MTA (Hevia *et al*, 2004). Indeed, Hevia *et al*. reported that coincubation of RAW 264.7 macrophages with LPS and MTA abrogated TNF production and iNOS induction, while potentiating their IL-10 response (Hevia *et al*, 2004). These effects were caused by

attenuated p38 MAPK signaling, c-jun phosphorylation and I κ B α degradation as a result of MTA exposure (Hevia *et al*, 2004). *In vivo*, MTA can be recycled into methionine - and subsequently into SAM - during the methionine salvage pathway, which further increases the complexity of this subject. Therefore, while our results suggest that methylation processes hinder the establishment of AM memory, they should be interpreted with caution. Furthermore, the epigenetic program of tissue-resident AMs likely differs from that of cultured mexAMs due to lack of tissue-specific factors and influences.

Humans are continuously exposed to varying concentrations of airborne endotoxin, which may either occur in an occupational or in an environmental context. These two types of exposure differ in several aspects, including the periodicity and amount of LPS inhalation, as well as its impact on human health (Shamsollahi *et al*, 2019). Occupational endotoxin exposure frequently causes adverse effects, such as fever, lung cancer, or atopic asthma, whereas exposure to environmental LPS (especially if happening during early life) was shown to reduce the incidence of allergic asthma in adolescence (Shamsollahi *et al*, 2019). We here identified that intranasal treatment with 1 ng LPS (a dose corresponding to 0.15 – 3.3 EU per breath in humans, assuming 0.5 L tidal volume (Hallett *et al*, 2022)) protected mice from pneumococcal pneumonia six days later. While these findings underline the immunomodulatory potential of environmental agents, it remains to be investigated whether and how ambient LPS exposure affects the outcome of other respiratory diseases, such as allergic asthma or fibrosis.

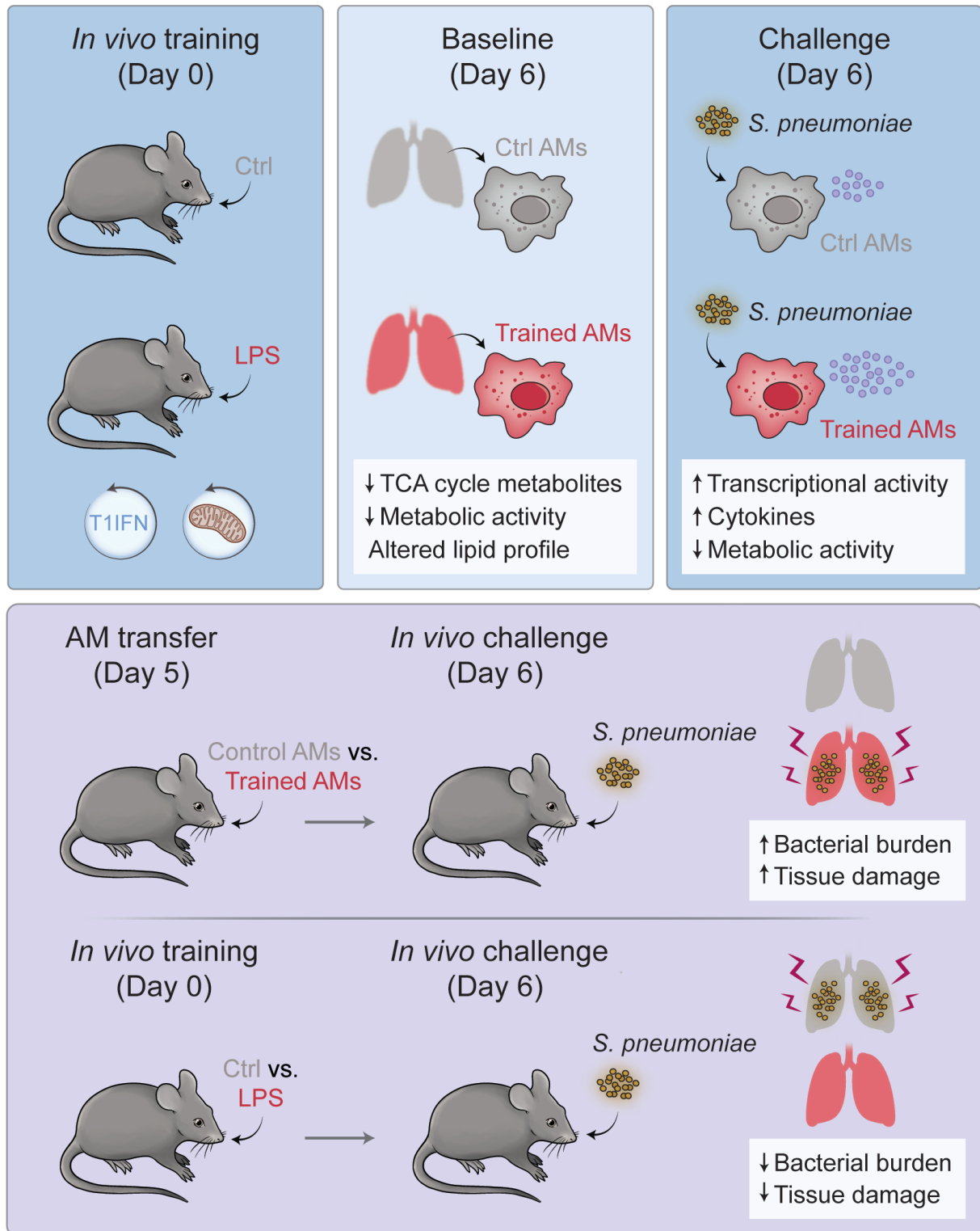
The concept of trained immunity was established based on observations of protective cross-reactivity in organisms lacking an adaptive immune system (Netea *et al*, 2011). Indeed, continuous evidence supports the notion that enhanced activation of trained innate immune cells can play a beneficial role in host immunity. However, excessive immune activation, if left unconstrained, may have a maladaptive impact on chronic inflammatory conditions, such as atherosclerosis, arthritis, or autoimmune diseases (Bekkering *et al*, 2021).

AM activation is fine-tuned to maintain tissue homeostasis and, at the same time, mount appropriate responses to environmental signals or infectious agents (Hussell & Bell, 2014). Therefore, imbalanced or dysregulated AM activity may potentially drive hyper- or hypoinflammation, and consequently hinder tissue repair or pathogen removal. We here showed that adoptive transfer of LPS-trained AMs impaired host defense against *S. pneumoniae*, and promoted lung inflammation. In contrast, intranasal exposure to LPS (six days prior to infection) promoted pneumococcal clearance and resolution of inflammation. While our study did not aim to dissect the complexity of these opposing findings, I would like to discuss potential explanations for those observations. LPS is a potent immunomodulatory agent, which, upon intranasal administration, may affect any lung-resident myeloid, lymphoid

or structural cell population. It is therefore possible that LPS exposure not only induces AM training but also reprograms other (non-AM) cell populations, thereby altering their responsiveness to a subsequent infection. Such additional reprogramming effects may be essential to restrain/cooperate with trained AM responses and/or optimize host defense during pneumococcal challenge. In an adoptive transfer setup, however, such non-AM effects are taken out of the equation, which could ultimately lead to impaired bacterial clearance, excessive inflammation and worsened disease outcome. At the same time it needs to be considered that adoptive transfer experiments harbor intrinsic difficulties, which may affect experimental outcomes due to concomitant inflammation and non-physiological conditions. The sole transfer of naïve AMs may, for instance, alter the recipient's immune response and general susceptibility to an infectious challenge. Furthermore, the isolation and subsequent, immediate transfer of AMs might impact their metabolic and immunological activity, which may not be comparable to their actual physiological behavior.

Last but not least, the tissue-specific microenvironment can have a fundamental impact on immune cell function and activity. As such, the regulatory milieu of the lungs (including e.g. non-cellular, soluble mediators) may be necessary to fine-tune LPS-induced AM memory *in vivo*.

In summary, we provide evidence that environmental pathogen-associated compounds can elicit trained immunity in the lungs, and identified a novel mechanism of AM training, which is dependent on type 1 IFN signaling and metabolic reprogramming (s. Thesis Figure 13). Our findings illustrate that the cellular characteristics of LPS-trained AMs are influenced by their unique mucosal environment, and highlight the necessity to investigate trained immunity in a tissue-specific context.



Thesis figure 13 - Graphical abstract

Trained immunity of alveolar macrophages requires metabolic rewiring and type 1 interferon signaling.

Conclusion & future prospects

The burgeoning field of trained immunity has allowed us to gain new insights into the diversity and adaptability of our innate immune system. Yet, we are only beginning to understand how versatile the mechanisms and consequences of innate memory can be. As such, traditional hallmarks of trained immunity (e.g. increased glycolytic activity, beneficial impact on host defense) may not be applicable to innate immune cells residing in specialized mucosal environments. In our study, we discovered that LPS, a ubiquitous microbial compound, has the potential to elicit trained immunity in AMs, and identified unique features of LPS-induced AM memory. Considering that AMs are permanently exposed to environmental agents, it will be necessary to dissect whether other airborne PAMPs, but also non-microbial particles, are able to induce AM training. Furthermore, while we demonstrated a critical role of LPS-induced AM memory in the context of bacterial pneumonia, it is possible that its impact on host immunity is influenced by the type of secondary challenge. Therefore, this phenomenon should be addressed in additional disease models and scenarios in order to fully uncover the immunomodulatory potential of AM training.

Research of the past decades enabled the development of promising immunotherapeutic approaches, which continue to provide great benefits to patients suffering from immune-related diseases. However, current treatment strategies predominantly focus on the neutralization of small effector molecules and on the engagement of adaptive immunity. Innate immune reprogramming may therefore open a novel therapeutic avenue, aiming to treat conditions of, both, hyperinflammation and immunosuppression. Trained immunity-based vaccines could offer non-specific, heterologous protection against different pathogens, and/or could be used in synergy with existing adaptive immunotherapies to improve their performance. As the clinical translation of trained immunity is currently facing technical limitations and challenges (s. chapter 1.4.5), a profound understanding of its biological principles is essential to fuel the development of innovative therapies. In context with our findings, it will be important to assess a potential role of AM training in human health and disease. As such, the identification of inducers and/or inhibitors of human AM memory, combined with a thorough investigation of its underlying mechanisms, may ultimately enable its therapeutic exploitation, for instance in the form of adoptive AM transfers or inhalation exposure.

At the same time, however, potential adverse effects of AM training need to be taken into account, as they might lead to chronic hyperinflammation and modulate the host's immune response to future infections. Our study emphasizes the need to investigate and characterize the impact of AM memory in a physiological setting, and raises awareness for potential

maladaptive consequences resulting from the adoptive transfer of an isolated, single cell population.

Assessing the longevity of LPS-induced AM memory, we found that the increased IL-6 production capacity of trained AMs persisted for (at least) six weeks. While we demonstrated that the resident AM population was not replenished by incoming monocytes early after *in vivo* training, we did not investigate AM turnover at later timepoints. Although it appears unlikely that the local AM pool gets repopulated several weeks after (low-dose) LPS exposure, it cannot be excluded that the increased reactivity of the trained AM population may be attributed to recruited moAMs rather than to the long half-life of tissue-resident AMs. In this context, future studies will be required to identify the precise duration of AM memory responses, as this information will be relevant for potential therapeutic applications. Similarly, it will be necessary to investigate whether AM memory is pertained following respiratory infectious challenges that cause AM depletion. Along these lines, it remains to be determined whether inducing agents of trained immunity lead to the formation of distinct AM subpopulations, which acquire distinct phenotypic properties and take on differential tasks during subsequent pulmonary exposures. The advancing field of single-cell analysis should allow to tackle these research questions in the near future.

In conclusion, our data point out the need to explore and understand the concepts and mechanisms of trained immunity in tissue-resident macrophages, with the ultimate goal of developing novel therapeutic approaches that exploit innate memory for the benefit of patients.

References

- Abdelaziz MH, Abdelwahab SF, Wan J, Cai W, Huixuan W, Jianjun C, Kumar KD, Vasudevan A, Sadek A, Su Z *et al* (2020) Alternatively activated macrophages; a double-edged sword in allergic asthma. *J Transl Med* 18: 58
- Abel AM, Yang C, Thakar MS, Malarkannan S (2018) Natural Killer Cells: Development, Maturation, and Clinical Utilization. *Front Immunol* 9: 1869
- Aberdein JD, Cole J, Bewley MA, Marriott HM, Dockrell DH (2013) Alveolar macrophages in pulmonary host defence the unrecognized role of apoptosis as a mechanism of intracellular bacterial killing. *Clin Exp Immunol* 174: 193-202
- Acevedo OA, Berrios RV, Rodriguez-Guilarte L, Lillo-Dapremont B, Kalergis AM (2021) Molecular and Cellular Mechanisms Modulating Trained Immunity by Various Cell Types in Response to Pathogen Encounter. *Front Immunol* 12: 745332
- Aegerter H, Kulikauskaite J, Crotta S, Patel H, Kelly G, Hessel EM, Mack M, Beinke S, Wack A (2020) Influenza-induced monocyte-derived alveolar macrophages confer prolonged antibacterial protection. *Nat Immunol* 21: 145-157
- Allard B, Panariti A, Martin JG (2018) Alveolar Macrophages in the Resolution of Inflammation, Tissue Repair, and Tolerance to Infection. *Front Immunol* 9: 1777
- Alon R, Sportiello M, Kozlovski S, Kumar A, Reilly EC, Zarbock A, Garbi N, Topham DJ (2021) Leukocyte trafficking to the lungs and beyond: lessons from influenza for COVID-19. *Nat Rev Immunol* 21: 49-64
- Arts RJ, Joosten LA, Netea MG (2016a) Immunometabolic circuits in trained immunity. *Semin Immunol* 28: 425-430
- Arts RJ, Novakovic B, Ter Horst R, Carvalho A, Bekkering S, Lachmandas E, Rodrigues F, Silvestre R, Cheng SC, Wang SY *et al* (2016b) Glutaminolysis and Fumarate Accumulation Integrate Immunometabolic and Epigenetic Programs in Trained Immunity. *Cell Metab* 24: 807-819
- Arts RJW, Carvalho A, La Rocca C, Palma C, Rodrigues F, Silvestre R, Kleinnijenhuis J, Lachmandas E, Goncalves LG, Belinha A *et al* (2016c) Immunometabolic Pathways in BCG-Induced Trained Immunity. *Cell Rep* 17: 2562-2571
- Arts RJW, Moorlag S, Novakovic B, Li Y, Wang SY, Oosting M, Kumar V, Xavier RJ, Wijmenga C, Joosten LAB *et al* (2018) BCG Vaccination Protects against Experimental Viral Infection in Humans through the Induction of Cytokines Associated with Trained Immunity. *Cell Host Microbe* 23: 89-100 e105
- Bain CC, MacDonald AS (2022) The impact of the lung environment on macrophage development, activation and function: diversity in the face of adversity. *Mucosal Immunol* 15: 223-234
- Baker EH, Baines DL (2018) Airway Glucose Homeostasis: A New Target in the Prevention and Treatment of Pulmonary Infection. *Chest* 153: 507-514

Baker EH, Clark N, Brennan AL, Fisher DA, Gyi KM, Hodson ME, Philips BJ, Baines DL, Wood DM (2007) Hyperglycemia and cystic fibrosis alter respiratory fluid glucose concentrations estimated by breath condensate analysis. *J Appl Physiol* (1985) 102: 1969-1975

Baker RE, Mahmud AS, Miller IF, Rajeev M, Rasambainarivo F, Rice BL, Takahashi S, Tatem AJ, Wagner CE, Wang LF *et al* (2022) Infectious disease in an era of global change. *Nat Rev Microbiol* 20: 193-205

Bals R (2005) Lipopolysaccharide and the lung: a story of love and hate. *Eur Respir J* 25: 776-777

Bals R, Hiemstra PS (2004) Innate immunity in the lung: how epithelial cells fight against respiratory pathogens. *Eur Respir J* 23: 327-333

Basinas I, Sigsgaard T, Kromhout H, Heederik D, Wouters IM, Schlunssen V (2015) A comprehensive review of levels and determinants of personal exposure to dust and endotoxin in livestock farming. *J Expo Sci Environ Epidemiol* 25: 123-137

Bazzan E, Turato G, Tine M, Radu CM, Balestro E, Rigobello C, Biondini D, Schiavon M, Lunardi F, Baraldo S *et al* (2017) Dual polarization of human alveolar macrophages progressively increases with smoking and COPD severity. *Respir Res* 18: 40

Beatty SR, Rose CE, Jr., Sung SS (2007) Diverse and potent chemokine production by lung CD11b^{high} dendritic cells in homeostasis and in allergic lung inflammation. *J Immunol* 178: 1882-1895

Bejjani F, Evanno E, Zibara K, Piechaczyk M, Jariel-Encontre I (2019) The AP-1 transcriptional complex: Local switch or remote command? *Biochim Biophys Acta Rev Cancer* 1872: 11-23

Bekkering S, Arts RJW, Novakovic B, Kourtzelis I, van der Heijden C, Li Y, Popa CD, Ter Horst R, van Tuijl J, Netea-Maier RT *et al* (2018) Metabolic Induction of Trained Immunity through the Mevalonate Pathway. *Cell* 172: 135-146 e139

Bekkering S, Dominguez-Andres J, Joosten LAB, Riksen NP, Netea MG (2021) Trained Immunity: Reprogramming Innate Immunity in Health and Disease. *Annu Rev Immunol* 39: 667-693

Bekkering S, Quintin J, Joosten LA, van der Meer JW, Netea MG, Riksen NP (2014) Oxidized low-density lipoprotein induces long-term proinflammatory cytokine production and foam cell formation via epigenetic reprogramming of monocytes. *Arterioscler Thromb Vasc Biol* 34: 1731-1738

Bekkering S, Stiekema LCA, Bernelot Moens S, Verweij SL, Novakovic B, Prange K, Versloot M, Roeters van Lennep JE, Stunnenberg H, de Winther M *et al* (2019) Treatment with Statins Does Not Revert Trained Immunity in Patients with Familial Hypercholesterolemia. *Cell Metab* 30: 1-2

Bistoni F, Vecchiarelli A, Cenci E, Puccetti P, Marconi P, Cassone A (1986) Evidence for macrophage-mediated protection against lethal *Candida albicans* infection. *Infect Immun* 51: 668-674

Blumenthal RL, Campbell DE, Hwang P, DeKruyff RH, Frankel LR, Umetsu DT (2001) Human alveolar macrophages induce functional inactivation in antigen-specific CD4 T cells. *J Allergy Clin Immunol* 107: 258-264

- Boada-Romero E, Martinez J, Heckmann BL, Green DR (2020) The clearance of dead cells by efferocytosis. *Nat Rev Mol Cell Biol* 21: 398-414
- Borger JG, Lau M, Hibbs ML (2019) The Influence of Innate Lymphoid Cells and Unconventional T Cells in Chronic Inflammatory Lung Disease. *Front Immunol* 10: 1597
- Branger J, Knapp S, Weijer S, Leemans JC, Pater JM, Speelman P, Florquin S, van der Poll T (2004) Role of Toll-like receptor 4 in gram-positive and gram-negative pneumonia in mice. *Infect Immun* 72: 788-794
- Briken V, Mosser DM (2011) Editorial: switching on arginase in M2 macrophages. *J Leukoc Biol* 90: 839-841
- Brooks LRK, Mias GI (2018) Streptococcus pneumoniae's Virulence and Host Immunity: Aging, Diagnostics, and Prevention. *Front Immunol* 9: 1366
- Brunekreef B (2018) [Air pollution and health]. *Ned Tijdschr Geneesk* 162
- Buenrostro JD, Giresi PG, Zaba LC, Chang HY, Greenleaf WJ (2013) Transposition of native chromatin for fast and sensitive epigenomic profiling of open chromatin, DNA-binding proteins and nucleosome position. *Nat Methods* 10: 1213-1218
- Byrne AJ, Mathie SA, Gregory LG, Lloyd CM (2015) Pulmonary macrophages: key players in the innate defence of the airways. *Thorax* 70: 1189-1196
- Byrne AJ, Powell JE, O'Sullivan BJ, Ogger PP, Hoffland A, Cook J, Bonner KL, Hewitt RJ, Wolf S, Ghai P *et al* (2020) Dynamics of human monocytes and airway macrophages during healthy aging and after transplant. *J Exp Med* 217
- Cai S, Batra S, Lira SA, Kolls JK, Jeyaseelan S (2010) CXCL1 regulates pulmonary host defense to Klebsiella Infection via CXCL2, CXCL5, NF-kappaB, and MAPKs. *J Immunol* 185: 6214-6225
- Carlin LM, Stamatiades EG, Auffray C, Hanna RN, Glover L, Vizcay-Barrena G, Hedrick CC, Cook HT, Diebold S, Geissmann F (2013) Nr4a1-dependent Ly6C(low) monocytes monitor endothelial cells and orchestrate their disposal. *Cell* 153: 362-375
- Carrington JM, Hershberger DM (2022) Pulmonary Alveolar Proteinosis. In: *StatPearls*, Treasure Island (FL)
- Castoldi A, Monteiro LB, van Teijlingen Bakker N, Sanin DE, Rana N, Corrado M, Cameron AM, Hassler F, Matsushita M, Caputa G *et al* (2020) Triacylglycerol synthesis enhances macrophage inflammatory function. *Nat Commun* 11: 4107
- Chakarov S, Lim HY, Tan L, Lim SY, See P, Lum J, Zhang XM, Foo S, Nakamizo S, Duan K *et al* (2019) Two distinct interstitial macrophage populations coexist across tissues in specific subtissular niches. *Science* 363
- Chang EY, Guo B, Doyle SE, Cheng G (2007) Cutting edge: involvement of the type I IFN production and signaling pathway in lipopolysaccharide-induced IL-10 production. *J Immunol* 178: 6705-6709
- Cheng SC, Quintin J, Cramer RA, Shepardson KM, Saeed S, Kumar V, Giamarellos-Bourboulis EJ, Martens JH, Rao NA, Aghajanirofeh A *et al* (2014) mTOR- and HIF-1alpha-mediated aerobic glycolysis as metabolic basis for trained immunity. *Science* 345: 1250684

- Chiu S, Bharat A (2016) Role of monocytes and macrophages in regulating immune response following lung transplantation. *Curr Opin Organ Transplant* 21: 239-245
- Chow KV, Sutherland RM, Zhan Y, Lew AM (2017) Heterogeneity, functional specialization and differentiation of monocyte-derived dendritic cells. *Immunol Cell Biol* 95: 244-251
- Christ A, Gunther P, Lauterbach MAR, Duewell P, Biswas D, Pelka K, Scholz CJ, Oosting M, Haendler K, Bassler K *et al* (2018) Western Diet Triggers NLRP3-Dependent Innate Immune Reprogramming. *Cell* 172: 162-175 e114
- Ciarlo E, Heinonen T, Theroude C, Asgari F, Le Roy D, Netea MG, Roger T (2020) Trained Immunity Confers Broad-Spectrum Protection Against Bacterial Infections. *J Infect Dis* 222: 1869-1881
- Cohen M, Giladi A, Gorki AD, Solodkin DG, Zada M, Hladik A, Miklosi A, Salame TM, Halpern KB, David E *et al* (2018) Lung Single-Cell Signaling Interaction Map Reveals Basophil Role in Macrophage Imprinting. *Cell* 175: 1031-1044 e1018
- Coker RK, Laurent GJ, Shahzeidi S, Hernandez-Rodriguez NA, Pantelidis P, du Bois RM, Jeffery PK, McAnulty RJ (1996) Diverse cellular TGF-beta 1 and TGF-beta 3 gene expression in normal human and murine lung. *Eur Respir J* 9: 2501-2507
- Condon TV, Sawyer RT, Fenton MJ, Riches DW (2011) Lung dendritic cells at the innate-adaptive immune interface. *J Leukoc Biol* 90: 883-895
- Corces MR, Buenrostro JD, Wu B, Greenside PG, Chan SM, Koenig JL, Snyder MP, Pritchard JK, Kundaje A, Greenleaf WJ *et al* (2016) Lineage-specific and single-cell chromatin accessibility charts human hematopoiesis and leukemia evolution. *Nat Genet* 48: 1193-1203
- Davies LC, Jenkins SJ, Allen JE, Taylor PR (2013) Tissue-resident macrophages. *Nat Immunol* 14: 986-995
- Desch AN, Henson PM, Jakubzick CV (2013) Pulmonary dendritic cell development and antigen acquisition. *Immunol Res* 55: 178-186
- Desch AN, Randolph GJ, Murphy K, Gautier EL, Kedl RM, Lahoud MH, Caminschi I, Shortman K, Henson PM, Jakubzick CV (2011) CD103+ pulmonary dendritic cells preferentially acquire and present apoptotic cell-associated antigen. *J Exp Med* 208: 1789-1797
- Di Luzio NR, Williams DL (1978) Protective effect of glucan against systemic *Staphylococcus aureus* septicemia in normal and leukemic mice. *Infect Immun* 20: 804-810
- Diseases GBD, Injuries C (2020) Global burden of 369 diseases and injuries in 204 countries and territories, 1990-2019: a systematic analysis for the Global Burden of Disease Study 2019. *Lancet* 396: 1204-1222
- Divangahi M, Aaby P, Khader SA, Barreiro LB, Bekkering S, Chavakis T, van Crevel R, Curtis N, DiNardo AR, Dominguez-Andres J *et al* (2021) Trained immunity, tolerance, priming and differentiation: distinct immunological processes. *Nat Immunol* 22: 2-6
- Divangahi M, King IL, Pernet E (2015) Alveolar macrophages and type I IFN in airway homeostasis and immunity. *Trends Immunol* 36: 307-314

- Doyle AG, Herbein G, Montaner LJ, Minty AJ, Caput D, Ferrara P, Gordon S (1994) Interleukin-13 alters the activation state of murine macrophages in vitro: comparison with interleukin-4 and interferon-gamma. *Eur J Immunol* 24: 1441-1445
- El-Zayat SR, Sibaii H, Mannaa FA (2019) Toll-like receptors activation, signaling, and targeting: an overview. *Bulletin of the National Research Centre* 43: 187
- Evren E, Ringqvist E, Tripathi KP, Sleiers N, Rives IC, Alisjahbana A, Gao Y, Sarhan D, Halle T, Sorini C *et al* (2021) Distinct developmental pathways from blood monocytes generate human lung macrophage diversity. *Immunity* 54: 259-275 e257
- Fanucchi S, Dominguez-Andres J, Joosten LAB, Netea MG, Mhlanga MM (2021) The Intersection of Epigenetics and Metabolism in Trained Immunity. *Immunity* 54: 32-43
- Fernandez S, Jose P, Avdiushko MG, Kaplan AM, Cohen DA (2004) Inhibition of IL-10 receptor function in alveolar macrophages by Toll-like receptor agonists. *J Immunol* 172: 2613-2620
- Fessler MB, Summer RS (2016) Surfactant Lipids at the Host-Environment Interface. Metabolic Sensors, Suppressors, and Effectors of Inflammatory Lung Disease. *Am J Respir Cell Mol Biol* 54: 624-635
- Feuerstein R, Forde AJ, Lohrmann F, Kolter J, Ramirez NJ, Zimmermann J, Gomez de Agüero M, Henneke P (2020) Resident macrophages acquire innate immune memory in staphylococcal skin infection. *Elife* 9
- Fillion I, Ouellet N, Simard M, Bergeron Y, Sato S, Bergeron MG (2001) Role of chemokines and formyl peptides in pneumococcal pneumonia-induced monocyte/macrophage recruitment. *J Immunol* 166: 7353-7361
- Foster SL, Hargreaves DC, Medzhitov R (2007) Gene-specific control of inflammation by TLR-induced chromatin modifications. *Nature* 447: 972-978
- Gawish R, Martins R, Böhm B, Wimberger T, Sharif O, Lakovits K, Schmidt M, Knapp S (2015) Triggering receptor expressed on myeloid cells-2 fine-tunes inflammatory responses in murine Gram-negative sepsis. *FASEB J* 29: 1247-1257
- Gazon H, Barbeau B, Mesnard JM, Peloponese JM, Jr. (2017) Hijacking of the AP-1 Signaling Pathway during Development of ATL. *Front Microbiol* 8: 2686
- Gheibi Hayat SM, Bianconi V, Pirro M, Sahebkar A (2019) Efferocytosis: molecular mechanisms and pathophysiological perspectives. *Immunol Cell Biol* 97: 124-133
- Ginhoux F (2014) Fate PPAR-titoning: PPAR-gamma 'instructs' alveolar macrophage development. *Nat Immunol* 15: 1005-1007
- Ginhoux F, Williams M (2016) Tissue-Resident Macrophage Ontogeny and Homeostasis. *Immunity* 44: 439-449
- Goritzka M, Durant LR, Pereira C, Salek-Ardakani S, Openshaw PJ, Johansson C (2014) Alpha/beta interferon receptor signaling amplifies early proinflammatory cytokine production in the lung during respiratory syncytial virus infection. *J Virol* 88: 6128-6136

Gorki AD, Symmank D, Zahalka S, Lakovits K, Hladik A, Langer B, Maurer B, Sexl V, Kain R, Knapp S (2022) Murine Ex Vivo Cultured Alveolar Macrophages Provide a Novel Tool to Study Tissue-Resident Macrophage Behavior and Function. *Am J Respir Cell Mol Biol* 66: 64-75

Grabner GF, Xie H, Schweiger M, Zechner R (2021) Lipolysis: cellular mechanisms for lipid mobilization from fat stores. *Nat Metab* 3: 1445-1465

Grubor B, Meyerholz DK, Ackermann MR (2006) Collectins and cationic antimicrobial peptides of the respiratory epithelia. *Vet Pathol* 43: 595-612

Guilliams M, Svedberg FR (2021) Does tissue imprinting restrict macrophage plasticity? *Nat Immunol* 22: 118-127

Haczku A (2008) Protective role of the lung collectins surfactant protein A and surfactant protein D in airway inflammation. *J Allergy Clin Immunol* 122: 861-879; quiz 880-861

Hallett S, Toro F, Ashurst JV (2022) Physiology, Tidal Volume. In: *StatPearls*, Treasure Island (FL)

Hamada A, Torre C, Drancourt M, Ghigo E (2018) Trained Immunity Carried by Non-immune Cells. *Front Microbiol* 9: 3225

Hao Z, Rajewsky K (2001) Homeostasis of peripheral B cells in the absence of B cell influx from the bone marrow. *J Exp Med* 194: 1151-1164

Hartl D, Tirouvanziam R, Laval J, Greene CM, Habiels D, Sharma L, Yildirim AO, Dela Cruz CS, Hogaboam CM (2018) Innate Immunity of the Lung: From Basic Mechanisms to Translational Medicine. *J Innate Immun* 10: 487-501

Hashimoto D, Chow A, Noizat C, Teo P, Beasley MB, Leboeuf M, Becker CD, See P, Price J, Lucas D *et al* (2013) Tissue-resident macrophages self-maintain locally throughout adult life with minimal contribution from circulating monocytes. *Immunity* 38: 792-804

Hayes MP, Freeman SL, Donnelly RP (1995) IFN-gamma priming of monocytes enhances LPS-induced TNF production by augmenting both transcription and mRNA stability. *Cytokine* 7: 427-435

Hetzel M, Ackermann M, Lachmann N (2021) Beyond "Big Eaters": The Versatile Role of Alveolar Macrophages in Health and Disease. *Int J Mol Sci* 22

Hevia H, Varela-Rey M, Corrales FJ, Berasain C, Martinez-Chantar ML, Latasa MU, Lu SC, Mato JM, Garcia-Trevijano ER, Avila MA (2004) 5'-methylthioadenosine modulates the inflammatory response to endotoxin in mice and in rat hepatocytes. *Hepatology* 39: 1088-1098

Hiemstra PS, Amatngalim GD, van der Does AM, Taube C (2016) Antimicrobial Peptides and Innate Lung Defenses: Role in Infectious and Noninfectious Lung Diseases and Therapeutic Applications. *Chest* 149: 545-551

Hoeffel G, Ginhoux F (2018) Fetal monocytes and the origins of tissue-resident macrophages. *Cell Immunol* 330: 5-15

Hole CR, Wager CML, Castro-Lopez N, Campuzano A, Cai H, Wozniak KL, Wang Y, Wormley FL, Jr. (2019) Induction of memory-like dendritic cell responses in vivo. *Nat Commun* 10: 2955

- Hou F, Xiao K, Tang L, Xie L (2021) Diversity of Macrophages in Lung Homeostasis and Diseases. *Front Immunol* 12: 753940
- Hu G, Christman JW (2019) Editorial: Alveolar Macrophages in Lung Inflammation and Resolution. *Front Immunol* 10: 2275
- Huang L, Nazarova EV, Tan S, Liu Y, Russell DG (2018) Growth of Mycobacterium tuberculosis in vivo segregates with host macrophage metabolism and ontogeny. *J Exp Med* 215: 1135-1152
- Huang S, Hendriks W, Althage A, Hemmi S, Bluethmann H, Kamijo R, Vilcek J, Zinkernagel RM, Aguet M (1993) Immune response in mice that lack the interferon-gamma receptor. *Science* 259: 1742-1745
- Hussell T, Bell TJ (2014) Alveolar macrophages: plasticity in a tissue-specific context. *Nat Rev Immunol* 14: 81-93
- Ifrim DC, Quintin J, Joosten LA, Jacobs C, Jansen T, Jacobs L, Gow NA, Williams DL, van der Meer JW, Netea MG (2014) Trained immunity or tolerance: opposing functional programs induced in human monocytes after engagement of various pattern recognition receptors. *Clin Vaccine Immunol* 21: 534-545
- Ignatiadis N, Klaus B, Zaugg JB, Huber W (2016) Data-driven hypothesis weighting increases detection power in genome-scale multiple testing. *Nat Methods* 13: 577-580
- Iwasaki A, Foxman EF, Molony RD (2017) Early local immune defences in the respiratory tract. *Nat Rev Immunol* 17: 7-20
- Jakubzick C, Tacke F, Ginhoux F, Wagers AJ, van Rooijen N, Mack M, Merad M, Randolph GJ (2008) Blood monocyte subsets differentially give rise to CD103⁺ and CD103⁻ pulmonary dendritic cell populations. *J Immunol* 180: 3019-3027
- Kapellos TS, Bonaguro L, Gemund I, Reusch N, Saglam A, Hinkley ER, Schultze JL (2019) Human Monocyte Subsets and Phenotypes in Major Chronic Inflammatory Diseases. *Front Immunol* 10: 2035
- Kar UK, Joosten LAB (2020) Training the trainable cells of the immune system and beyond. *Nat Immunol* 21: 115-119
- Kaufmann E, Sanz J, Dunn JL, Khan N, Mendonca LE, Pacis A, Tzelepis F, Pernet E, Dumaine A, Grenier JC *et al* (2018) BCG Educates Hematopoietic Stem Cells to Generate Protective Innate Immunity against Tuberculosis. *Cell* 172: 176-190 e119
- Khaing P, Summer R (2020) Maxed Out on Glycolysis: Alveolar Macrophages Rely on Oxidative Phosphorylation for Cytokine Production. *Am J Respir Cell Mol Biol* 62: 139-140
- Kim EY, Battaile JT, Patel AC, You Y, Agapov E, Grayson MH, Benoit LA, Byers DE, Alevy Y, Tucker J *et al* (2008) Persistent activation of an innate immune response translates respiratory viral infection into chronic lung disease. *Nat Med* 14: 633-640
- Kim TH, Lee HK (2014) Differential roles of lung dendritic cell subsets against respiratory virus infection. *Immune Netw* 14: 128-137

Knapp S, Leemans JC, Florquin S, Branger J, Maris NA, Pater J, van Rooijen N, van der Poll T (2003) Alveolar macrophages have a protective antiinflammatory role during murine pneumococcal pneumonia. *Am J Respir Crit Care Med* 167: 171-179

Knapp S, Wieland CW, van 't Veer C, Takeuchi O, Akira S, Florquin S, van der Poll T (2004) Toll-like receptor 2 plays a role in the early inflammatory response to murine pneumococcal pneumonia but does not contribute to antibacterial defense. *J Immunol* 172: 3132-3138

Kopf M, Schneider C, Nobs SP (2015) The development and function of lung-resident macrophages and dendritic cells. *Nat Immunol* 16: 36-44

Krahenbuhl JL, Sharma SD, Ferraresi RW, Remington JS (1981) Effects of muramyl dipeptide treatment on resistance to infection with *Toxoplasma gondii* in mice. *Infect Immun* 31: 716-722

Kruger P, Saffarzadeh M, Weber AN, Rieber N, Radsak M, von Bernuth H, Benarafa C, Roos D, Skokowa J, Hartl D (2015) Neutrophils: Between host defence, immune modulation, and tissue injury. *PLoS Pathog* 11: e1004651

Kudva A, Scheller EV, Robinson KM, Crowe CR, Choi SM, Slight SR, Khader SA, Dubin PJ, Enelow RI, Kolls JK *et al* (2011) Influenza A inhibits Th17-mediated host defense against bacterial pneumonia in mice. *J Immunol* 186: 1666-1674

Kulikauskaite J, Wack A (2020) Teaching Old Dogs New Tricks? The Plasticity of Lung Alveolar Macrophage Subsets. *Trends Immunol* 41: 864-877

Lagler H, Sharif O, Haslinger I, Matt U, Stich K, Furtner T, Doninger B, Schmid K, Gattlinger R, de Vos AF *et al* (2009) TREM-1 activation alters the dynamics of pulmonary IRAK-M expression in vivo and improves host defense during pneumococcal pneumonia. *J Immunol* 183: 2027-2036

Lavin Y, Winter D, Blecher-Gonen R, David E, Keren-Shaul H, Merad M, Jung S, Amit I (2014) Tissue-resident macrophage enhancer landscapes are shaped by the local microenvironment. *Cell* 159: 1312-1326

Lawrence SM, Corriden R, Nizet V (2017) Age-Appropriate Functions and Dysfunctions of the Neonatal Neutrophil. *Front Pediatr* 5: 23

Lee B, Robinson KM, McHugh KJ, Scheller EV, Mandalapu S, Chen C, Di YP, Clay ME, Enelow RI, Dubin PJ *et al* (2015) Influenza-induced type I interferon enhances susceptibility to gram-negative and gram-positive bacterial pneumonia in mice. *Am J Physiol Lung Cell Mol Physiol* 309: L158-167

Liu GY, Liu Y, Lu Y, Qin YR, Di GH, Lei YH, Liu HX, Li YQ, Wu C, Hu XW *et al* (2016) Short-term memory of danger signals or environmental stimuli in mesenchymal stem cells: implications for therapeutic potential. *Cell Mol Immunol* 13: 369-378

Love MI, Huber W, Anders S (2014) Moderated estimation of fold change and dispersion for RNA-seq data with DESeq2. *Genome Biol* 15: 550

MacGillivray DM, Kollmann TR (2014) The role of environmental factors in modulating immune responses in early life. *Front Immunol* 5: 434

Machiels B, Dourcy M, Xiao X, Javaux J, Mesnil C, Sabatel C, Desmecht D, Lallemand F, Martinive P, Hammad H *et al* (2017) A gammaherpesvirus provides protection against allergic

asthma by inducing the replacement of resident alveolar macrophages with regulatory monocytes. *Nat Immunol* 18: 1310-1320

Mackanness GB (1962) Cellular resistance to infection. *J Exp Med* 116: 381-406

Maier BB, Hladik A, Lakovits K, Korosec A, Martins R, Kral JB, Mesteri I, Strobl B, Muller M, Kalinke U *et al* (2016) Type I interferon promotes alveolar epithelial type II cell survival during pulmonary *Streptococcus pneumoniae* infection and sterile lung injury in mice. *Eur J Immunol* 46: 2175-2186

Malley R, Henneke P, Morse SC, Cieslewicz MJ, Lipsitch M, Thompson CM, Kurt-Jones E, Paton JC, Wessels MR, Golenbock DT (2003) Recognition of pneumolysin by Toll-like receptor 4 confers resistance to pneumococcal infection. *Proc Natl Acad Sci U S A* 100: 1966-1971

Mantovani A, Sica A, Sozzani S, Allavena P, Vecchi A, Locati M (2004) The chemokine system in diverse forms of macrophage activation and polarization. *Trends Immunol* 25: 677-686

Martinez FO, Gordon S (2014) The M1 and M2 paradigm of macrophage activation: time for reassessment. *F1000Prime Rep* 6: 13

Martinez-Gonzalez I, Matha L, Steer CA, Ghaedi M, Poon GF, Takei F (2016) Allergen-Experienced Group 2 Innate Lymphoid Cells Acquire Memory-like Properties and Enhance Allergic Lung Inflammation. *Immunity* 45: 198-208

Martinez-Reyes I, Chandel NS (2020) Mitochondrial TCA cycle metabolites control physiology and disease. *Nat Commun* 11: 102

Mazgaeen L, Gurung P (2020) Recent Advances in Lipopolysaccharide Recognition Systems. *Int J Mol Sci* 21

McNab F, Mayer-Barber K, Sher A, Wack A, O'Garra A (2015) Type I interferons in infectious disease. *Nat Rev Immunol* 15: 87-103

Melgert BN, Oriss TB, Qi Z, Dixon-McCarthy B, Geerlings M, Hylkema MN, Ray A (2010) Macrophages: regulators of sex differences in asthma? *Am J Respir Cell Mol Biol* 42: 595-603

Melgert BN, ten Hacken NH, Rutgers B, Timens W, Postma DS, Hylkema MN (2011) More alternative activation of macrophages in lungs of asthmatic patients. *J Allergy Clin Immunol* 127: 831-833

Merad M, Manz MG, Karsunky H, Wagers A, Peters W, Charo I, Weissman IL, Cyster JG, Engleman EG (2002) Langerhans cells renew in the skin throughout life under steady-state conditions. *Nat Immunol* 3: 1135-1141

Mills CD, Kincaid K, Alt JM, Heilman MJ, Hill AM (2000) M-1/M-2 macrophages and the Th1/Th2 paradigm. *J Immunol* 164: 6166-6173

Mirastschijski U, Dembinski R, Maedler K (2020) Lung Surfactant for Pulmonary Barrier Restoration in Patients With COVID-19 Pneumonia. *Front Med (Lausanne)* 7: 254

Misharin AV, Morales-Nebreda L, Reyfman PA, Cuda CM, Walter JM, McQuattie-Pimentel AC, Chen CI, Anekalla KR, Joshi N, Williams KJN *et al* (2017) Monocyte-derived alveolar macrophages drive lung fibrosis and persist in the lung over the life span. *J Exp Med* 214: 2387-2404

- Moorlag S, Roring RJ, Joosten LAB, Netea MG (2018) The role of the interleukin-1 family in trained immunity. *Immunol Rev* 281: 28-39
- Mosser DM, Edwards JP (2008) Exploring the full spectrum of macrophage activation. *Nat Rev Immunol* 8: 958-969
- Mulder WJM, Ochando J, Joosten LAB, Fayad ZA, Netea MG (2019) Therapeutic targeting of trained immunity. *Nat Rev Drug Discov* 18: 553-566
- Muller U, Steinhoff U, Reis LF, Hemmi S, Pavlovic J, Zinkernagel RM, Aguet M (1994) Functional role of type I and type II interferons in antiviral defense. *Science* 264: 1918-1921
- Munoz N, Van Maele L, Marques JM, Rial A, Sirard JC, Chabalgoity JA (2010) Mucosal administration of flagellin protects mice from *Streptococcus pneumoniae* lung infection. *Infect Immun* 78: 4226-4233
- Murphy K, Weaver C (2016) *Janeway's immunobiology*. Garland Science/Taylor & Francis Group, LLC, New York, NY
- Murray PJ (2017) Macrophage Polarization. *Annu Rev Physiol* 79: 541-566
- Murray PJ, Allen JE, Biswas SK, Fisher EA, Gilroy DW, Goerdts S, Gordon S, Hamilton JA, Ivashkiv LB, Lawrence T *et al* (2014) Macrophage activation and polarization: nomenclature and experimental guidelines. *Immunity* 41: 14-20
- Nathan CF, Murray HW, Wiebe ME, Rubin BY (1983) Identification of interferon-gamma as the lymphokine that activates human macrophage oxidative metabolism and antimicrobial activity. *J Exp Med* 158: 670-689
- Navarini AA, Recher M, Lang KS, Georgiev P, Meury S, Bergthaler A, Flatz L, Bille J, Landmann R, Odermatt B *et al* (2006) Increased susceptibility to bacterial superinfection as a consequence of innate antiviral responses. *Proc Natl Acad Sci U S A* 103: 15535-15539
- Nayak DK, Zhou F, Xu M, Huang J, Tsuji M, Hachem R, Mohanakumar T (2016) Long-Term Persistence of Donor Alveolar Macrophages in Human Lung Transplant Recipients That Influences Donor-Specific Immune Responses. *Am J Transplant* 16: 2300-2311
- Netea MG, Dominguez-Andres J, Barreiro LB, Chavakis T, Divangahi M, Fuchs E, Joosten LAB, van der Meer JWM, Mhlanga MM, Mulder WJM *et al* (2020) Defining trained immunity and its role in health and disease. *Nat Rev Immunol* 20: 375-388
- Netea MG, Joosten LA, Latz E, Mills KH, Natoli G, Stunnenberg HG, O'Neill LA, Xavier RJ (2016) Trained immunity: A program of innate immune memory in health and disease. *Science* 352: aaf1098
- Netea MG, Quintin J, van der Meer JW (2011) Trained immunity: a memory for innate host defense. *Cell Host Microbe* 9: 355-361
- Nicod LP (2005) Lung defences: an overview. *European Respiratory Review* 14: 45-50
- Nieuwenhuizen NE, Kirstein F, Jayakumar J, Emedi B, Hurdal R, Horsnell WG, Lopata AL, Brombacher F (2012) Allergic airway disease is unaffected by the absence of IL-4R α -dependent alternatively activated macrophages. *J Allergy Clin Immunol* 130: 743-750 e748

- Noviello S, Huang DB (2019) The Basics and the Advancements in Diagnosis of Bacterial Lower Respiratory Tract Infections. *Diagnostics (Basel)* 9
- Ogger PP, Byrne AJ (2021) Macrophage metabolic reprogramming during chronic lung disease. *Mucosal Immunol* 14: 282-295
- Ohar JA, Donohue JF, Spangenthal S (2019) The Role of Guaifenesin in the Management of Chronic Mucus Hypersecretion Associated with Stable Chronic Bronchitis: A Comprehensive Review. *Chronic Obstr Pulm Dis* 6
- Parkhitko AA, Jouandin P, Mohr SE, Perrimon N (2019) Methionine metabolism and methyltransferases in the regulation of aging and lifespan extension across species. *Aging Cell* 18: e13034
- Pechkovsky DV, Prasse A, Kollert F, Engel KM, Dentler J, Luttmann W, Friedrich K, Muller-Quernheim J, Zissel G (2010) Alternatively activated alveolar macrophages in pulmonary fibrosis-mediator production and intracellular signal transduction. *Clin Immunol* 137: 89-101
- Penaloza HF, Nieto PA, Munoz-Durango N, Salazar-Echegarai FJ, Torres J, Parga MJ, Alvarez-Lobos M, Riedel CA, Kalergis AM, Bueno SM (2015) Interleukin-10 plays a key role in the modulation of neutrophils recruitment and lung inflammation during infection by *Streptococcus pneumoniae*. *Immunology* 146: 100-112
- Pham LN, Dionne MS, Shirasu-Hiza M, Schneider DS (2007) A specific primed immune response in *Drosophila* is dependent on phagocytes. *PLoS Pathog* 3: e26
- Pivniouk V, Gimenes Junior JA, Honeker LK, Vercelli D (2020) The role of innate immunity in asthma development and protection: Lessons from the environment. *Clin Exp Allergy* 50: 282-290
- Pletz MW, Maus U, Krug N, Welte T, Lode H (2008) Pneumococcal vaccines: mechanism of action, impact on epidemiology and adaption of the species. *Int J Antimicrob Agents* 32: 199-206
- Puchelle E, de Bentzmann S, Zahm JM (1995) Physical and functional properties of airway secretions in cystic fibrosis--therapeutic approaches. *Respiration* 62 Suppl 1: 2-12
- Quintin J, Saeed S, Martens JHA, Giamarellos-Bourboulis EJ, Ifrim DC, Logie C, Jacobs L, Jansen T, Kullberg BJ, Wijnnga C *et al* (2012) *Candida albicans* infection affords protection against reinfection via functional reprogramming of monocytes. *Cell Host Microbe* 12: 223-232
- Rajaram MV, Brooks MN, Morris JD, Torrelles JB, Azad AK, Schlesinger LS (2010) *Mycobacterium tuberculosis* activates human macrophage peroxisome proliferator-activated receptor gamma linking mannose receptor recognition to regulation of immune responses. *J Immunol* 185: 929-942
- Ranta A, Kumar S (2020) Recent advancements in role of TAM receptors on efferocytosis, viral infection, autoimmunity, and tissue repair. *Int Rev Cell Mol Biol* 357: 1-19
- Ribes S, Meister T, Ott M, Redlich S, Janova H, Hanisch UK, Nessler S, Nau R (2014) Intraperitoneal prophylaxis with CpG oligodeoxynucleotides protects neutropenic mice against intracerebral *Escherichia coli* K1 infection. *J Neuroinflammation* 11: 14

Rijneveld AW, Florquin S, Branger J, Speelman P, Van Deventer SJ, van der Poll T (2001) TNF-alpha compensates for the impaired host defense of IL-1 type I receptor-deficient mice during pneumococcal pneumonia. *J Immunol* 167: 5240-5246

Riksen NP, Netea MG (2021) Immunometabolic control of trained immunity. *Mol Aspects Med* 77: 100897

Rojas A, Padidam M, Cress D, Grady WM (2009) TGF-beta receptor levels regulate the specificity of signaling pathway activation and biological effects of TGF-beta. *Biochim Biophys Acta* 1793: 1165-1173

Rolph CA, Gwyther CL, Tyrrel SF, Nasir ZA, Drew GH, Jackson SK, Khera S, Hayes ET, Williams B, Bennett A *et al* (2018) Sources of Airborne Endotoxins in Ambient Air and Exposure of Nearby Communities—A Review. *Atmosphere* 9: 375

Roquilly A, Jacqueline C, Davieau M, Molle A, Sadek A, Fourgeux C, Rooze P, Broquet A, Misme-Aucouturier B, Chaumette T *et al* (2020) Author Correction: Alveolar macrophages are epigenetically altered after inflammation, leading to long-term lung immunoparalysis. *Nat Immunol* 21: 962

Roth MD, Golub SH (1993) Human pulmonary macrophages utilize prostaglandins and transforming growth factor beta 1 to suppress lymphocyte activation. *J Leukoc Biol* 53: 366-371

Rubins JB (2003) Alveolar macrophages: wielding the double-edged sword of inflammation. *Am J Respir Crit Care Med* 167: 103-104

Sabatel C, Radermecker C, Fievez L, Paulissen G, Chakarov S, Fernandes C, Olivier S, Toussaint M, Pirottin D, Xiao X *et al* (2017) Exposure to Bacterial CpG DNA Protects from Airway Allergic Inflammation by Expanding Regulatory Lung Interstitial Macrophages. *Immunity* 46: 457-473

Sadhu C, Ting HJ, Lipsky B, Hensley K, Garcia-Martinez LF, Simon SI, Staunton DE (2007) CD11c/CD18: novel ligands and a role in delayed-type hypersensitivity. *J Leukoc Biol* 81: 1395-1403

Saluzzo S, Gorki AD, Rana BMJ, Martins R, Scanlon S, Starkl P, Lakovits K, Hladik A, Korosec A, Sharif O *et al* (2017) First-Breath-Induced Type 2 Pathways Shape the Lung Immune Environment. *Cell Rep* 18: 1893-1905

Sano H, Kuroki Y (2005) The lung collectins, SP-A and SP-D, modulate pulmonary innate immunity. *Mol Immunol* 42: 279-287

Schneider C, Nobs SP, Heer AK, Kurrer M, Klinke G, van Rooijen N, Vogel J, Kopf M (2014a) Alveolar macrophages are essential for protection from respiratory failure and associated morbidity following influenza virus infection. *PLoS Pathog* 10: e1004053

Schneider C, Nobs SP, Kurrer M, Rehrauer H, Thiele C, Kopf M (2014b) Induction of the nuclear receptor PPAR-gamma by the cytokine GM-CSF is critical for the differentiation of fetal monocytes into alveolar macrophages. *Nat Immunol* 15: 1026-1037

Schyns J, Bureau F, Marichal T (2018) Lung Interstitial Macrophages: Past, Present, and Future. *J Immunol Res* 2018: 5160794

- Seeley JJ, Ghosh S (2017) Molecular mechanisms of innate memory and tolerance to LPS. *J Leukoc Biol* 101: 107-119
- Serafini N, Jarade A, Surace L, Goncalves P, Sismeiro O, Varet H, Legendre R, Coppee JY, Disson O, Durum SK *et al* (2022) Trained ILC3 responses promote intestinal defense. *Science* 375: 859-863
- Shamsollahi HR, Ghoochani M, Jaafari J, Moosavi A, Sillanpaa M, Alimohammadi M (2019) Environmental exposure to endotoxin and its health outcomes: A systematic review. *Ecotoxicol Environ Saf* 174: 236-244
- Sharif O, Gawish R, Warszawska JM, Martins R, Lakovits K, Hladik A, Doninger B, Brunner J, Korosec A, Schwarzenbacher RE *et al* (2014) The triggering receptor expressed on myeloid cells 2 inhibits complement component 1q effector mechanisms and exerts detrimental effects during pneumococcal pneumonia. *PLoS Pathog* 10: e1004167
- Sharif O, Knapp S (2008) From expression to signaling: roles of TREM-1 and TREM-2 in innate immunity and bacterial infection. *Immunobiology* 213: 701-713
- Shaykhiev R, Krause A, Salit J, Strulovici-Barel Y, Harvey BG, O'Connor TP, Crystal RG (2009) Smoking-dependent reprogramming of alveolar macrophage polarization: implication for pathogenesis of chronic obstructive pulmonary disease. *J Immunol* 183: 2867-2883
- Song C, Li H, Li Y, Dai M, Zhang L, Liu S, Tan H, Deng P, Liu J, Mao Z *et al* (2019) NETs promote ALI/ARDS inflammation by regulating alveolar macrophage polarization. *Exp Cell Res* 382: 111486
- Stein M, Keshav S, Harris N, Gordon S (1992) Interleukin 4 potently enhances murine macrophage mannose receptor activity: a marker of alternative immunologic macrophage activation. *J Exp Med* 176: 287-292
- Stein MM, Hrusch CL, Gozdz J, Igartua C, Pivniouk V, Murray SE, Ledford JG, Marques Dos Santos M, Anderson RL, Metwali N *et al* (2016) Innate Immunity and Asthma Risk in Amish and Hutterite Farm Children. *N Engl J Med* 375: 411-421
- Summers C, Rankin SM, Condliffe AM, Singh N, Peters AM, Chilvers ER (2010) Neutrophil kinetics in health and disease. *Trends Immunol* 31: 318-324
- Sun Y, Jiang X, Chen S, Price BD (2006) Inhibition of histone acetyltransferase activity by anacardic acid sensitizes tumor cells to ionizing radiation. *FEBS Lett* 580: 4353-4356
- Sunshine H, Iruela-Arispe ML (2017) Membrane lipids and cell signaling. *Curr Opin Lipidol* 28: 408-413
- Svedberg FR, Brown SL, Krauss MZ, Campbell L, Sharpe C, Clausen M, Howell GJ, Clark H, Madsen J, Evans CM *et al* (2019) The lung environment controls alveolar macrophage metabolism and responsiveness in type 2 inflammation. *Nat Immunol* 20: 571-580
- Tan SY, Krasnow MA (2016) Developmental origin of lung macrophage diversity. *Development* 143: 1318-1327
- Tarca AL, Draghici S, Khatri P, Hassan SS, Mittal P, Kim JS, Kim CJ, Kusanovic JP, Romero R (2009) A novel signaling pathway impact analysis. *Bioinformatics* 25: 75-82

- Tecle T, Tripathi S, Hartshorn KL (2010) Review: Defensins and cathelicidins in lung immunity. *Innate Immun* 16: 151-159
- Torres A, Cilloniz C, Niederman MS, Menendez R, Chalmers JD, Wunderink RG, van der Poll T (2021) Pneumonia. *Nat Rev Dis Primers* 7: 25
- Torres A, Peetermans WE, Viegi G, Blasi F (2013) Risk factors for community-acquired pneumonia in adults in Europe: a literature review. *Thorax* 68: 1057-1065
- Travis MA, Sheppard D (2014) TGF-beta activation and function in immunity. *Annu Rev Immunol* 32: 51-82
- Uciechowski P, Dempke WCM (2020) Interleukin-6: A Masterplayer in the Cytokine Network. *Oncology-Basel* 98: 131-137
- Vadiveloo PK, Vairo G, Hertzog P, Kola I, Hamilton JA (2000) Role of type I interferons during macrophage activation by lipopolysaccharide. *Cytokine* 12: 1639-1646
- van de Laar L, Saelens W, De Prijck S, Martens L, Scott CL, Van Isterdael G, Hoffmann E, Beyaert R, Saeys Y, Lambrecht BN *et al* (2016) Yolk Sac Macrophages, Fetal Liver, and Adult Monocytes Can Colonize an Empty Niche and Develop into Functional Tissue-Resident Macrophages. *Immunity* 44: 755-768
- van der Poll T, Opal SM (2009) Pathogenesis, treatment, and prevention of pneumococcal pneumonia. *Lancet* 374: 1543-1556
- Varma TK, Lin CY, Toliver-Kinsky TE, Sherwood ER (2002) Endotoxin-induced gamma interferon production: contributing cell types and key regulatory factors. *Clin Diagn Lab Immunol* 9: 530-543
- Verma D, Parasa VR, Raffetseder J, Martis M, Mehta RB, Netea M, Lerm M (2017) Anti-mycobacterial activity correlates with altered DNA methylation pattern in immune cells from BCG-vaccinated subjects. *Sci Rep* 7: 12305
- Vernooy JH, Dentener MA, van Suylen RJ, Buurman WA, Wouters EF (2002) Long-term intratracheal lipopolysaccharide exposure in mice results in chronic lung inflammation and persistent pathology. *Am J Respir Cell Mol Biol* 26: 152-159
- Vivier E, Artis D, Colonna M, Diefenbach A, Di Santo JP, Eberl G, Koyasu S, Locksley RM, McKenzie ANJ, Mebius RE *et al* (2018) Innate Lymphoid Cells: 10 Years On. *Cell* 174: 1054-1066
- Wang H, Airola MV, Reue K (2017) How lipid droplets "TAG" along: Glycerolipid synthetic enzymes and lipid storage. *Biochim Biophys Acta Mol Cell Biol Lipids* 1862: 1131-1145
- Wang N, Liang H, Zen K (2014) Molecular mechanisms that influence the macrophage m1-m2 polarization balance. *Front Immunol* 5: 614
- Wculek SK, Dunphy G, Heras-Murillo I, Mastrangelo A, Sancho D (2022) Metabolism of tissue macrophages in homeostasis and pathology. *Cell Mol Immunol* 19: 384-408
- Weinberger SE, Cockrill BA, Mandel J (2019) Lung Defense Mechanisms. In: *Principles of Pulmonary Medicine*, Weinberger S.E., Cockrill B.A., Mandel J. (eds.) pp. 285-296. Elsevier: Philadelphia

- Weiser JN, Ferreira DM, Paton JC (2018) *Streptococcus pneumoniae*: transmission, colonization and invasion. *Nat Rev Microbiol* 16: 355-367
- Weizman OE, Song E, Adams NM, Hildreth AD, Riggan L, Krishna C, Aguilar OA, Leslie CS, Carlyle JR, Sun JC *et al* (2019) Mouse cytomegalovirus-experienced ILC1s acquire a memory response dependent on the viral glycoprotein m12. *Nat Immunol* 20: 1004-1011
- Wendeln AC, Degenhardt K, Kaurani L, Gertig M, Ulas T, Jain G, Wagner J, Hasler LM, Wild K, Skodras A *et al* (2018) Innate immune memory in the brain shapes neurological disease hallmarks. *Nature* 556: 332-338
- WHO (2020, December 9) The top 10 causes of death.
- Woo YD, Jeong D, Chung DH (2021) Development and Functions of Alveolar Macrophages. *Mol Cells* 44: 292-300
- Woods PS, Kimmig LM, Meliton AY, Sun KA, Tian Y, O'Leary EM, Gokalp GA, Hamanaka RB, Mutlu GM (2020) Tissue-Resident Alveolar Macrophages Do Not Rely on Glycolysis for LPS-induced Inflammation. *Am J Respir Cell Mol Biol* 62: 243-255
- Wu C, Xue Y, Wang P, Lin L, Liu Q, Li N, Xu J, Cao X (2014) IFN-gamma primes macrophage activation by increasing phosphatase and tensin homolog via downregulation of miR-3473b. *J Immunol* 193: 3036-3044
- Wu D, Sanin DE, Everts B, Chen Q, Qiu J, Buck MD, Patterson A, Smith AM, Chang CH, Liu Z *et al* (2016) Type 1 Interferons Induce Changes in Core Metabolism that Are Critical for Immune Function. *Immunity* 44: 1325-1336
- Wu Y, Hirschi KK (2020) Tissue-Resident Macrophage Development and Function. *Front Cell Dev Biol* 8: 617879
- Wynn TA, Vannella KM (2016) Macrophages in Tissue Repair, Regeneration, and Fibrosis. *Immunity* 44: 450-462
- Yan C, Boyd DD (2006) Histone H3 acetylation and H3 K4 methylation define distinct chromatin regions permissive for transgene expression. *Mol Cell Biol* 26: 6357-6371
- Yao Y, Jeyanathan M, Haddadi S, Barra NG, Vaseghi-Shanjani M, Damjanovic D, Lai R, Afkhami S, Chen Y, Dvorkin-Gheva A *et al* (2018) Induction of Autonomous Memory Alveolar Macrophages Requires T Cell Help and Is Critical to Trained Immunity. *Cell* 175: 1634-1650 e1617
- Yona S, Kim KW, Wolf Y, Mildner A, Varol D, Breker M, Strauss-Ayali D, Viukov S, Guillems M, Misharin A *et al* (2013) Fate mapping reveals origins and dynamics of monocytes and tissue macrophages under homeostasis. *Immunity* 38: 79-91
- Yu W, Wang Z, Zhang K, Chi Z, Xu T, Jiang D, Chen S, Li W, Yang X, Zhang X *et al* (2019) One-Carbon Metabolism Supports S-Adenosylmethionine and Histone Methylation to Drive Inflammatory Macrophages. *Mol Cell* 75: 1147-1160 e1145
- Yu X, Buttgerit A, Lelios I, Utz SG, Cansever D, Becher B, Greter M (2017) The Cytokine TGF-beta Promotes the Development and Homeostasis of Alveolar Macrophages. *Immunity* 47: 903-912 e904

Yu YR, O'Koren EG, Hotten DF, Kan MJ, Kopin D, Nelson ER, Que L, Gunn MD (2016) A Protocol for the Comprehensive Flow Cytometric Analysis of Immune Cells in Normal and Inflamed Murine Non-Lymphoid Tissues. *PLoS One* 11: e0150606

Zhang C, Yang M, Ericsson AC (2021a) Function of Macrophages in Disease: Current Understanding on Molecular Mechanisms. *Front Immunol* 12: 620510

Zhang H, He F, Li P, Hardwidge PR, Li N, Peng Y (2021b) The Role of Innate Immunity in Pulmonary Infections. *Biomed Res Int* 2021: 6646071

Zhang L, Wang Y, Wu G, Xiong W, Gu W, Wang CY (2018) Macrophages: friend or foe in idiopathic pulmonary fibrosis? *Respir Res* 19: 170

Zhang M, Angata T, Cho JY, Miller M, Broide DH, Varki A (2007) Defining the in vivo function of Siglec-F, a CD33-related Siglec expressed on mouse eosinophils. *Blood* 109: 4280-4287

Curriculum vitae

PERSONAL INFORMATION

Name: Sophie Zahalka

Nationality: Austrian

Contact: sophie.zahalka@meduniwien.ac.at

RESEARCH INTERESTS

Innate immunity, infection biology, macrophages, immunometabolism, host-pathogen interaction

EDUCATION

- | | |
|-------------------|---|
| 09/2016 – present | PhD studies, Medical University of Vienna (MUW)/Research Center for Molecular Medicine (CeMM) of the Austrian Academy of Sciences
Programs: Cell Communication in Health and Disease (CCHD), CeMM PhD program
Dissertation title: “Concepts and mechanisms of trained immunity in pulmonary macrophages”
Supervisor: Prof. Sylvia Knapp, MD, PhD
Department of Medicine I, MUW |
| 09/2014-08/2016 | Master studies, ETH Zurich
Program: Microbiology and Immunology
Dissertation title: “Effects of GM-CSF on neutrophil functions in the absence of regulatory T cells”
Supervisor: Prof. Burkhard Becher, PhD
Institute of Experimental Immunology, University of Zurich |
| 10/2010-08/2014 | Bachelor studies, University of Vienna
Program: Biology (Microbiology and Genetics)
Dissertation title: “Epidemiologic and molecular analysis of a sarcoid outbreak in a herd of 111 donkeys in Northern Italy”
Supervisor: Dipl.-Ing. Dr. Sabine Brandt
Clinical Unit of Equine Surgery, University of Veterinary Medicine Vienna |

RESEARCH EXPERIENCE

- | | |
|-----------------|--|
| 04/2018-12/2018 | Visiting scientist, Max Planck Institute of Immunobiology & Epigenetics, Freiburg, Germany
Research focus: Metabolic regulation of macrophage reprogramming
Supervisor: Prof. Edward J. Pearce, PhD |
|-----------------|--|

- 01/2015 – 05/2015 **MSc Research internship, Institute of Molecular Biology & Biophysics, ETH Zurich**
Research focus: Cryo-EM, bacterial secretion systems
Supervisor: Prof. Martin Pilhofer, PhD
- 09/2014 – 12/2014 **MSc Research internship, Institute of Molecular Systems Biology, ETH Zurich**
Research focus: *Drosophila melanogaster*
Supervisor: Prof. Ernst Hafen, PhD
- 08/2012 **Summer internship, Kaiser Franz Joseph Hospital, Vienna**

CONFERENCE CONTRIBUTIONS

Oral presentation at the *Next Generation Immunologists (NGI)* video symposium/annual *Austrian Society for Allergy and Immunology (ÖGAI)* meeting 2021

“Exploring tissue-specific aspects of trained immunity in lung macrophages”

Poster presentation at the *European Macrophage and Dendritic Cell Society* conference 2021 (online); “Low-dose LPS exposure induces trained immunity in alveolar macrophages”

Poster presentation at the *Young Scientist Association (YSA)* PhD Symposium 2021 (online)
“Low-dose LPS exposure induces trained immunity in alveolar macrophages”

Oral presentation at the YSA PhD Symposium 2019; Vienna, Austria
“Exploring trained immunity in pulmonary infection”

Oral presentation at the *Keystone* symposium “Regulation and Dysregulation of Innate immunity in disease” 2018; Vancouver, Canada; “Exploring trained immunity in lung infection”

AWARDS & FELLOWSHIPS

YSA oral presentation award (2019)

European Molecular Biology Organization (EMBO) Short Term Fellowship (2018)

ÖGAI travel grant (2018)

EXTRACURRICULAR ACTIVITIES

Editorial board member at the volunteer-run journal *Phenotype*

Scientific illustration and graphic design

MEMBERSHIPS

Austrian Association for Allergy and Immunology (ÖGAI)

Austrian Association of Molecular Life Sciences and Biotechnology (ÖGMBT)

PUBLICATIONS

Zahalka, S., Starkl, P., Watzenboeck, M.L., Farhat, A., Radhouani, M., Deckert, F., Hladik, A., Lakovits, K., Oberndorfer, F., Lassnig, C., Strobl, B., Klavins, K., Matsushita, M., Sanin, D. E., Grzes, K., Pearce, E. J., Gorki, A. D., & Knapp, S. (2022). [Trained immunity of alveolar macrophages requires metabolic rewiring and type 1 interferon signaling](#). Accepted for publication in *Mucosal Immunology*.

Grzes, K. M., Sanin, D. E., Kabat, A. M., Stanczak, M. A., Edwards-Hicks, J., Matsushita, M., Hackl, A., Hassler, F., Knoke, K., **Zahalka, S.**, Villa, M., Kofler, D. M., Voll, R. E., Zigrino, P., Fabri, M., Pearce, E. L., & Pearce, E. J. (2021). [Plasmacytoid dendritic cell activation is dependent on coordinated expression of distinct amino acid transporters](#). *Immunity*, 54(11):2514-2530. <https://doi.org/10.1016/j.immuni.2021.10.009>

Gorki, A. D., Symmank, D., **Zahalka, S.**, Lakovits, K., Hladik, A., Langer, B., Maurer, B., Sexl, V., Kain, R., & Knapp, S. (2022). [Murine ex vivo Cultured Alveolar Macrophages Provide a Novel Tool to Study Tissue-Resident Macrophage Behavior and Function](#). *Am J Respir Cell Mol Biol*, 66(1):64-75. <https://doi.org/10.1165/rcmb.2021-0190OC>

Watzenboeck, M. L., Gorki, A. D., Quattrone, F., Gawish, R., Schwarz, S., Lambers, C., Jaksch, P., Lakovits, K., **Zahalka, S.**, Rahimi, N., Starkl, P., Symmank, D., Artner, T., Pattaroni, C., Fortelny, N., Klavins, K., Frommlet, F., Marsland, B. J., Hoetzenecker, K., Widder, S., & Knapp, S. (2021). [Multi-omics profiling predicts allograft function after lung transplantation](#). *Eur Respir J*, 59(2):2003292. <https://doi.org/10.1183/13993003.03292-2020>

Watzenboeck, M. L., Drobits, B., **Zahalka, S.**, Gorki, A. D., Farhat, A., Quattrone, F., Hladik, A., Lakovits, K., Richard, G. M., Lederer, T., Strobl, B., Versteeg, G. A., Boon, L., Starkl, P., & Knapp, S. (2021). [Lipocalin 2 modulates dendritic cell activity and shapes immunity to influenza in a microbiome dependent manner](#). *PLoS Pathog*, 17(4):e1009487. <https://doi.org/10.1371/journal.ppat.1009487>

Starkl, P., Watzenboeck, M. L., Popov, L. M., **Zahalka, S.**, Hladik, A., Lakovits, K., Radhouani, M., Haschemi, A., Marichal, T., Reber, L. L., Gaudenzio, N., Sibilano, R., Stulik, L., Fontaine, F., Mueller, A. C., Amieva, M. R., Galli, S. J., & Knapp, S. (2020). [IgE Effector Mechanisms, in Concert with Mast Cells, Contribute to Acquired Host Defense against Staphylococcus aureus](#). *Immunity*, 53(4):793-804. <https://doi.org/10.1016/j.immuni.2020.11.012>

Abel-Reichwald, H., Hainisch, E. K., **Zahalka, S.**, Corteggio, A., Borzacchiello, G., Massa, B., Merlone, L., Nasir, L., Burden, F., & Brandt, S. (2016). [Epidemiologic analysis of a sarcoid outbreak involving 12 of 111 donkeys in Northern Italy](#). *Vet Microbiol*, 196:85-92. <https://doi.org/10.1016/j.vetmic.2016.10.021>